

LYMPHOCYTE EGRESS SIGNAL SPHINGOSINE-1-PHOSPHATE PROMOTES ERM-GUIDED,
BLEB-BASED MIGRATION

Tanner Ford Robertson

A DISSERTATION

in

Immunology

Presented to the Faculties of the University of Pennsylvania

in

Partial Fulfillment of the Requirements for the

Degree of Doctor of Philosophy

2021

Supervisor of Dissertation

Janis K. Burkhardt, Ph.D.

Professor of Pathology and Laboratory Medicine

Graduate Group Chairperson

David M. Allman, Ph.D.

Professor of Pathology and Laboratory Medicine

Dissertation Committee

Taku Kambayashi, M.D., Ph.D., (Chair) Professor of Pathology and Laboratory Medicine

Michael S. Marks, Ph.D., Professor of Pathology and Laboratory Medicine

Pamela L. Schwartzberg, M.D., Ph.D., Chief, Cell Signaling and Immunity Section

Phillip Scott, Ph.D., Professor of Microbiology and Immunology

LYMPHOCYTE EGRESS SIGNAL SPHINGOSINE-1-PHOSPHATE PROMOTES ERM-
GUIDED BLEB-BASED MIGRATION

COPYRIGHT

2021

Tanner Ford Robertson

This work is licensed under the

Creative Commons Attribution-NonCommercial-ShareAlike 4.0 License

To view a copy of this license, visit:

<https://creativecommons.org/licenses/by-nc-sa/4.0/us/>

DEDICATION

This thesis is dedicated to my parents, Rex and Debra Robertson, whose love and support have been unwavering.

ACKNOWLEDGMENTS

I would first like to acknowledge Joseph Acker and Fran Legband for sparking an interest in science and a love for learning when I was young and impressionable. I am incredibly grateful for Dr. David Minter, who was convinced I was supposed to be a scientist long before I was. Dr. Michael Chumley made immunology immediately accessible and fascinating to me, a feat I'm only able to truly appreciate in hindsight. I am forever indebted to him, and would certainly not be where I am today without his devotion to undergraduate mentorship. I would also like to thank Drs. Phil Hartman and Matt Chumchal for their encouragement during my undergraduate years. Nathan Roy taught me everything I needed to know to start this project, his patience and mentoring abilities are unparalleled. My cohort – Tom, Brenal, Glendon, and Omar – made the years fly by and are each destined for brilliant careers. I would especially like to thank Madeleine Salvatore, whose friendship made my time at Penn immensely better than it otherwise would have been.

I was fortunate to work with and learn from a number of extremely talented collaborators while working on this project. I would like to thank Daniella Gomez Atria, for her expertise in immunofluorescence histology, and Pragati Chengappa, for being perhaps the only person I know with the patience to measure intracellular pressure in T cells. Christine Wu made my life in lab immensely better these past two years, and when she eventually unlearns all the bad habits I've taught her she will do great things in science. I would like to thank my thesis committee – Taku Kambayashi, Mickey Marks, Pamela Schwartzberg, and Phil Scott – for their guidance and support during my thesis work. I would also like to thank Daniel Blumenthal, Lyndsay Avery, Xing Li, Ed Williamson, Franklin Staback, and other members of the Burkhardt lab that touched on this project in some way. Finally, I was extremely fortunate to train under Janis K. Burkhardt, who is simultaneously a tremendous scientist and devoted mentor. I will be forever grateful to her.

ABSTRACT

LYMPHOCYTE EGRESS SIGNAL SPHINGOSINE-1-PHOSPHATE PROMOTES ERM- GUIDED, BLEB-BASED MIGRATION

Tanner Ford Robertson

Janis K. Burkhardt

Ezrin, radixin, and moesin (ERM) family proteins regulate cytoskeletal responses by tethering the plasma membrane to the underlying actin cortex. Mutations in ERM proteins lead to severe combined immunodeficiency, but the function of these proteins in T cells remains poorly defined. Using mice in which T cells lack all ERM proteins, we demonstrate a selective role for these proteins in facilitating egress from lymphoid organs in response to sphingosine-1-phosphate (S1P), a pleiotropic signaling lipid abundant in the blood and lymph. ERM-deficient T cells display defective S1P-induced migration *in vitro*, despite normal responses to standard protein chemokines that control entry into and migration within lymphoid organs. Analysis of these defects revealed that S1P promotes a fundamentally different mode of migration than chemokines, characterized by intracellular pressurization and bleb-based motility. ERM proteins facilitate this process, controlling directional migration by limiting blebbing to the leading edge. We propose that the distinct modes of motility induced by S1P and chemokines are specialized to allow T cell migration across lymphatic barriers and through tissue stroma, respectively.

TABLE OF CONTENTS

DEDICATION	iii
ACKNOWLEDGEMENTS	iv
ABSTRACT	v
TABLE OF CONTENTS	vi
LIST OF FIGURES	viii
LIST OF ABBREVIATIONS	x
CHAPTER 1: INTRODUCTION	1
1.1 Cell Migration and Immunity	1
1.2 Lymphocyte Surveillance	2
1.3 Migration Strategies	10
1.4 Ezrin, Radixin, and Moesin (ERM) Family Proteins	15
1.5 Sphingosine-1-Phosphate (S1P) and S1P receptors	21
1.6 Structure of Thesis and Contributions	27
1.7 Figures	30
CHAPTER 2: ERM PROTEINS FACILITATE S1P-DEPENDENT T CELL EGRESS	33
2.1 Results	33
2.2 Figures	38
CHAPTER 3: S1P PROMOTES ERM-GUIDED, BLEB-BASED MIGRATION	46
3.1 Results	46
3.2 Figures	54
CHAPTER 4: DISCUSSION	61
4.1 Summary and Reconciliation with Previous Work	61
4.2 S1PR1 vs Chemokine Receptor Signaling	63
4.3 The Role of Lamellipodia, Blebs, and Other Protrusions for Migration <i>in vivo</i>	68
4.4 Concluding Remarks	75
4.5 Figures	77

Materials and Methods	78
BIBLIOGRAPHY	85

LIST OF FIGURES

Figure 1.1	Diagram of T cell homeostatic immune surveillance.....	30
Figure 1.2	Illustration of lamellipodia, filipodia, and blebs at the leading edge	31
Figure 1.3	Illustration of ERM protein domains and conformational regulation.....	32
Figure 2.1	Schematic of Msn targeting strategy.....	38
Figure 2.2	Verification of the deletion of ezrin and moesin.....	39
Figure 2.3	ERM-deficient lymphocytes assume an altered tissue distribution with severe lymphopenia.....	40
Figure 2.4	Organization of secondary lymphoid organs in DKO mice.....	41
Figure 2.5	ERM deficiency results in the accumulation of mature, single positive thymocytes.....	42
Figure 2.6	ERM-deficient T cells have a cell-intrinsic egress defect.....	43
Figure 2.7	Overnight culture improves S1PR1 responses in T cells.....	44
Figure 2.8	DKO T cells have a selective transmigration defect towards S1P.....	45
Figure 3.1	ERM proteins are dispensable for S1PR1 expression, endocytosis and signaling.....	54
Figure 3.2	S1P-induced ERM inactivation is short-lived relative to chemokines.....	55
Figure 3.3	S1P promotes a rapid, highly transient mode of migration.....	56
Figure 3.4	ERM proteins are required for S1P-induced chemokinetic responses.....	57
Figure 3.5	S1P promotes bleb-based migration.....	58

Figure 3.6	S1P activates myosin to drive intracellular pressurization and bleb-based migration.....	59
Figure 3.7	ERM proteins facilitate S1P-induced migration by limiting blebs to the leading edge.....	60
Figure 4.1	A model for the role of ERM proteins in lamellipodial and bleb-based migration.....	77

LIST OF ABBREVIATIONS

ABD	Actin-binding domain
APC	Antigen-presenting cell
ApoM	Apolipoprotein M
Arp2/3	Actin-related proteins-2/3
ATP	Adenosine Triphosphate
ATX	Autotaxin
BCR	B cell receptor
C-ERMAD	C-terminal ERM association domain
CCL19	Chemokine (C-C motif) ligand 19
CCL21	Chemokine (C-C motif) ligand 21
CCR4	C-C chemokine receptor type 4
CCR7	C-C chemokine receptor type 7
CCR9	C-C chemokine receptor type 9
CCR10	C-C chemokine receptor type 10
CD4	Cluster of Differentiation 4
CD8	Cluster of Differentiation 8
CD44	Cluster of Differentiation 44
CD69	Cluster of Differentiation 69
CHO Cells	Chinese Hamster Ovary Epithelial Cells
CXCL12	Chemokine (C-X-C motif) ligand 12
CXCL13	Chemokine (C-X-C motif) ligand 13
CXCR5	C-C chemokine receptor type 5
EBI2	Epstein-Barr virus-induced G-protein receptor 2
Edg	Endothelial differentiation gene
ELC	Essential light chain
ERM	Ezrin, Radixin, Moesin
FDCs	Follicular dendritic cells
FERM	F for 4.1 protein, E for ezrin, R for radixin and M for moesin
FRCs	Fibroblastic reticular cells
GCB cell	Germinal center B cell
GGG	S-geranylgeranyl-L-glutathione
GlyCAM-1	Glycosylation-dependent cell adhesion molecule-1
GPCR	G protein-coupled receptor
HDL	High-density lipoprotein
HEV	High endothelial venule
HeLa cells	Henrietta Lacks cervical epithelial cells
IL-15	Interleukin-15
LECs	lymphatic endothelial cells
LFA-1	Lymphocyte function-associated antigen 1
LOK	Lymphocyte-oriented kinase
LPA	Lysophosphatidic acid
Lpar2	Lysophosphatidic acid receptor 2
MAdCAM-1	Mucosal addressin cell adhesion molecule 1
MAP Kinase	Mitogen-activated protein kinase
MHC	Major histocompatibility complex
MLC	Myosin light chain

MLCK	Myosin light chain kinase
MRC	Marginal reticular cells
MZ B cell	Marginal Zone B cell
NIK	NF-kappa-B-inducing kinase
P2RY8	P2Y purinoreceptor 8
PI3K	Phosphoinositide 3-kinases
PIP	Phosphatidylinositol
PIP2/PtdIns(4,5)P2	Phosphatidylinositol (4,5)-bisphosphate
PIP3/PtdIns(3,4,5)P3	Phosphatidylinositol (3,4,5)-trisphosphate
PKC α	Protein Kinase C alpha
PKC θ	Protein Kinase C Theta
PM	Plasma membrane
PNAd	Peripheral Node Addressin
PP1a	Protein Phosphatase 1 alpha
PTEN	Phosphatase and tensin homolog
PVS	Perivascular space
ROCK	Rho-associated protein kinase
S1P	Sphingosine-1-phosphate
S1PR1	Sphingosine-1-phosphate Receptor 1
S1PR2	Sphingosine-1-phosphate Receptor 2
S1PR3	Sphingosine-1-phosphate Receptor 3
S1PR4	Sphingosine-1-phosphate Receptor 4
S1PR5	Sphingosine-1-phosphate Receptor 5
SCID	Severe combined immunodeficiency
Spns2	Spinster homolog 2
STK10	Serine/threonine-protein kinase 10
TCR	T cell receptor
TES	Thymic epithelial space
Tfh cells	T follicular helper cells
VCAM-1	Vascular cell adhesion protein 1
VEGF	Vascular endothelial growth factor
VLA-4	Very late antigen 4
X-MAID	X-linked moesin-associated immunodeficiency

CHAPTER 1: INTRODUCTION

1.1: Cell Migration and Immunity

From bacteria to mammals, cellular motility is integral to life. Single-cell organisms rely on motility for the acquisition of nutrients and the evasion of harsh or toxic environments [1]. In multicellular organisms, motility plays a fundamental role in development, but most terminally differentiated cells are non-motile [2]. Some cells, like erythrocytes, move throughout the body passively via blood flow, but do not actively migrate on their own. In the mature host, cell motility is particularly important for the hematopoietic compartment, where it plays an indispensable role in immunity. Among his many observations, Élie Metchnikoff noted that leukocytes not only extravasate into inflamed tissues, but that this process continues even after the death of the host when blood flow has ceased – an early indication of leukocytes' intrinsic migratory capacity [3].

Leukocytes use their special migratory abilities to survey the host for infections. Fundamental differences in how myeloid and lymphoid cells detect microbes has resulted in two complementary but distinct surveillance programs. Innate immune cells use germline-encoded receptors to detect common microbial products, allowing a small number of tissue-resident sentinel cells at barrier sites to recognize a wide variety of pathogenic threats and mobilize circulating myeloid cells to the site of infection *en masse* [4, 5]. Generic pathogen recognition is a luxury not afforded to lymphocytes. Genetic recombination events during lymphocyte development produce a pool of T and B cells with immense diversity in their antigen receptor specificity [6], but this creates a separate problem. In an adult mouse, this resulting repertoire contains only ~100 naïve T cells capable of responding to any given antigen [7, 8]. Since naïve lymphocytes have

no way of knowing where their specific or “cognate” antigen may appear, they must perpetually traffic throughout the host in a process termed homeostatic immune surveillance. This introductory chapter details this surveillance process first at the organismal level (trafficking) and then at the cellular and molecular levels (migration).

1.2: Lymphocyte Surveillance

Naïve T cell Trafficking

The main purpose of T cell homeostatic surveillance is the detection of rare, cognate antigens. Antigens and antigen-presenting cells (APCs) collect regionally in lymph nodes and other secondary lymphoid tissues distributed strategically throughout the host, allowing naïve lymphocytes to sample locally available antigens without surveying the entirety of the tissue [9]. For T cells, homeostatic immune surveillance occurs in four discrete steps:

1. Circulating T cells enter into lymph nodes from the blood.
2. T cells migrate intranodally, scanning APCs for cognate antigen in the form of peptide-MHC complexes.
3. If no cognate antigen is detected, T cells egress from the lymph node via efferent lymphatic vessels.
4. Lymphatics merge with the vasculature, returning to step 1.

If T cells spend too little time in a given lymph node, they are prone to missing rare cognate antigen. If T cells linger for too long, they may take unacceptably long to discover cognate antigen that has collected in a different node. In both cases, the result is the same: delayed onset of adaptive immunity. These two opposing evolutionary

forces have created an extremely efficient process guided by a variety of soluble and cell-bound migratory cues. Each step in this homeostatic immune pathway is outlined below.

Lymph Node Entry

Initial entry into lymph nodes from the blood is a highly regulated process. Lymphocytes in the blood first interact with specialized high endothelial venules (HEVs; [10]) and gain access to the lymph node through the sequential function of three receptors: CD62L (L-selectin), C-C Chemokine Receptor Type 7 (CCR7), and lymphocyte function-associated antigen 1 (LFA-1). HEVs uniquely express a sulfotransferase that modifies cell surface proteins including CD34, GlyCAM-1, and MAdCAM-1 with a 6-sulfo sialyl Lewis^X carbohydrate group [11, 12]. These modified proteins are collectively referred to as peripheral node addressin (PNAd) and act as the ligand for CD62L [13]. The interaction between CD62L and PNAd captures circulating lymphocytes and causes them to begin rolling along the HEV surface [14]. T cell rolling along the endothelium permits CCR7 to bind to one of its ligands, CCL21, which is immobilized on the HEV luminal surface through an interaction with cell surface heparan sulfate [15]. CCR7-dependent signaling then drives LFA-1 from a bent, inactive conformation to an extended, highly active conformation. Extended LFA-1 binds to HEV-expressed ICAM-1, and this interaction terminates rolling and promotes firm adhesion on the HEV walls [16]. Deletion or blockade of CD62L, CCR7, or LFA-1 prevents T cells from entering into lymph nodes, indicating that each homing receptor is necessary [17-20]. Along those lines, neutrophils express CD62L and LFA-1 but not CCR7 and are therefore excluded from lymph nodes under normal conditions [21].

In contrast to tethering, rolling, and firm adhesion, the actual process of transendothelial migration across the HEV or signals that prompt it are poorly understood. Autotaxin (ATX), an enzyme that converts the ubiquitous blood lipid lysophosphatidyl choline into lysophosphatidic acid (LPA), is highly expressed at HEVs. Pharmacological inhibition of ATX abrogates transendothelial passage and results in lymphocytes accumulating at HEVs, apparently unable to transverse [22]. Likewise, LPA promotes T cell polarization, motility, and transendothelial migration *in vitro* [23, 24]. However, T cells express multiple LPA receptors, and HEV cells themselves are responsive to LPA, which warrants further research into how LPA prompts transendothelial passage [24]. Along these lines, HEVs are not simple portals into the lymph nodes, but rather function as trafficking controllers by retaining T cells near the entry point to regulate T cell abundance in the lymph node parenchyma [25].

Intranodal Migration

Within lymph nodes, various non-hematopoietic cell populations create a structural network that doubles as a migratory roadway for T, B, and Dendritic Cells [26]. T cells that enter lymph nodes through the HEVs are guided to the paracortex by a network of fibroblastic reticular cells (FRCs; [27, 28]). These cells highly express the chemokines CCL19 and CCL21, both ligands for CCR7, in addition to ligands for LFA-1 and a second integrin, very late antigen 4 (VLA-4). T cells migrate directly on these FRC networks, which restricts migration to the paracortex, where T cells can scan APCs for cognate peptide-MHC complexes [29]. Deletion of CCR7 or its ligands results in T cell disorganization, migration defects, and associated immune deficiencies [18, 30]. Although CCR7 plays a major role in lymph node entry, these intranodal migratory defects are apparent even when HEV entry is bypassed by direct injection of T cells into

afferent lymphatics, indicating a clear role for CCR7 in intranodal guidance [31]. Further, CCR7-deficient T cells are severely disorganized in the spleen, which does not possess HEVs or utilize CCR7-dependent entry [18].

Follicular dendritic cells (FDCs) and marginal reticular cells (MRCs), two other non-hematopoietic stromal cell populations, form a corresponding network in the lymph node follicles. Unlike FRCs, FDCs and MRCs highly express the chemokine CXCL13, a ligand for the B cell chemokine receptor CXCR5 [32, 33]. CXCR5 thus guides recent B cell immigrants into the B cell follicle, but follows the same basic principles of migration guided by non-hematopoietic stromal cell networks as T cell migration to the paracortex [34]. Naïve T and B cell populations are therefore largely segregated from one another in secondary lymphoid organs. [34].

Egress

T cells spend approximately 12 hours in a given lymph node searching for antigen and, if none is found, will leave via the efferent lymphatics [35]. T cells first egress by passing through lymphatic sinuses present in the lymph node cortex near the T cell zone. From there, lymphatic flow carries them to macrophage-rich medullary sinuses, then through the subcapsular space, and ultimately into the efferent lymphatic vessels [36]. The central signal guiding T cell egress is sphingosine-1-phosphate (S1P), a pleiotropic signaling lipid present in high concentrations in the blood and lymph, but maintained in low concentrations in the interstitial fluid of lymphoid organs [37]. This distribution creates a high-to-low S1P gradient between the circulatory fluids and lymphoid organs that T cells recognize with S1P receptor 1 (S1PR1, *Edg1*). Recognition of this S1P gradient with S1PR1 prompts T cell passage into the lymphatic sinuses from

the lymph node parenchyma [38, 39]. While lymph nodes typically exist in series, these lymphatics ultimately merge with the thoracic duct, which places lymphocytes back into blood, restarting the successive process of lymph node entry, intranodal migration, and egress.

Variations in the Spleen

The spleen is the largest secondary lymphoid organ and maintains several distinctive features compared to lymph nodes that alter how T cells survey the organ. First, the majority of the splenic parenchyma, termed “red pulp”, is devoted blood filtration and other immunologically-independent functions [40]. Lymphocytes are concentrated in discrete regions termed “white pulp” [40]. Unlike lymph nodes, the spleen has no high endothelial venules. Instead, lymphocytes and antigen alike are transported into the spleen via the central arteriole, which carries them to the marginal zone – the demarcation between the red and white pulp [41]. Thus, relative to the lymph nodes, entry into the spleen is considered a passive process. Once in the splenic marginal zone, T and B cells segregate in the white pulp based on similar principles as the lymph nodes. T cells responding to CCL19 and CCL21 segregate from B cells responding to CXCL12 and CXCL13 [18, 42]. Marginal zone B cells, which are spleen-resident and do not recirculate, are the primary APC population in the spleen [43-45]. The route of T cell egress from the spleen has remained ill-defined, but occurs directly into the vasculature in an S1PR1-dependent fashion [46]

Effector Lymphocyte Trafficking

The majority of naïve T cells never find cognate antigen, but those that do enter a rapid proliferative phase that coincides with large-scale transcriptional changes [47, 48]. In addition to the acquisition of effector functions, activation results in profound

alterations in the expression of various chemoattractant receptors and adhesion proteins, which endows effector T cells with new surveillance and migratory capabilities. Shortly after T cell receptor (TCR) stimulation, T cells downregulate S1PR1, which causes them to remain lymph node resident during their highly proliferative phase [49]. Some effector T cells, especially CD8⁺ cells, will subsequently re-express S1PR1 to leave the lymph node and traffic to infected or inflamed peripheral tissues [50]. Entry into inflamed peripheral tissues by effector T cells is facilitated by the upregulation of VLA-4 and expression of CD44, which bind to VCAM-1 and hyaluronic acid, respectively, both components of inflamed endothelia [51-53]. Activated T cells also shed CD62L, which prevents further entry into lymph nodes and thus facilitates peripheral homing [54-56].

T follicular helper (Tfh) cells and germinal center B (GCB) cells remain in the draining lymph node following activation but alter their expression of chemoattractant receptors to coordinate germinal center responses. Naïve B cells normally localize to the follicle by virtue of CXCR5, with signaling through the receptor EBI2 biasing B cells to the outer perimeter [18, 34, 57]. Following activation, B cells downregulate CXCR5 and express the T cell chemokine receptor CCR7, which prompts their migration to the border of the T cell zone or paracortex [58]. At the T cell border, activated B cells interact with antigen-specific CD4⁺ T cells to form highly dynamic and mobile cell conjugates [59]. These B cells then migrate, guided by the receptor EBI2 and its oxysterol ligand, to the outer regions of the follicle near the subcapsular space (interfollicular zone) where they proliferate for 1-2 days prior to the formation of a proper germinal center [60-62]. Cognate T cells are also present at this interfollicular zone either through their own EBI2 guidance [63] or by virtue of being dragged there by B cells [59]. Several days post-activation, GCB cells and Tfh cells begin organizing formal germinal centers in the

center of the primary follicle. Movement from the interfollicular region to the nascent germinal center is mediated by the loss of EBI2 and expression of S1PR2 and P2RY8 by both Tfh and GCB cells. While S1P concentrations are substantially lower in lymphoid organs than blood or lymph, concentrations are not uniform across the tissue parenchyma. S1P concentrations are lowest in the center of the follicle, and the same is likely true for the ligand of P2RY8, S-Geranylgeranyl-L-glutathione [64, 65]. S1PR2 and P2RY8 simultaneously inhibit lymphocyte migration to chemokines and appear to drive chemorepulsion away from gradients of S1P or S-Geranylgeranyl-L-glutathione, which culminates in Tfh and GCB cells tightly clustering in the center of the follicle [65-68]. Light and dark zones subsequently form, and GCB cells use CXCR4 to move into the dark zones and CXCR5 to move into the light zones [69].

Memory T cell Trafficking

Memory T cells that form after pathogen clearance can be divided into “central memory” and “effector memory” subsets based on their expression of trafficking proteins [70]. Central memory T cells retain expression of the critical homeostatic surveillance receptors CD62L and CCR7 and therefore continue a surveillance program of secondary lymphoid organs similar to naïve T cells [71]. Effector memory populations downregulate CCR7 and CD62L, which reduces their capacity to enter peripheral lymph nodes [70, 72]. Effector memory cells primarily survey peripheral non-lymphoid tissue, but can enter lymph nodes through alternative receptors under some situations [73, 74]. Some memory T cell populations express tissue-specific homing receptors that allows them to preferentially survey tissues where a pathogenic threat was initially encountered. For example, expression of the chemokine receptors CCR4 and CCR10 promote preferential

trafficking to the skin [75-77], and expression of the integrin $\alpha 4\beta 7$ along with the chemokine receptor CCR9 promotes trafficking to the intestines [78-81].

Tissue-resident memory cells are a more recently-described subset that remain in peripheral tissues with no apparent re-circulation [82]. Tissue-resident memory cells have been observed in the skin [83, 84], intestines [85], lungs [86], salivary glands [87], and brain [88]. This tissue residency depends on the sustained suppression of S1PR1 function, which otherwise prompts T cell movement into the circulatory fluids [89, 90]. Further, tissue-resident memory cells upregulate the integrin $\alpha E\beta 7$, which is dispensable for entry into peripheral sites but is crucial for retention, likely by facilitating T cell interactions with tissue epithelial cells [88, 90-92].

In summary, T cell trafficking is integral to adaptive immunity. Antigen search, effector function, and memory surveillance are all orchestrated by the local production of chemoattractants, chemo repellents, adhesion ligands, and the cell-specific expression of their various receptors. Protein chemokines and lipid chemoattractants like S1P appear to play complementary but functionally distinct roles in this trafficking process. Much of the data presented in this dissertation is devoted to comparing how S1P and chemokines differentially influence T cell migration, and how that reflects their unique *in vivo* functions. We were able to address these questions by developing a cell culture technique that makes primary mouse T cells responsive to S1P through S1PR1 *in vitro*, and utilized this technique to compare and contrast S1PR1 and chemokine receptor signaling and migratory strategies. With the organismal-level picture of T cell trafficking now described, this introduction will now focus in on migration at the cellular and molecular levels.

1.3 Migration Strategies

In its simplest form, cell migration occurs when a protrusion at one pole of the cell is coupled to subsequent retraction on the opposite pole. This process results in net displacement, especially when performed in cycles: protrusion, retraction, protrusion, retraction, and so on. While this is simple in principle, cells display an incredible amount of plasticity in how they move. This migratory diversity reflects both the heterogeneous environments cells must migrate through and the biological purpose for their migration. For instance, straight line “ballistic” migration is ideal for a neutrophil chasing a pathogen, but impractical for a T cell searching numerous APCs for rare, cognate antigen. Additionally, cells may need to produce qualitatively different types of protrusions for crossing endothelial barriers compared to migrating within tissue parenchyma.

Actin and Myosin

There are two central components that facilitate migration in cells: actin and myosin. Actin is a small globular protein that can be polymerized into filaments in a regulated fashion. In resting cells, actin filaments assemble subjacent to the plasma membrane to form the actin cortex [93]. These actin filaments are cross-linked by myosin, resulting in a higher order structure referred to as the actomyosin complex or simply actomyosin. Actomyosin controls fundamental biological properties like cell shape, membrane tension, and intracellular pressure and is central to all modes of migration [94-97].

Humans express up to 40 different myosin genes organized into more than 20 distinct classes [98, 99]. All myosins possess an N-terminal catalytic motor domain that binds to actin [100, 101], but show great diversity in their C-terminal regions. This

diversity allows myosins to bind cargoes, assemble into filaments, and perform other functions. Myosin proteins operate by utilizing the energy gained from ATP hydrolysis to walk along actin filaments [102]. Depending on the myosin isoform and what the C-terminus is interacting with, walking along actin filaments can transport cargo proteins or cause a cellular contraction [103].

The Myosin II subfamily is the largest group of myosins, and it encompasses the myosins that carry out the well-known contractile functions in cardiac, skeletal, and smooth muscle cells as well as three additional members termed non-muscle myosin IIs (NMIIIs) that are expressed more broadly [99]. The C-terminus of myosin II heavy chain does not bind cargo but instead dimerizes with another myosin II protein in parallel fashion [104]. Each myosin II heavy chain in this dimer further associates with one essential light chain (ELC), which provides structural stability, and one regulatory myosin light chain (MLC), which modulates the activity of the catalytic motor domain [105, 106]. As a whole, this forms a hetero hexamer myosin complex, which further assembles into bipolar filaments [107]. When these myosin filaments collectively walk along actin, they cause the actin filaments to slide towards each other. This is an actomyosin contraction. When myosin is distributed unevenly over the cell cortex, actomyosin contractions can facilitate unique biological outcomes. Contractile activity at the cleavage furrow, for instance, mediate cytokinesis [108, 109]. In migratory cells, myosin classically localizes to the rear and powers trailing edge retractions [110-112].

Non-muscle myosin II shows low levels of activity even in resting cells, which keeps the plasma membrane under slight tension and creates a heightened intracellular pressure [97, 113, 114]. This contractile activity is modulated by phosphorylation of the MLC, especially at the tandem Thr18 and Ser19 positions, which increases the ATPase

activity of the catalytic head domain [115-117]. These crucial sites are phosphorylated by Rho-associated protein kinase (ROCK), myosin light-chain kinase (MLCK), or other kinases to increase actomyosin contractile activity in response to various stimuli [118-120].

Protrusions – actin-polymerization vs blebs

Cellular protrusions are typically driven by actin polymerization against the plasma membrane. The initial polymerization of actin is energetically unfavorable and must be initiated by a class of proteins called nucleation promoting factors. Depending on the factors at play, actin can be polymerized into a dense, highly-branched meshwork, which generates sheet-like protrusions called lamellipodia or it can be polymerized into parallel linear bundles that generate finger-like projections called filipodia (Illustrated in Fig. 1.2A-B). Lamellipodia are generated by the Arp2/3 complex, which binds pre-existing filaments and nucleates a new filament at a 70-degree angle from the initial filament [121, 122]. Filipodia are generated by the formin family of proteins, which generate long actin cables by simultaneously promoting polymerization and blocking filament capping [123-125]. While some cells almost exclusively use lamellipodia or filipodia, cells frequently utilize a blend, with Arp2/3 contributing to filipodia formation [126] and formins contributing to lamellipodia formation [127]. Irrespective of the type of actin structure that cells use for their leading-edge protrusions, myosin plays a key role in trailing edge retraction [110-112].

Blebs are a fundamentally different type of protrusion than those generated by localized actin polymerization. Blebs occur when intracellular pressure causes the plasma membrane to herniate from the underlying actin cortex (Illustrated in Fig 1.2C). Blebs occur in three discrete phases: initiation, expansion, and retraction [128]. Under

normal conditions, the plasma membrane is tightly associated with the underlying actin cortex. Bleb initiation occurs when there is a decrease in the membrane-cortex association, an increase in intracellular pressure, or some combination of the two [129-131]. Bleb expansion lasts only a few seconds, during which time the flow of cytosol causes inflation of the nascent bleb. The protrusion is devoid of actin or other major cytoskeletal machinery at this stage. Bleb formation is associated with an apparent increase in cell surface area [132], but lipid membranes can only stretch 2-3% before rupturing [133]. Bleb expansion thus appears to occur through the localized unfolding of small lipid invaginations to supply membrane during the expansion phase [134]. The actin cortex eventually reforms underneath the new protrusion, which ceases expansion [135, 136]. This reformation occurs sequentially, with ezrin, radixin, and moesin (ERM) family proteins first localizing the bleb membrane followed by actin, actin-bundling proteins, then myosin [137]. What promotes actin nucleation at the bleb membrane is unclear, as Arp2/3 and formins are conspicuously absent from nascent bleb at this time of cortex repolymerization [137]. Retraction is typically not observed in motile cells, with new blebs sprouting from old blebs as soon as the cortex has been repolymerized [135].

For blebs to drive productive migration, they must occur in a polarized manner. One initial study found that the driving force behind blebs – cytoplasmic pressure – could be unequally distributed throughout the cell, which could theoretically drive polarized blebbing [138]. Subsequent studies have challenged the notion of unequal cytoplasmic pressure, or at least its ability to drive polarized blebbing [139, 140]. Polarized blebbing could also occur under uniform intracellular pressure but localized weaknesses in the membrane-cortex interaction. Two studies in bleb-prone cancer cell models have shown that membrane-cortex linker proteins, especially ERM family proteins, accumulate at the

periphery and rear of migrating cells to limit blebbing outside the leading edge [141, 142]. Defects in bleb-based migration have also been observed in ERM-deficient zebrafish progenitor cells [143]. Thus, ERM proteins serve dual roles in bleb prevention and retraction, with the former function playing a critical role in steering bleb-based motility.

While blebs have long been observed at the leading edge of migratory cells [144-147], they have historically been less well-studied than actin-based protrusions [148], perhaps due to their association with apoptosis [149]. More recent studies showing that bleb-based migration occurs *in vivo* during development have quelled any notion that blebs are somehow artefactual or less physiologically relevant than their actin-based counterpart [135, 150]. Cells can alternate between actin-based protrusions or blebs depending on the extracellular environment, with cells preferring actin-rich pseudopods in two-dimensional settings and preferring blebs in confined settings [151, 152]. Further, lamellipodia seem optimized for migration on high-adhesion surfaces whereas bleb-based motility largely relies on the traction afforded by confinement for net displacement. While most research on bleb-based motility has focused on non-hematopoietic cells, lymphocytes also display bleb-based motility in three-dimensional or confined settings [153]. A crucial open question is whether T cells toggle between actin polymerization and bleb-based motility for different migratory goals *in vivo*. Intravital imaging experiments have shown some indications of T cells using lamellipodia for intranodal migration and transendothelial migration through the HEVs [27, 154], but the transiency and protein-dim nature of blebs makes them difficult to study by these methods. Thus, a role for bleb-based migration in lymphocyte trafficking, if any, remains to be determined. In this thesis, I identify a role for bleb-based motility in response to S1P but not

chemokines, which will be covered extensively in the results and discussion portions of this document.

1.4 Ezrin, Radixin, and Moesin Family Proteins

Discovery and Evolution

Ezrin, radixin, and moesin are the three members of the ERM protein family. Ezrin was first identified as a component of the brush border of chicken intestinal epithelial cells in 1983 and named after Ezra Cornell, the founder of Cornell University [155]. This was followed up by the identification of moesin in bovine uterus smooth muscle cells [156] and radixin from rat hepatocytes [157, 158]. Moesin is an acronym for membrane-organizing extension spike protein, and radixin, first identified as a component of adherens junctions was named after radix, the Latin word for “root” or “foundation”. Ezrin, radixin, and moesin are highly homologous at the amino acid level (~85% in mice and humans) and are generally considered to be functionally overlapping if not simply redundant when co-expressed in a cell [159-161]. Most cells express multiple ERM family members [162], and deletions of individual members typically only cause overt phenotypes in cells or tissues where that isoform is exclusively expressed. Radixin, for instance, is uniquely expressed in the cochlear stereocilia, and global deletion results in progressive auditory loss in mice with limited phenotypes observed in other tissues [163].

A single ERM ortholog most closely related to moesin is common in non-vertebrates including fruit flies (*Drosophila melanogaster*; [164]), nematodes (*Caenorhabditis elegans*; [165, 166]), and tunicates (*Ciona intestinalis*; [167]). Ezrin and

radixin are suspected to have arisen from gene duplication events in a common ancestor to vertebrate animals [168, 169]. While most vertebrates encode ezrin, radixin, and moesin in their genomes, several animals, especially birds and fish, deviate from these norms. For instance, Atlantic Salmon (*Salmo salar*) harbor ten ERM genes (2 ezrin, 4 radixin, and 4 moesin), and complete loss of the moesin gene is observed in many species of birds [169] .

Structure, Function, and Regulation

The primary function of ERM family proteins is to link the plasma membrane to the underlying actin cortex in a regulatable manner. All ERM proteins have an approximately 300 amino acid N-terminal FERM (4.1 protein, ezrin, radixin, moesin) domain that binds to the membrane phosphatidyl inositol (PtdIns) lipid PtdIns(4,5)P₂ (PIP₂) at the inner leaflet of the plasma membrane, an approximately 200 amino acid intermediary region, and an approximately 100 amino acid C-terminal region (C-ERMAD) that contains an actin-binding domain (ABD; Fig. 1.3a; [170-172]). By simultaneously binding to the membrane and the actin cortex, ERM proteins are able to tether these two structures together (Fig. 1.3b).

ERM proteins are conformationally regulated, existing in either inactive or active forms. The inactive form occurs through a head-to-tail intramolecular interaction that masks both the membrane and actin binding sites (Fig. 1.3b [173, 174]). ERM proteins undergo a two-step transition into the active conformation. First, an initial interaction with PIP₂ causes a slight conformational change that unmasks a critical threonine residue (Thr558 for moesin) in the ABD [175-177]. Second, phosphorylation of this threonine residue destabilizes the interaction between the FERM and ABD domains, driving a conformational change into the active, open state where the protein can simultaneously

bind the membrane and actin [178-180]. The PIP2 binding and threonine phosphorylation occur sequentially, with both being critical for ERM linker function [175, 181]. Replacing this critical threonine residue with aspartate creates a phospho-mimetic mutant that is constitutively active. Overexpression of this mutant generates aberrant actin-dependent membrane structures like microvilli and often interferes with cellular functions [182-185]. In the open conformation, the FERM domain is also reported to bind to numerous protein binding partners at the plasma membrane to help organize and regulate signaling events [186].

Various kinases are reported to phosphorylate the regulatory threonine residue in the ABD including PKC α [187], PKC θ [188], ROCK [178, 182, 189], NIK [190], LOK [191, 192], and several others [193]. Many of these kinases act in a context-specific manner, enabling specialized functions of ERM proteins across different tissues. The most compelling evidence for the relevant ERM kinase in lymphocytes is for LOK (lymphocyte-oriented kinase, STK10). In the absence of LOK, cells from the spleen, lymph nodes, and bone marrow all display substantial reductions (~80%) in resting ERM phosphorylation levels along with altered migratory responses [191]. On the other end, both myosin phosphatase and protein phosphatase 1 α (PP1 α) have been reported to dephosphorylate ERM proteins at the regulatory threonine residue [194-197]. The dynamic regulation of ERM protein activity through dephosphorylation/rephosphorylation is critical to several biological processes. For example, during cell division, broad ERM phosphorylation first promotes cell rounding and spindle alignment and subsequent dephosphorylation selectively at the poles facilitates cytokinesis [198-202].

The Role of ERM Proteins in Epithelial Cells

ERM proteins are also regulated by subcellular localization. In a variety of tissue and cell types, phosphatidyl inositol kinases, phosphatases, and lipases coordinate to form asymmetrical distributions of PtdIns species variably phosphorylated on their inositol ring [203-207]. In tubular organs, PIP2 is concentrated in the apical membranes of epithelial cells and absent from basolateral regions, whereas PtdIns(3,4,5)P3 (PIP3) shows the opposite distribution [205, 206]. Through their interaction with PIP2, ERM proteins are commonly localized to the apical membranes where they play crucial roles in maintaining actin-dependent structures. Ezrin, for instance, localizes to apical domain of intestinal epithelial layers and controls villus morphogenesis. In the absence of ezrin, mice die perinatally due to defective nutrient absorption secondary to issues with their brush border organization [208]. The sole ERM protein in *Drosophila* plays a similar role in maintaining epithelial polarity during development [209].

The Role of ERM proteins in Leukocytes

As in epithelial morphogenesis and maintenance, phosphatidylinositol species display a polarized distribution in migratory cells. From amoebas to leukocytes, PI3K and PTEN coordinate to concentrate PIP3 at the leading edge and PIP2 at the periphery and rear of polarized, migrating cells [203, 210-212]. Just like PIP2, ERM proteins localize to the periphery and rear of migratory amoebas [213], neutrophils [214], lymphocytes [215], and various cell lines [142]. However, the role of ERM proteins in cell migration has remained enigmatic.

Lymphocytes express high levels of moesin, moderate amount of ezrin, and negligible amounts of radixin [216, 217]. Chemokine stimulation in both T and B cells drives rapid ERM dephosphorylation lasting between 10-60 minutes [184, 217, 218]. The

fraction of ERM proteins that remain phosphorylated following chemokine stimulation localize to the uropod, a specialized membrane structure in the rear of polarized lymphocytes [215, 219]. The importance of the remaining pool of active ERM proteins, if any, is unclear as ERM-deficient T cells can chemotax normally in most scenarios [220].

Several groups have investigated a role for ERM proteins in lymphocyte polarization or the formation of uropod structures, often yielding conflicting results. Stephen Shaw's group reported that expression of a phospho-mimetic moesin (T558D) potentially interfered with chemokine-induced T cell polarization [184], whereas Martinelli et al. reported that expression of an analogous phospho-mimetic ezrin (T567D) led to excessive T cell polarization, even in the absence of chemokine [221]. This discrepancy doesn't appear to be an ezrin vs moesin difference, as the Shaw group later reported that transgenic expression of phospho-mimetic ezrin (T567E) also blocked T cell polarization and potentially interfered with migratory responses [185]. Martinelli et al. reported that a dominant negative version of ezrin blocked chemokine-induced polarization, but these data must be interpreted with caution since this construct has the potential to interfere with any PIP2-binding protein or PIP2-dependent process [221]. Using ezrin-knockout, moesin-knockdown (ERM-deficient) T cell blasts, Chen et al. found that ERM proteins were important for uropod formation in response to $\beta 1$, but not $\beta 2$ integrin engagement [220]. These data indicate that ERM proteins are not required for polarization *per se*, but may facilitate it under some conditions. Likewise, ERM-deficient neutrophils stimulated with the chemokine CXCL1 show only mild polarization defects [222].

Irrespective of these context-dependent alterations in uropod formation or polarization, ERM proteins are largely dispensable for actual migratory responses under

most circumstances. ERM-deficient T cells chemotax normally in transwell assays and migrate normally in collagen gel matrices [220]. When the pore size in the transwell is reduced from 5-microns to 3-microns, ERM-deficient T cells do show consistent migratory defects, likely indicating a preferential need for ERM proteins in confined settings [220].

While much of the *in vitro* work on the migration of ERM-deficient T cells shows underwhelming phenotypes, there is compelling *in vivo* data from both mice and humans that these proteins play a critical role in lymphocyte trafficking. First, mice with a germline deletion in moesin were originally reported to be phenotypically normal [223], but closer analysis revealed these mice are lymphopenic due to a cell-intrinsic lymphocyte egress defect [224]. How moesin facilitates egress remains unclear. Second, hemizygous missense mutations in moesin cause severe combined immunodeficiency (SCID) in humans, with patient T cells showing potent migratory defects *in vitro* [225]. This disease, termed X-linked moesin-associated immunodeficiency (X-MAID), is characterized clinically by profound lymphopenia, moderate neutropenia, poor vaccine responses, and recurrent bacterial and viral infections [225]. Six out of the seven patients described in this initial cohort have the same hemizygous missense R171W mutation in the moesin FERM domain, but the effect of this mutation on moesin function is still unknown. Since 2016, four additional SCID patients with this same R171W mutation have been identified by newborn screens or whole exome sequencing [226-228].

In addition to their role in lymphocyte trafficking, ERM proteins also appear to carry out additional, often disparate, functions in lymphocytes. Although B cells express high levels of moesin, loss of ezrin alone results in augmented B cell receptor (BCR)

signaling and dysregulated humoral immune responses. Ezrin-deficient B cells display enlarged BCR microclusters at the membrane following stimulation and exhibit a corresponding increase in downstream signaling [229]. This effect is not recapitulated in ezrin-deficient T cells, which show modest diminution of TCR signaling and associated defects in cytokine production and activation [217]. In T cells, ezrin and moesin localize to the posterior region during immunological synapse formation, forming a membrane domain termed the distal pole complex. In this way, they are proposed to promote T cell activation by sequestering several negative regulators of TCR signaling [217, 230]. Finally, moesin has been implicated in maintaining CD8⁺ regulatory T cells by regulating IL-15-mediated signaling, and moesin-deficient T cells develop lupus erythematosus-like autoimmune phenotype with age [231].

1.5 Sphingosine-1-Phosphate (S1P) and S1P Receptors

Regulation of S1P concentrations

Sphingosine-1-Phosphate (S1P) is a pleiotropic signaling lipid, and its concentrations in various tissues are tightly regulated. S1P is produced during normal sphingolipid metabolism and is therefore found in low concentrations in virtually all cells [232-234]. The transportation of intracellularly-generated S1P into the extracellular space, however, is highly specialized. S1P is most abundant in the circulatory fluids, and different cellular sources contribute S1P to the blood and lymph. In blood, extracellular S1P is produced by the hematopoietic compartment, with erythrocytes being the primary contributor [235]. Platelets also store large amounts of S1P that is released upon stimulation [236, 237], but platelet-derived S1P doesn't appear to contribute to the

homeostatic serum or lymph S1P levels critical for egress [235, 238]. Both erythrocytes and platelets utilize the transporter Mfsd2b for S1P secretion. Deletion of Mfsd2b reduces serum S1P concentrations by approximately 50%, resulting in mild lymphopenia [239]. Additional S1P transporters in erythrocytes are suspected but not yet identified.

Lymphatic endothelial cells (LECs) are the major supplier of extracellular S1P to the lymph and are thus critical for egress from the lymph nodes [240]. LECs utilize the S1P transporter Spns2, and its deletion ablates virtually all lymph S1P [241]. The contribution of Spns2 to blood S1P is contested, with different groups reporting mild to severe reductions in serum S1P concentrations in the absence of the transporter [241-243].

Many biological functions depend not just on the presence of S1P but on the high-to-low concentration gradient that exists between the circulatory fluids and tissues, including lymphoid organs. S1P is irreversibly degraded into phosphoethanolamine and hexadecenal by S1P lyase, an intracellular enzyme located in the endoplasmic reticulum and mitochondria of various cells [244]. Pharmacologically inhibiting or genetically reducing S1P lyase activity creates a uniformly high S1P environment between lymphoid organs and circulatory fluids, and potently interferes with lymphocyte egress [37, 245]. S1P lyase is abundantly expressed by non-hematopoietic cells, but deletion in these cell lineages has no apparent impact on S1P concentrations in the interstitial fluid of lymphoid organs. Instead, the egress-relevant S1P lyase activity is restricted largely to CD11c⁺ dendritic cells that are positioned near egress sites [246].

S1P receptors in lymphocytes

Both mice and humans express five dedicated G protein-coupled receptors (GPCRs) for S1P (S1PR1-5). Naïve T cells express high levels of S1PR1 (*Edg1*), and deletion of this receptor severely reduces egress from primary and secondary lymphoid organs in a T cell-intrinsic manner [38, 39]. Within the lymph node, CCR7 and S1PR1 act as competing retention and egress signals, respectively [247]. T cells limit the influence of S1PR1 in this balancing act through ligand-induced endocytosis. Cells in the S1P-rich circulatory fluids endocytose S1PR1, diminishing their attraction to blood or lymph and permitting their subsequent entry lymphoid organs [248]. Within the S1P-poor environment of the lymph node, T cells progressively upregulate surface S1PR1, restoring their sensitivity to S1P egress signals. In addition to controlling responsiveness to S1P, ligand-induced endocytosis also plays an important role in proper signaling through S1PR1 [249]. While ligand-induced endocytosis is crucial for homeostatic trafficking of naïve T cells, the lymph node retention of recently activated T cells is controlled by other mechanisms. Following T cell receptor recognition of cognate peptide-MHC or interferon signaling, T cells upregulate CD69, which interacts with S1PR1 on the plasma membrane and prompts its internalization [49]. Activation-induced S1PR1 downregulation is transient, and effector T cells eventually utilize S1PR1 to leave the lymph node, enter the blood, and access infected or inflamed peripheral tissues [50]. Memory T cells display different trafficking patterns than their naïve counterparts including the ability to survey non-lymphoid tissues [250, 251]. Tissue-resident memory T cells embed themselves in peripheral tissues and stop recirculating, a process that depends on the loss of S1PR1 expression [89].

While most research on S1PR1 in lymphocytes has focused on its role in trafficking, the importance of S1PR1 is not limited to egress. The periodic burst of S1PR1 signaling that occurs during egress is also critical for maintenance of mitochondrial content and long-term survival of naïve lymphocytes [252]. S1P signaling through S1PR1 limits proliferation of common lymphoid progenitor cells to regulate lymphopoiesis [253]. Two- to three-fold overexpression of S1PR1 in T cells in vivo simultaneously inhibits the formation of regulatory T cells while promoting Th1 differentiation [254]. Given that S1PR1 signaling appears to modulate T cell differentiation, it is worth exploring whether S1P concentrations change in draining lymph nodes or circulatory fluids during different kinds of pathogenic challenges.

In addition to S1PR1, naïve T cells express high levels of S1PR4, but the impact of S1PR4 on naïve CD4⁺ T cell trafficking is still subject to debate [255]. The weak phenotypes observed following loss of S1PR4 are somewhat surprising because unlike all other S1P receptors, S1PR4 is exclusively expressed in the hematopoietic compartment under normal conditions. One recent study found that S1PR4 does appear to synergize with S1PR1 for effector and memory T cells in peripheral tissues to gain access to draining lymphatics [256], but the role for S1PR4 in naïve T cell homeostatic surveillance is still unclear.

Various S1P receptors play critical roles in the function of other lymphocyte populations. S1PR5 is highly expressed by mature natural killer cells and controls their egress from the bone marrow into the blood [257, 258], playing a similar role as S1PR1 does for T cells. S1PR3 is highly expressed by marginal zone B cells and functions alongside S1PR1 and CXCR5 to control Marginal Zone (MZ) B cell shuttling between the follicle and marginal zone in the spleen [45, 259].

S1PR2 is distinct from the other S1P receptors. Poorly expressed in naïve lymphocytes, S1PR2 is strongly upregulated in GCB cells and Tfh cells [64, 67]. In both cell populations, S1PR2 promotes clustering in the germinal center where Tfh and GCB cells coordinate to produce high-affinity antibodies. In addition to controlling localization, S1PR2 limits the proliferation and signaling of GC B cells, and extreme outgrowths of these cell populations in chronically-established germinal centers occur in about half of S1PR2-deficient mice [64]. Whereas S1PR1, 3, 4, and 5 all promote chemotaxis in various lymphocyte populations in transwell assays, S1PR2 does not [39, 45, 256, 257]. On the contrary, when S1P is sensed through S1PR2 it can impede migration to chemokines or induce chemorepulsion on its own [64, 260]. Thus, while S1PR1, 3, 4, 5 drive either egress or migration in response to S1P, S1PR2 appears to limit motility to control organization and positioning within lymphoid organs [261].

S1PR1 function in non-lymphocytes

S1PR1 plays critical roles in non-lymphocytes, especially during development. Global deletion or knockdown of S1PR1 results in severe developmental defects in both mice and zebrafish due to impaired vascular development and associated edema [262-264]. During vascularization, S1PR1 acts in a cell-intrinsic manner to promote mature blood vessel formation by antagonizing VEGF-driven angiogenic sprouting [265]. S1PR1 is also crucial to platelet production, and conditional deletion of S1PR1 in megakaryocytes results in severe thrombocytopenia. In these cells, S1PR1 responding to S1P gradients guides megakaryocyte proplatelet extensions into bone marrow sinusoids to permit platelet release [266]. How a single ligand-receptor pair drives such disparate biological outcomes in different cell types remains a fascinating question. Interestingly, ligand-induced S1PR1 endocytosis occurs quickly in lymphocytes but

slowly in endothelia following S1P exposure [267]. S1PR1 has been shown to exhibit sustained signaling from endosomes in some contexts [268], which creates the possibility that cells may derive different outcomes from S1PR1 ligation by shunting the receptor to different subcellular localizations where it may engage in different signaling pathways. While this has not demonstrated for S1PR1, internalization-dependent signaling events have been demonstrated for other GPCRs [269].

S1PR1 structure and ligand binding

Due to its lipid nature, S1P also binds to its receptors in an atypical fashion. Like all GPCRs, S1PR1 possesses a seven-pass transmembrane region, but the extracellular region normally involved in ligand binding is occluded by an N-terminal helical region in the crystal structure [270]. There is an abnormally large gap between helices I and VII in the transmembrane region, however, and S1P is thought to access the binding pocket by first integrating into the outer leaflet of the plasma membrane and then diffusing laterally into this pocket [270-272]. This method of ligation explains why S1P shows such slow saturation of S1PR1 binding sites and how S1P within the endosomal membrane can activate S1P receptors [273, 274].

One additional layer of complexity for S1P is the very nature of peptide/protein vs lipid chemoattractants. While chemokines like CCL19 are readily soluble in aqueous solutions of the body, lipids like S1P are not. S1P is transported by binding non-covalently to carrier proteins, with the primary partners being Apolipoprotein M (ApoM), the major protein component of high-density lipoproteins (HDL), and albumin [275, 276]. The degree to which the carrier protein impacts the outcome of S1P-S1PR1 interactions remains an open question. S1P-ApoM and S1P-albumin both stimulate the MAP kinase cascade through S1PR1 to similar degrees in endothelial cells, but the intracellular tail of

S1PR1 appears to bind differently to scaffolding proteins and promote different cellular responses depending on the carrier [277, 278]. Surprisingly, S1P bound to ApoM appears to be completely dispensable for T cell trafficking [253]. Even in mice doubly deficient in ApoM and albumin, lymphopenia isn't observed, although other proteins are reported fulfill the S1P-carrying function in these animals [279]. It seems likely that S1PR1-dependent T cell egress is largely indifferent to the S1P carrier protein so long as sufficiently high S1P levels are maintained in the circulatory fluids. More work is needed to verify that this is the case. Most of the *in vitro* data on T cell responses to S1P, including the experiments detailed in chapters 2-3, utilize S1P conjugated to albumin.

1.6 Structure of Thesis and Contributions

Following this introductory **Chapter 1**, this dissertation contains two chapters (Chapters 2 & 3) devoted to data. **Chapter 2** details our characterization of a novel mouse model in which T cells are devoid of all ERM proteins, and concludes with the major finding that ERM proteins are particularly critical for S1P-dependent egress *in vivo* and S1P-induced migration *in vitro*. **Chapter 3** then describes an atypical pressure-driven bleb-based mode of migration elicited by S1P, and how this contrasts with standard actin-based motility elicited by chemokines. Chapter 3 concludes by showing that ERM proteins are selectively critical for S1P-induced bleb-based migration because they limit blebbing to the leading edge. In **Chapter 4**, I discuss the results from Chapters 2-3 with a particular focus on how S1P could elicit such a profoundly different mode of migration than chemokines, and why bleb-based motility may be particularly useful for crossing specialized endothelial barrier during egress events.

The contents of this dissertation contain modified text and figures from a manuscript this is currently being revised for resubmission to the Journal of Cell Biology with the following author list, title, author affiliations, and author contributions:

[Preparing Resubmission] Tanner F. Robertson^{1,2}, Pragati Chengappa³, Daniela Gomez Atria⁴, Christine F. Wu^{1,2}, Lyndsay Avery^{1,2}, Nathan H. Roy^{1,2}, Ivan Maillard⁴, Ryan J. Petrie³, Janis K. Burkhardt^{1,2}. Lymphocyte Egress Signal Sphingosine-1-Phosphate Promotes ERM-Guided, Bleb-Based Migration. *Journal of Cell Biology* (2021)

¹Department of Pathology and Laboratory Medicine, Children's Hospital of Philadelphia Research Institute, Philadelphia, PA, USA.

²Perelman School of Medicine, University of Pennsylvania, Philadelphia, PA, USA.

³Department of Biology, Drexel University, Philadelphia, PA, USA.

⁴Division of Hematology-Oncology, Department of Medicine, Abramson Family Cancer Research Institute, University of Pennsylvania Perelman School of Medicine, Philadelphia, PA, USA.

Author Contributions

T.F.R. designed and executed most experiments, interpreted the data, and guided the project. D.G.A and I.P.M designed and performed the immunohistochemistry studies, and P.C. and R.J.P designed and performed the intracellular pressure experiments. C.F.W assisted with T cell purification and culture, transwell migration assays, video analysis, and western blots. L.A. helped design and execute competitive in vivo

migration experiments, and N.H.R provided conceptual and technical assistance with cell motility and blebbing. J.K.B oversaw the project.

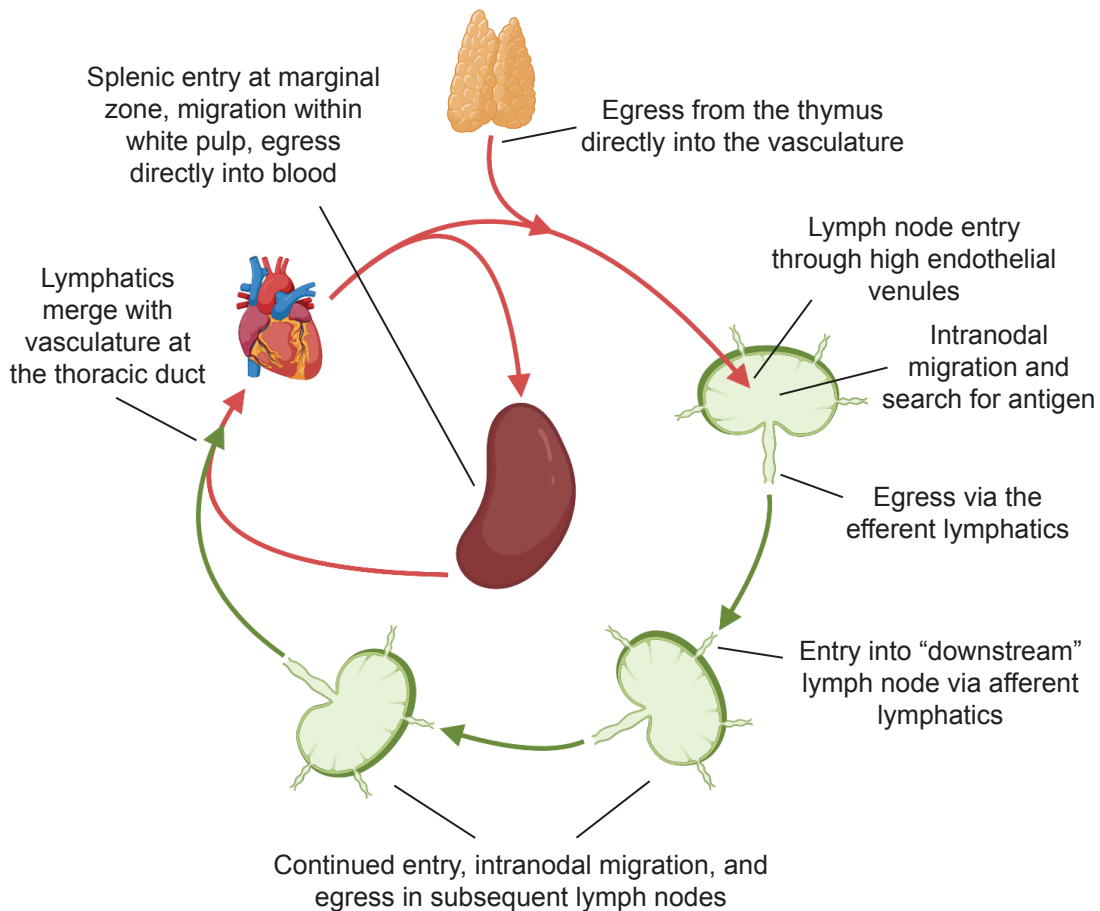


Figure 1.1. Diagram of T cell Homeostatic Immune Surveillance

T cell surveillance can be illustrated as a simple circuit. Moving clockwise, T cells first egress from the thymus directly into the vasculature. From the blood, T cells enter into lymph nodes through the high endothelial venules. Within the lymph node, T cells search for cognate antigen, and, if unsuccessful, egress via the efferent lymphatics. For lymph nodes that exist in series, these lymphatics carry the T cells directly into a downstream lymph node, where the T cells continues to search for antigen and, if unsuccessful, egress via the efferent lymphatics. The efferent lymphatics eventually merge with the vasculature at the thoracic duct, which puts the T cell back into circulation, permitting subsequent lymph node entry through the high endothelial venules. T cells can also access the spleen through the blood. In this case, T cells enter via the central arteriole, which places them at the marginal zone. These cells migrate within the white pulp, and then egress directly into the vasculature.

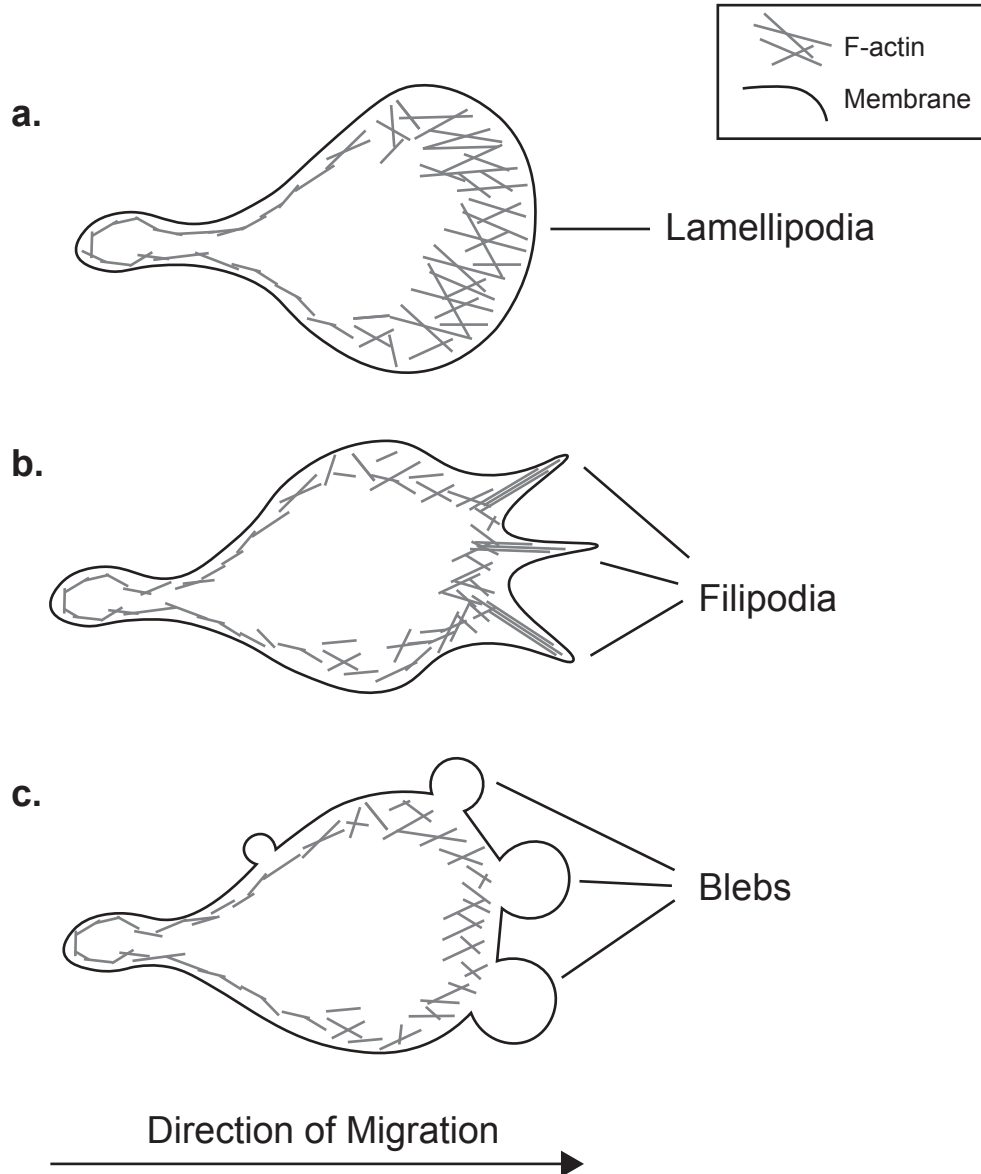


Figure 1.2 Illustration of lamellipodia, filipodia, and blebs at the leading edge

Illustrations showing leading edge morphology in cells migrating with lamellipodia (a), filipodia (b), or blebs (c). **(a)** In lamellipodia, actin organizes into a thin, flat meshwork. **(b)** In filipodial migraton, actin organizes into long protrusive bundles. **(c)** In bleb-based migration, the plasma membrane separates from the underlying actin cortex at the leading edge.

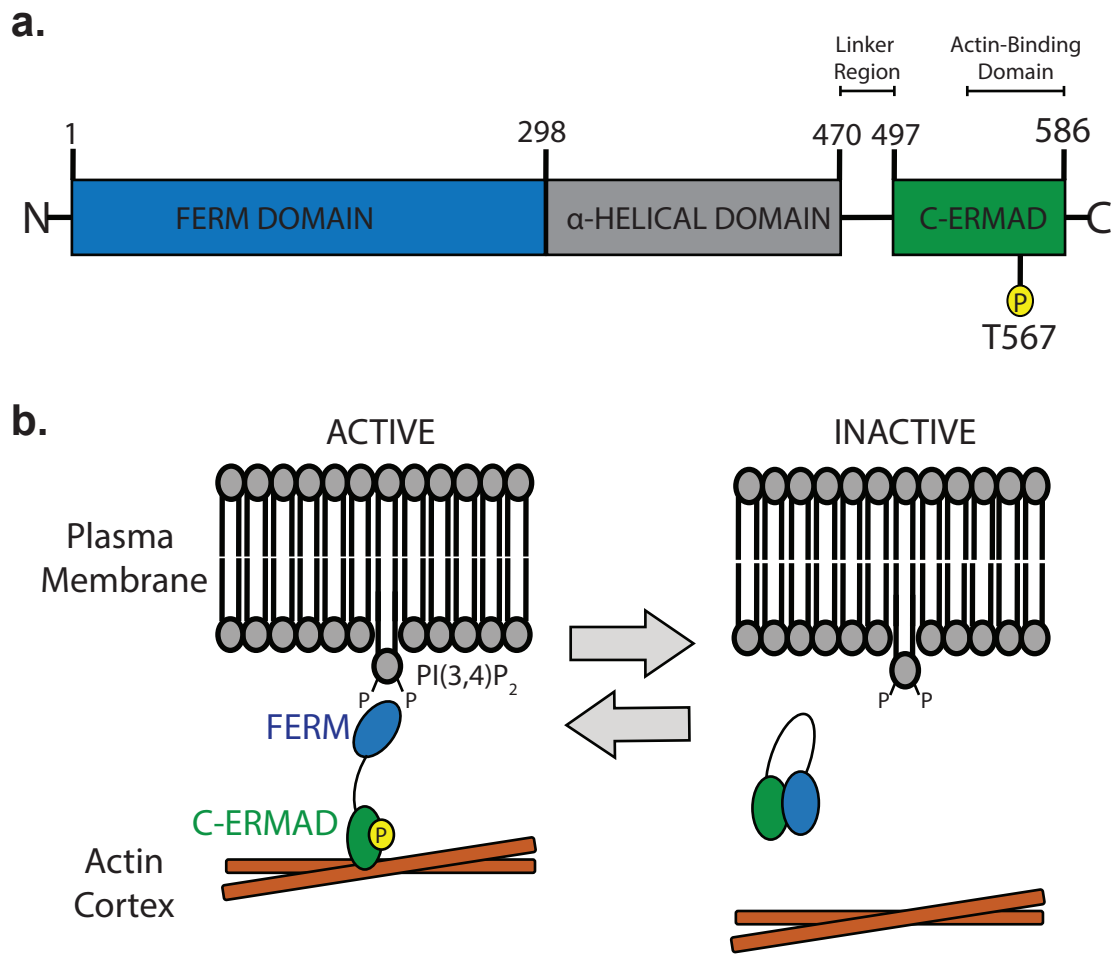


Figure 1.3. ERM Protein Structure, Function, and Conformational Regulation

(a) The domain organization ERM proteins. All ERM proteins have an N-terminal FERM domain followed by an intermediary alpha-helical domain, a short linker region, and a C-terminal region (C-ERMAD) that contains an actin-binding domain. The indicated amino acid positions are for specific to ezrin, but radizin and moesin contain analogous sites. The critical threonine residue, T5667, is shown. **(b)** In the open conformation (left) ERM proteins simultaneously bind to $\text{PI}(3,4)\text{P}_2$ in the inner leaflet of the plasma membrane through their FERM domain and to the actin cortex through their C-ERMAD region. In the inactive, closed conformation, the protein assumes a head-to-tail autoinhibited conformation that masks the membrane- and actin-binding sites.

CHAPTER 2: ERM DEFICIENCY RESULTS IN A T CELL- INTRINSIC EGRESS DEFECT FROM LYMPHOID ORGANS

2.1 Results

ERM-deficient lymphocytes show an altered distribution among lymphoid organs and blood

Co-expressed ERM proteins functionally overlap, and T cells express high levels of both moesin and ezrin. We generated germline moesin knockout mice (MKO) by targeted disruption of the *Msn* gene (Fig 2.1) and crossed them to mice with a conditional deletion of *Ezn* in the T cell compartment (*ezrin*^{Flox/Flox:CD4Cre}, EKO; [217]) to generate animals in which mature T cells lack both gene products (double knockout, DKO). These mice were born at expected Mendelian frequencies and were visibly indistinguishable from wildtype littermates. Additionally, histological analysis did not reveal any overt pathology or aberrant accumulation of leukocytes in non-lymphoid organs (skin, liver, kidney, collected at 8-16 weeks of age, data not shown). Western blot analysis of CD4⁺ T cells confirmed that ezrin and moesin were deleted as expected from the single and double knockouts; radixin levels remained low (Fig. 2.2). Note that B cells in both MKO and DKO mice lack moesin, but continue to express ezrin.

Analysis of secondary lymphoid organs from both MKO and DKO mice revealed marked alterations in lymphocyte distribution. Spleens were larger in size compared to WT mice and showed elevated cellularity and lymphocyte numbers, while inguinal and mesenteric lymph nodes showed diminished total cellularity and T cell numbers (Fig.

2.3a-e). Numbers of lymph node B cells were also reduced, although this did not reach statistical significance (Fig. 2.3d-e). Despite these alterations, ERM-deficient lymphocytes generally segregated into the correct anatomical locations within the spleens and lymph nodes, although the organization of these zones was more diffuse than in WT mice (Fig. 2.4a-g). Most striking, MKO and DKO mice displayed sharp reductions in the numbers of all lymphocytes in the blood (Fig. 2.3f). Overall, the phenotype of MKO and DKO mice was similar, but DKO mice consistently exhibited more pronounced phenotypes. This likely reflects the fact that moesin is the more abundant isoform in T cells, and the existence of functional overlap between ezrin and moesin in this setting. Given the more profound defects in DKO mice, only these animals were used for further experiments.

Within the thymus of DKO mice, double negative and double positive thymocytes appeared in normal numbers and frequency, indicating no gross perturbations in T cell development (Fig. 2.5a-b). CD4 and CD8 single positive populations showed a mild increase; further analysis demonstrated that this was due to a significant accumulation of mature (CD24^{low}, S1PR1^{hi}) single positive thymocytes (Fig. 2.5c-f). This phenotype as well as the peripheral lymphopenia in DKO mice (Fig. 1f) are common features of mouse models with egress defects from lymphoid organs [38, 39]. Taken together, these data suggest that ERM proteins are important for homeostatic lymphocyte trafficking.

ERM deficiency results in cell-intrinsic defects in egress from lymphoid organs

To ask whether the altered distribution of ERM-deficient lymphocytes reflects a cell-intrinsic trafficking defect, we performed competitive *in vivo* migration assays by labelling congenic WT and DKO naïve CD4⁺ T cells with cell tracking dyes and co-

injecting them into the lateral tail veins of WT recipients (Fig. 2.6a). To distinguish between entry and egress defects, cells were analyzed 1-hour after injection, when egress is minimal, and 24-hours after injection, when trafficking is reaching equilibrium [35, 280]. 1-hour post-injection, DKO T cells showed a 30-40% reduction in lymph node entry and a corresponding elevation in the blood (Fig. 2.6b). This points to a role for ERM proteins in promoting T cell passage into lymph nodes across high endothelial venules. Entry into the spleen, which occurs via an open system continuous with blood [281, 282], was equally efficient for WT and DKO T cells. By 24 hours, DKO T cells accumulated in the spleen and showed a corresponding decrease in the blood (Fig. 2.6c), indicating that DKO T cells fail to egress properly from the spleen. The relative paucity of DKO T cells in lymph nodes was maintained from 1 to 24 hours post injection, most likely because the reduced entry rate evident at 1-hr is matched by a reduced lymph node egress rate [35]. Importantly, the distribution of transferred T cells at 24 hours matched the altered tissue distribution observed in the DKO mice (Fig. 2.2), indicating that the observed alterations in the DKO mice are T cell intrinsic. Taken together, these studies show that although loss of ERM proteins impairs both entry and egress from lymphoid organs, the egress defects drive the most profound phenotypes, including accumulation of mature thymocytes, splenomegaly, and severe peripheral lymphopenia. Thus, we focused on understanding the molecular basis for this egress defect.

ERM proteins are selectively required for S1P-induced migratory responses

The central signal that governs lymphocyte egress from lymphoid organs is sphingosine-1-phosphate (S1P), a pleiotropic signaling lipid that is rich in blood and lymph but low in interstitial fluids of lymphoid organs [37]. T cells recognize S1P through

the receptor S1PR1 (*Edg1*), which prompts egress [38, 39]. Our initial attempts to study S1P-induced migration in WT and DKO T cells were stymied by the fact that T cells are notoriously unresponsive to S1P *in vitro* [248, 249], a problem that is further complicated by the presence of S1P in cell culture serum. In other cell types, optimal S1P responses can be achieved by overnight culture in serum-free media [283], but this strategy results in unacceptable levels of death for primary T cells (data not shown). To maintain T cell viability, we utilized charcoal-stripped FBS (CS-FBS), which is devoid of lipophilic components. T cells cultured overnight in media supplemented with CS-FBS were mostly viable and displayed dramatically enhanced transmigration to S1P relative to freshly-isolated cells cultured for one hour in the same media (Fig 2.7a). Inhibiting S1PR1 with the selective antagonist Ex26 [284] completely abrogated transmigration, verifying that the response was S1PR1-dependent (Fig 2.7a).

We initially hypothesized that T cells were sensing S1P during the isolation process and subsequently endocytosing S1PR1, which diminished responsiveness in our *in vitro* assays. However, freshly-isolated cells had only a slight reduction in surface S1PR1 relative to those cultured overnight, which seemed insufficient to explain the transmigration defect (Fig 2.7b). Although they started off with elevated F-actin content, freshly isolated cells polymerized actin in response to S1P comparably to those cultured overnight, with both groups returning to their own pre-stimulation set point (Fig. 2.7c). Despite this grossly normal actin response, downstream signaling through the ERK1/2 or AKT pathways in freshly isolated cells was severely reduced following S1P stimulation relative to those cultured overnight (Fig. 2.7d). Notably, this defective signaling in freshly-isolated cells did not extend to other chemoattractants like CCL19 (Fig. 2.7e). Both the actin and signaling responses to S1P were blocked by Ex26, indicating S1PR1

was driving both (data not shown). It remains unresolved why some aspects of S1PR1 function (actin responses) are intact in freshly isolated cells and others (signaling) are defective. These data indicate that the actin responses can be at least partially uncoupled from downstream signaling events and may indicate unique aspects of S1PR1 regulation. Despite the unresolved aspects of the overnight culture procedure, it provided a method for more rigorously testing T cell responses to S1P *in vitro* than previously possible.

Using this improved *in vitro* approach, we found that DKO T cells were highly defective in transmigrating towards S1P across multiple doses (Fig. 2.8a). Remarkably, transmigration towards CCL19 or CXCL12, two chemokines involved in naïve T cell trafficking [18, 285] was entirely normal (Fig. 2.8b-c). These data indicate that, while ERM proteins are not required for directed T cell migration generally, they are selectively critical for S1P-induced migratory responses. To understand why ERM proteins appear selectively critical for mediating S1P responses, I examined the modes of motility elicited by S1P versus chemokines in T cells. These experiments revealed fundamental differences between the responses to these various chemoattractants that explain the unique requirement for ERM proteins in S1P responses. These experiments are detailed in the following section, **Chapter 3**.

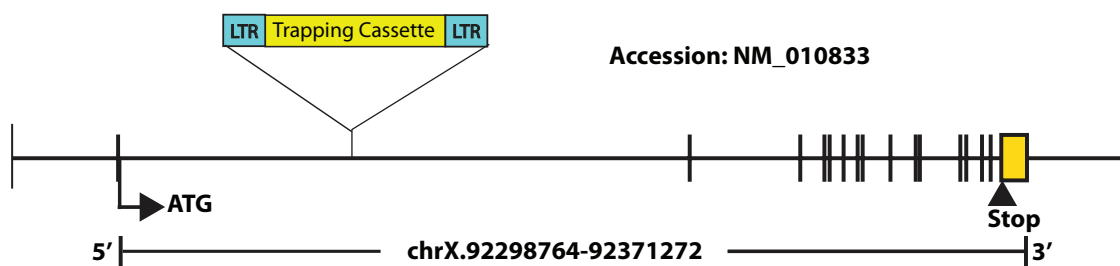


Figure 2.1 Schematic of *Msn* targeting strategy

The diagram shows the insertion of the trapping cassette into the first intron of the *Msn* gene in 129/Sv ES clones (OST4322827), which were used to generate the moesin knockout (MKO) mice used in this report.

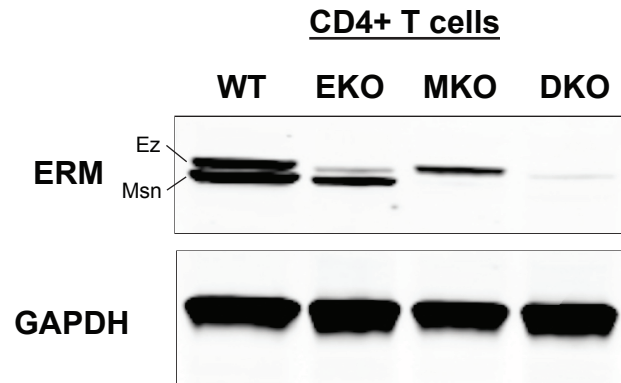


Figure 2.2 Verification of the deletion of ezrin and moesin

CD4+ T cells harvested from the spleens and lymph nodes of mice with a T cell conditional deletion in ezrin (EKO), a germline deletion in moesin (MKO), or both (DKO) were lysed and immunoblotted with a pan-ERM antibody and for GAPDH. The ezrin (Ez) and moesin (msn) bands are noted.

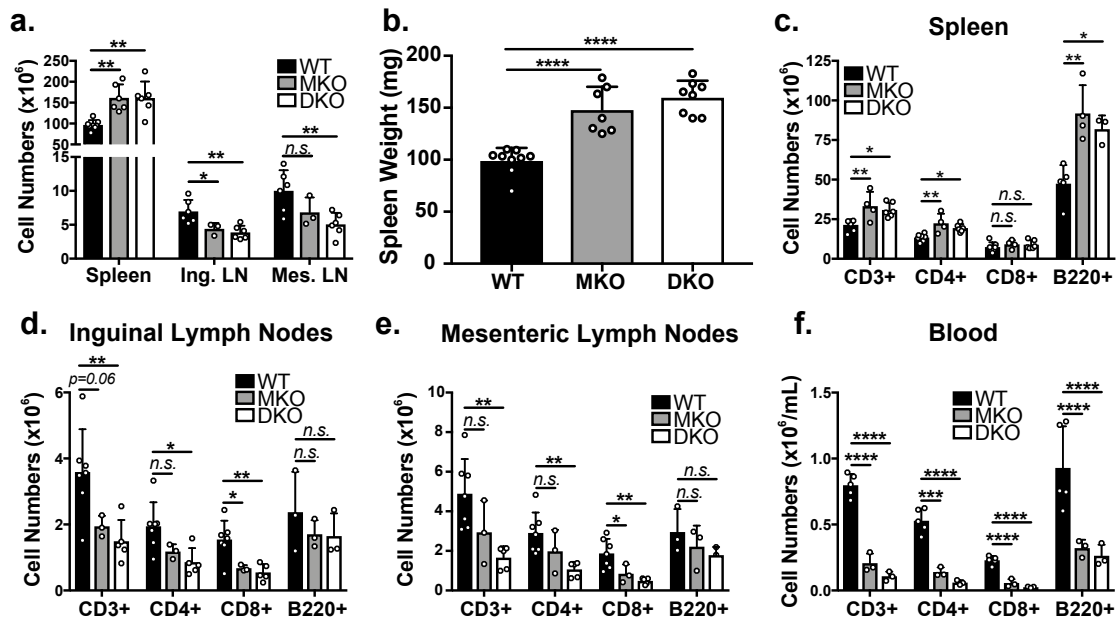


Figure 2.3. ERM-deficient lymphocytes assume an altered tissue distribution with severe lymphopenia.

(a) Total cell counts from spleens (post-RBC lysis), inguinal and mesenteric lymph nodes from 8-16-week-old mice. (b) Spleens from age matched mice of the indicated genotype were weighed. (c-f) Cell suspensions and PBMCs were labeled for the indicated surface markers, counted, and cell populations were quantified using flow cytometry. Data in a-f represent means \pm StDev. Each dot corresponds to an individual mouse. Statistical significance was determined using a standard one-way ANOVA. * $p < 0.05$, ** $p < 0.01$, *** $p < 0.001$, **** $p < 0.0001$

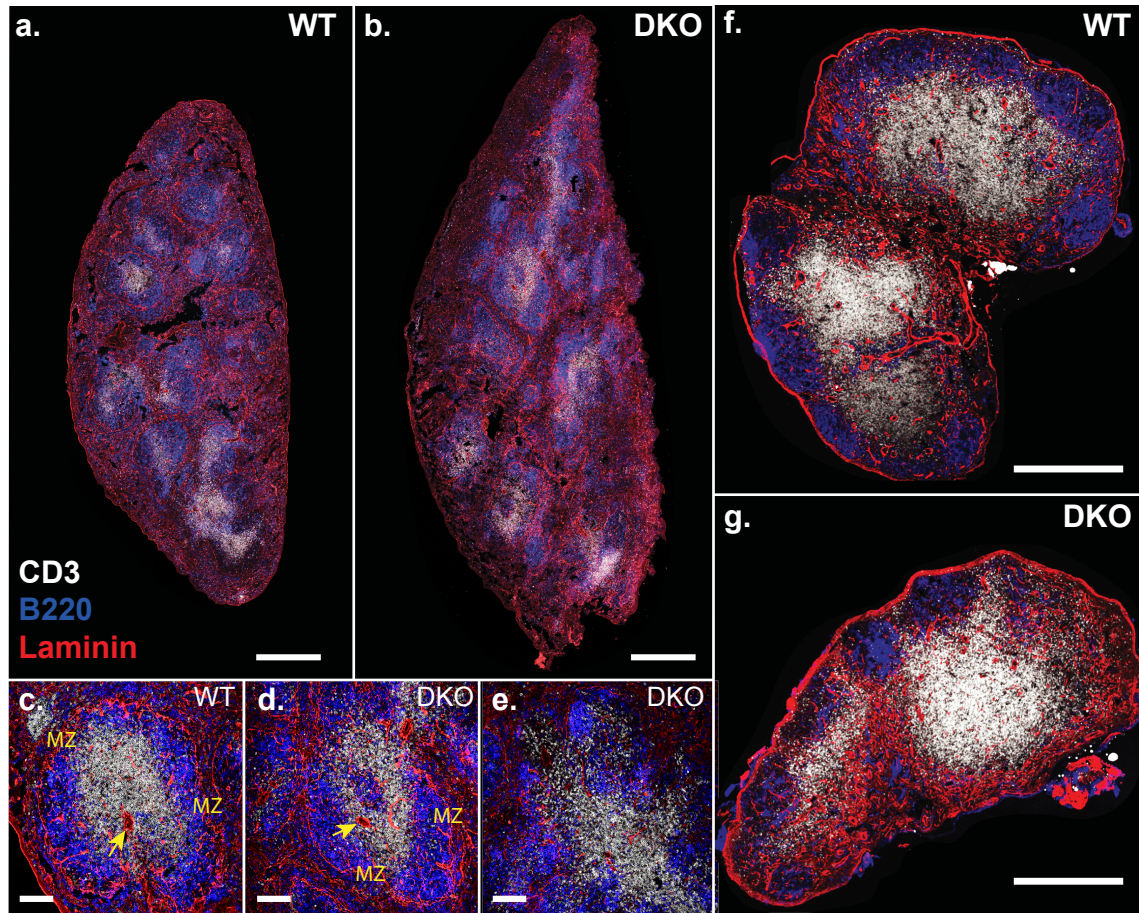


Figure 2.4 Organization of secondary lymphoid organs in DKO mice.

Immunofluorescence histology of spleens and lymph nodes from WT and DKO mice stained with antibodies against CD3 (white), B220 (blue) and laminin (red). **(a-b)** Confocal tile scans of whole spleens from WT and DKO mice, bar = 500 μ m. **(c-e)** Magnified regions of spleens with the central arterioles (arrows) and marginal zones (MZ) labelled. Normal lymphocyte organization in WT and DKO spleens shown (c-d) as well as a representative region of poor organization in DKO spleen (e), bar = 100 μ m. **(f-g)** Confocal tile scans of whole inguinal lymph nodes from WT and DKO mice, bar = 500 μ m.

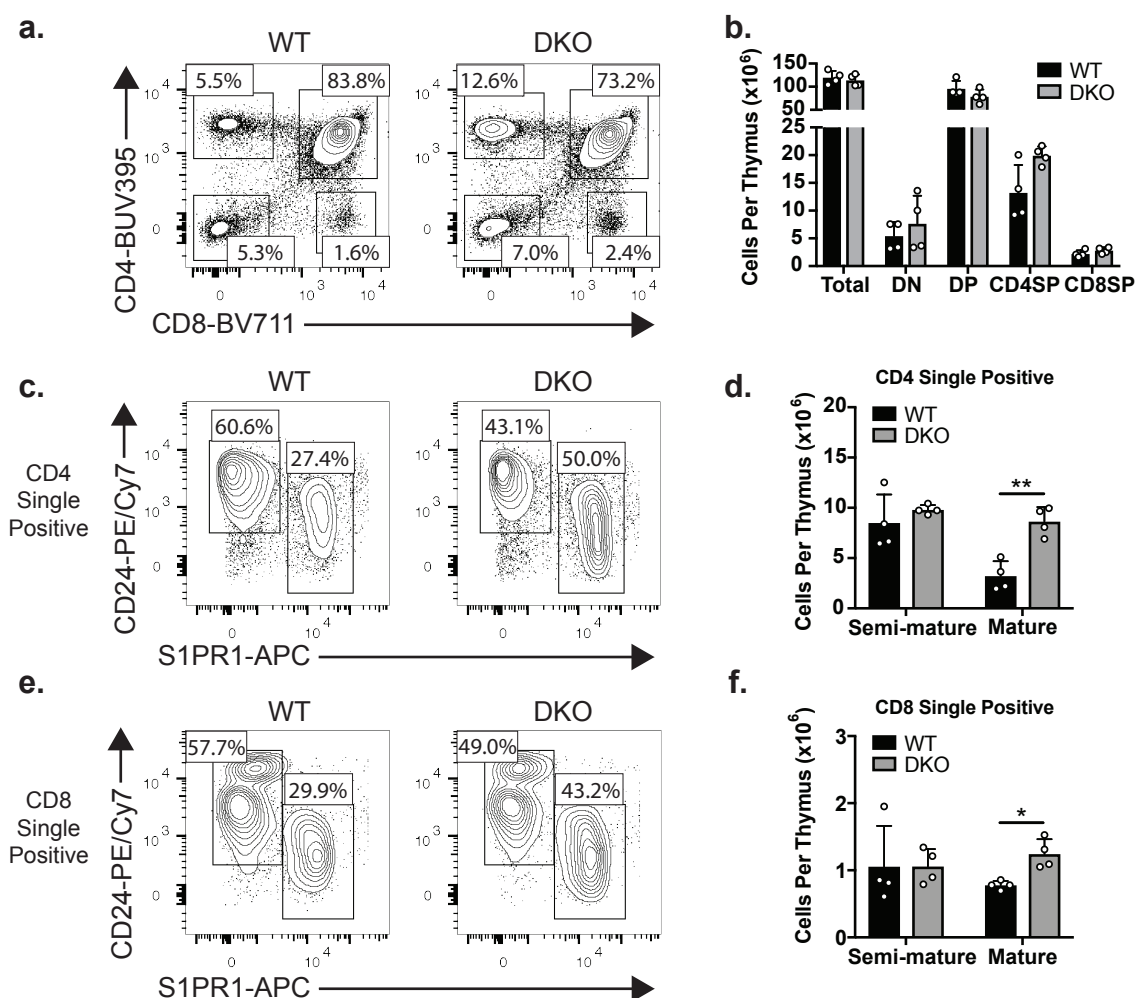


Figure 2.5 ERM-deficiency results in the accumulation of mature, single positive thymocytes

(a-b) Representative flow plots and total numbers of the major thymocyte populations based on CD4 and CD8 expression. (c-d) CD4 single positive populations further analyzed by CD24 and S1PR1 expression to determine the numbers of semi-mature (CD24^{Hi} S1PR1^{Low}) and mature (CD24^{Low} S1PR1^{Hi}) subpopulations in WT and DKO thymi. (e-f) CD8 single positive populations analyzed as in (c-d). Statistical significance for b, d, f determined by comparing the WT and DKO means using multiple t-tests and the Holm-Sidak method for correcting for multiple comparisons. *p<0.05, **p<0.01

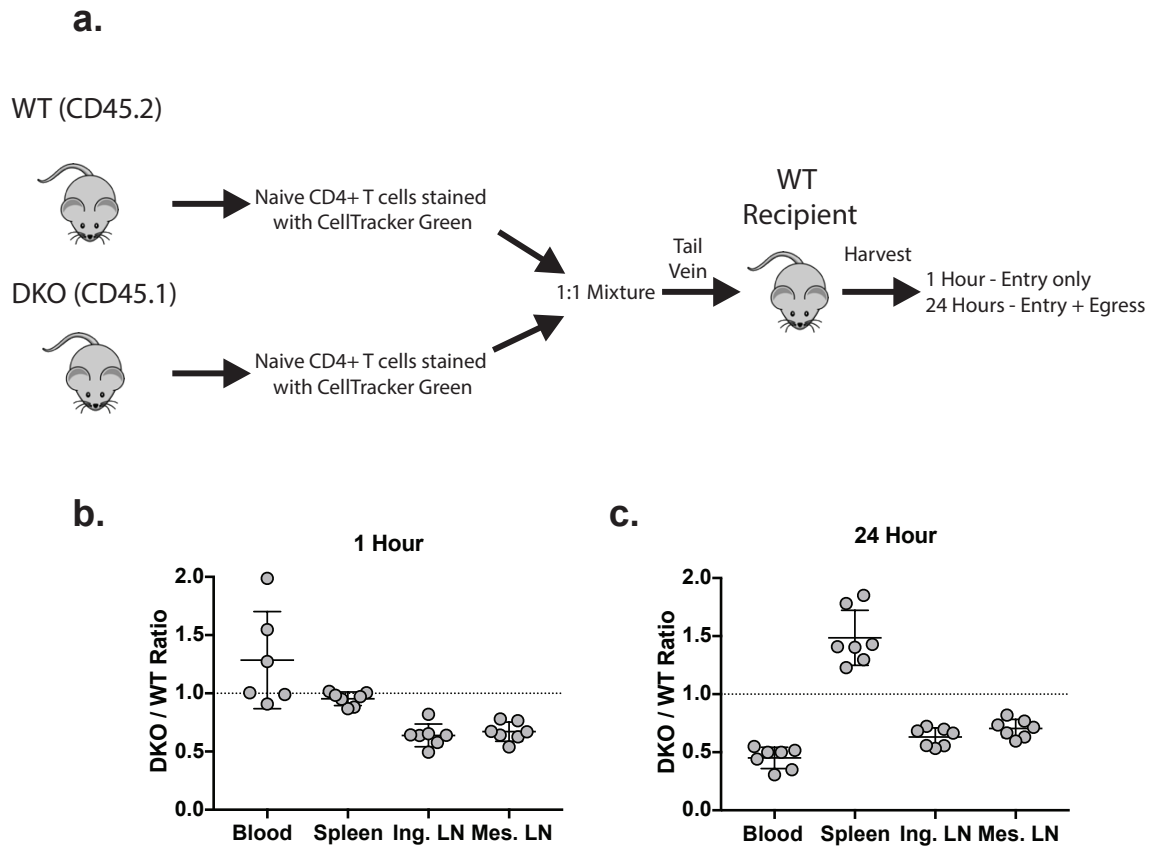


Figure 2.6 ERM-deficient T cells have a cell-intrinsic egress defect

(a) Competitive in vivo migration experimental design. CD45 congenic WT and DKO naïve CD4⁺ T cells labelled with CellTracker Green (CMFDA) were co-injected 1:1 into the tail vein of WT recipient mice and harvested from the blood or indicated organ 1 hour or 24 hours later. (b-c) The ratio of the number of transferred WT and DKO T cells isolated from blood, spleen, or lymph node at 1 hour (b) or 24 hours (c) post-transfer. Each dot corresponds to a recipient mouse, pooled from two independent experiments.

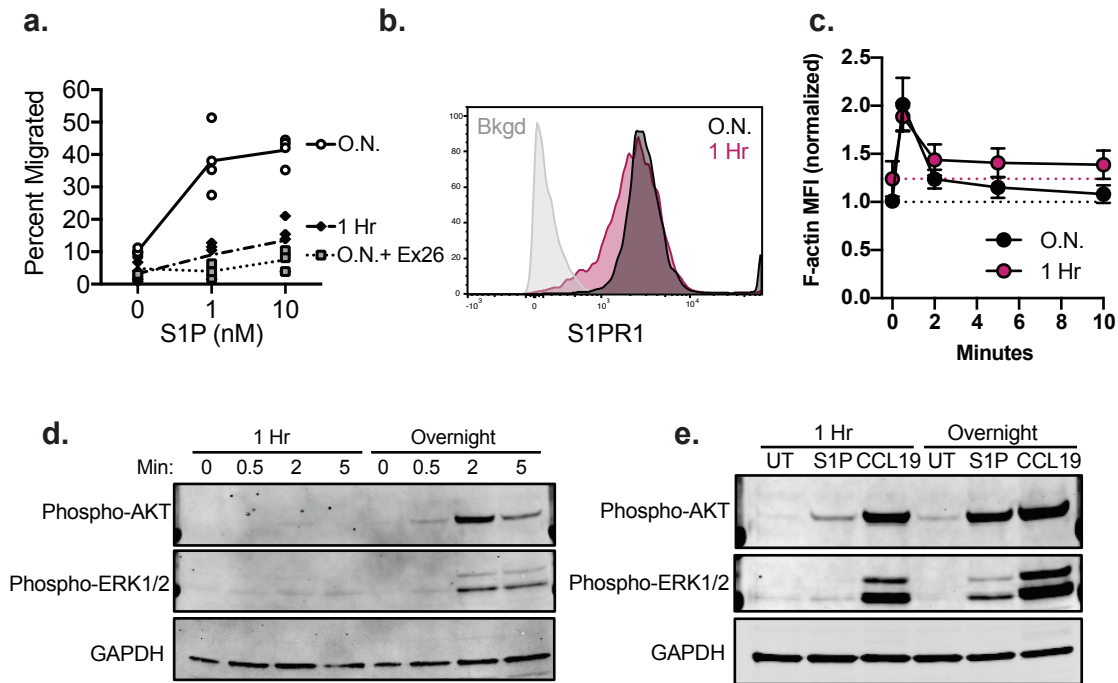


Figure 2.7 Overnight culture improves S1PR1 responses in T cells

Following isolation, naive CD4⁺ T cells were cultured either overnight (O.N) or for 1 hour (1 Hr) in media supplemented with 10% charcoal-stripped FBS. **(a)** Percent transmigration of O.N. or 1 Hr cells towards the indicated concentration of S1P in the bottom chamber of a transwell chamber. Cells in the Ex26 group were pretreated with 100 nM of the antagonist 20 minutes prior to the assay. Data pooled from 4 independent experiments. **(b)** Surface S1PR1 levels of O.N. and 1 Hr cells were determined by flow cytometry. Background (Bkgd) refers to cells stained without primary anti-S1PR1 antibody. Representative plot from 2 independent experiments. **(c)** O.N. and 1 Hr cells were stimulated with S1P for the indicated amounts of time, fixed with PFA, stained with fluorescently-conjugated phalloidin, and analyzed by flow cytometry. Data is normalized to untreated O.N. cells and pooled data from 3 independent experiments. **(d)** O.N. and 1 Hr cells were stimulated with S1P (1 nM), lysed after 0, 0.5, 2, or 5 minutes, and immunoblotted for phospho-Erk (Thr2020/Tyr204), phospho-Akt (Ser473), and GAPDH. Only performed once. **(e)** O.N. and 1 Hr cells were stimulated with S1P (1 nM) or CCL19 (100 ng/mL), lysed, and immunoblotted for phospho-Erk (Thr2020/Tyr204), phospho-Akt (Ser473), and GAPDH. Only performed once.

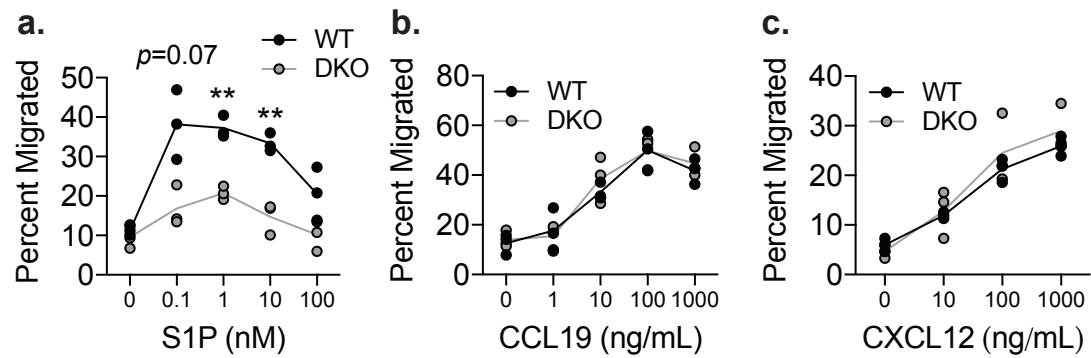


Figure 2.8 DKO T cells have a selective transmigration defect towards S1P.

(a-c) Percent transmigration of WT and DKO naïve CD4⁺ T cells cultured overnight to the indicated concentration of S1P (a), CCL19 (b), or CXCL12 (c) in the bottom chamber of a transwell chamber. Each data point represents one technical replicate from one experiment, representative of 3-5 independent experiments. WT and DKO transmigration means for each concentration of chemoattractant were compared with t-tests. * $p < 0.05$, ** $p < 0.01$.

CHAPTER 3: S1P ACTIVATES MYOSIN TO PROMOTE BLEB-BASED, ERM-GUIDED MOTILITY

3.1: Results

ERM proteins are dispensable for S1PR1 expression and endocytosis

After identifying that ERM deficiency results in a T cell-intrinsic egress defect and a corresponding defect in migration towards S1P, we next sought to determine how ERM proteins facilitate S1P responses. Since cell surface expression of S1PR1 and ligand-induced endocytosis are both known to impact S1P-dependent T cell egress [38, 39, 248, 249], we asked if ERM protein expression is required for these events. Across multiple secondary lymphoid organs, surface S1PR1 levels on naïve DKO CD4⁺ T cell were normal or slightly elevated (Fig. 3.1a). Surface S1PR1 expression also appeared normal in mature DKO thymocyte populations (Fig. 2.5c, e). Additionally, DKO T cells displayed low surface expression of S1PR1 when isolated from blood, a high S1P environment, indicating that receptor endocytosis *in vivo* is intact (Fig. 3.1a). To confirm that ERM proteins are dispensable for S1PR1 endocytosis, we treated cells with S1P *in vitro* for 30 seconds or 10 minutes, stained for surface S1PR1, and measured loss of receptor expression by flow cytometry. WT and DKO T cells showed similar surface levels of S1PR1 in culture, and no differences were detected in the efficiency or kinetics of endocytosis following S1P treatment (Fig. 3.1b-c). Thus, we conclude that receptor expression and ligand-induced internalization are intact in the absence of ERM proteins.

ERM proteins are dispensable for S1P-dependent signaling

Since ERM proteins interact with important signaling proteins at the PM [186], we asked if DKO T cells show signaling defects downstream of S1PR1 ligation. Studies on S1PR1 signaling in lymphocytes are lacking, but S1PR1 has been shown to signal through the PI3K/Akt and MAP Kinase pathways in other cell types [268, 286]. We stimulated WT and DKO T cells with S1P for various times and immunoblotted for phospho-Akt and phospho-Erk1/2. Both the magnitude and kinetics of signaling were similar for WT and DKO T cells (Fig. 3.1d). As a separate readout of S1PR1 signaling, we measured actin polymerization, and found no differences in the response of WT and DKO T cells (Fig. 3.1e-f). Treatment with the S1PR1 antagonist Ex26 effectively blocked actin polymerization, confirming the receptor specificity of this response (data not shown). Taken together, these studies show that ERM protein expression is not required for ligand-induced S1PR1 internalization or signaling.

S1P treatment induces rapid dephosphorylation and rephosphorylation of ERM proteins

Since S1PR1 appeared to be fully signaling-competent in DKO T cells, we considered alternative explanations for the transmigration defects observed. ERM proteins cycle between an activated conformation at the PM and an auto-inhibited head-to-tail conformation in the cytoplasm [173]. Activation is mediated by binding of the N-terminal FERM domain to PIP2 in PM, and by phosphorylation of a critical threonine residue in the C-terminal actin binding domain [181]. Chemokine receptor signaling in T cells promotes potent ERM dephosphorylation lasting 10-20 minutes, during which time the cell can undergo shape changes and molecular reorganization events needed for polarized cell motility [184, 217]. We asked if ERM proteins cycle differently in response to S1P stimulation. Interestingly, although both CCL19 and S1P induced ERM

dephosphorylation at 30 seconds, dephosphorylation was sustained in the CCL19-treated group, whereas S1P-treated cells showed rapid ERM re-phosphorylation between 2- and 5-minutes post stimulation (Fig. 3.2a-b). Thus, the ERM-dependent linkage of the actin cortex to the PM is largely intact during S1P but not chemokine responses.

S1P induces a rapid, highly transient mode of motility that depends on ERM proteins

To study the differences between S1P and chemokine induced migration, we developed a chemokinesis assay to visualize cell responses following chemoattractant stimulation. WT Naïve CD4⁺ T cells were added to chambers coated with vascular adhesion protein-1 (VCAM), and imaged for several minutes at which point S1P, CCL19, or CXCL12 was gently dripped into the chamber. Prior to stimulation, VCAM-bound cells mostly exhibited a rounded morphology. Addition of S1P induced a rapid burst of migration lasting only a few minutes, after which the cells rounded up and stopped moving (Supplemental Video 1). In contrast, both CCL19 and CXCL12 induced modest, but sustained, chemokinetic responses (Supplemental Videos 2, 3). Quantitative analysis of cell velocity confirmed this distinction; S1P induced strong, but short-lived responses that returned to baseline within 4-5 minutes whereas CCL19 and CXCL12 induced sustained migration (Fig. 3.3a). These distinct modes of motility are reflected in the kinetics of F-actin polymerization, which is short-lived in S1P-stimulated cells and sustained for at least 20 minutes in cells treated with CCL19 (Fig. 3.3b-c). Importantly, during the time when S1P treated T cells exhibit maximal motility (approximately 2 minutes after stimulation, Fig 3.3a), ERM protein phosphorylation has already returned

to significant levels (Fig. 3.2). This contrasts with chemokine-stimulated cells, where phospho-ERM protein levels remain low during migratory responses (Fig 3.2).

We next used this chemokinesis assay to conduct side-by-side analysis of WT and DKO T cells. We first quantified the number of cells that migrate in response to each chemoattractant, using a threshold of at least 10 microns of displacement. Similar to the transwell data (Fig 2.8a), fewer DKO T cells migrated in response to S1P (Fig 3.4a, Supplemental Videos 1, 4), whereas the frequency of DKO cells migrating to CCL19 and CXCL12 was normal (Fig. 3.4 b). Among the cells that did move at least 10 microns, DKO T cells showed reduced displacement and directionality in response to S1P (Fig. 3.4c, e), but not in response to CCL19 or CXCL12 (Fig. 3.4d, f). These selective defects in displacement and directionality are readily observed in plots of cell tracks (Fig. 3.4g-h).

S1P induces pressurized, bleb-based migration

When quantifying WT and DKO T cell dynamics, we observed that although WT cells responding to S1P and chemokines exhibited similar morphologies at early time points, their behavior differed dramatically after the first 2-3 minutes. Prior to stimulation, cells were rounded and poorly migratory (Fig. 3.5a-b, Pre-treat). Immediately after stimulation with either S1P or chemokine (CXCL12 and CCL19 promoted similar responses), T cells showed prominent membrane ruffling coincident with a burst of actin polymerization (Fig. 3.5a-b, Ruffle, Fig. 3.3b-c). Both sets of cells then polarized and began actively migrating. During this initial migratory phase (Fig. 3.5a-b, Lamellipodial), both sets of cells exhibited broad, flat lamellipodia at the leading edge (arrowheads), and a refractile uropod at the rear. For chemokine-stimulated cells, this morphology was

maintained throughout the course of the assay. In contrast, S1P-stimulated cells transitioned after 2-3 minutes from a lamellipodial mode of motility to one associated with prominent membrane blebbing. Blebbing continued until the end of the migratory response, approximately 5 minutes after stimulation (Fig 3.5a, Bleb-based, Supplemental Videos 5, 6). Blebs are sites of temporary PM separation from the actin cortex [128, 152, 287]. By DIC microscopy, they appear as rapidly-forming balloon-like protrusions (Fig. 3.5c). Blebs are highly transient in migrating cells, since actin-rich structures fill the space within seconds. Enumeration of these structures revealed that S1P stimulation drove a substantial increase in blebbing over unstimulated cells (control), whereas chemokine stimulation did not (Fig. 3.5d).

Unlike lamellipodia, blebs are pressure-driven protrusions [287]. Intracellular pressure is regulated primarily by actomyosin contractility [97]. To determine if S1P was driving bleb-based migration through enhanced myosin activity, we treated cells with either S1P or CCL19 and immunoblotted for phosphorylation of myosin light chain at Thr18/Ser19. Phosphorylation at these sites enhances ATPase activity of the catalytic head domain of myosin heavy chain and promotes contractility [115-117]. We also probed for AKT phosphorylation as a positive control. S1P and CCL19 both drove significant AKT phosphorylation at 0.5 minutes to similar degrees, but this response was highly transient for S1P treated relative to CCL19 (Fig. 3.6a, b). As AKT phosphorylation diminished, S1P-treated cells showed enhanced MLC phosphorylation peaking at 3.5 minutes post-stimulation (Fig. 3.6a, c), a time point that corresponds to high levels of blebbing in the chemokinesis assay (Fig. 3.5a). CCL19 did not drive any elevation in MLC phosphorylation, but did result in a substantial decrease at 0.5 minutes (Fig 3.6 a, c).

To determine if this myosin activation resulted in heightened intracellular pressure that could be used to drive bleb formation, we utilized the servo-null micropressure method, which uses a microelectrode to penetrate the cell membrane and directly quantify cytoplasmic pressure, to determine intracellular pressure in T cells [288]. Cells were left untreated (none) or stimulated with either S1P or CCL19, and intracellular pressure was determined. As shown in Fig. 3.6d, S1P stimulation resulted in a significant elevation in intracellular pressure, whereas CCL19 stimulation did not. To determine whether this pressure increase was dependent myosin activity, we treated the cells with the myosin inhibitor blebbistatin (BBS) prior to S1P stimulation. Treatment with BBS alone in resting cells resulted in a significant drop in pressure, consistent with a well-described homeostatic role for myosin contractility in regulating pressure [97]. Even with their lowered starting values, BBS-treated T cells did not elevate their intracellular pressure in response to S1P, indicating that myosin activity is necessary for S1P-induced pressurization. To determine if myosin inhibition also prevented bleb-formation, we repeated the chemokinesis assay in the presence or absence of BBS and quantified bleb formation. As shown in Fig 3.6e, S1P induced prominent blebbing, but these protrusions were potently inhibited by pre-treatment with BBS. Collectively, these data indicate that S1P activates myosin to drive pressurized, bleb-based migration and that this migratory response is fundamentally different from the responses elicited by CCL19 or CXCL12.

ERM proteins facilitate migration by limiting blebs to the leading edge

ERM proteins, which link the PM to the actin cortex, are known to play an important role in bleb prevention and resolution [137]. We therefore compared bleb formation in WT and DKO T cells during S1P-induced migration. At early times after S1P

addition, WT and DKO cells ruffled, polarized, and began to migrate similarly (Fig. 3.7a). However, when the transition to blebbing occurred, WT T cells primarily displayed blebbing at or near the leading edge, whereas DKO T cells showed indiscriminate blebbing all around the cell body (Fig. 3.7a, asterisks, Supplemental Videos 7, 8). To quantify this, cells were divided into thirds along the axis of migration (rear, middle, and front), and the front third was further divided into “front” and “lead” to distinguish blebs that occur strictly at the leading edge. Examples of blebs occurring in each region are shown in Figure 3.7b. Videos of WT and DKO T cells were then analyzed for the bleb frequency within each region. Blebbing in the rear third of the cell was rarely observed in either cell population. In WT T cells, blebbing was progressively more frequent in the regions closer to the leading edge (Fig. 3.7c). Relative to WT cells, DKO T cells showed elevated blebbing in the middle region and reduced blebbing at the leading edge (Fig. 3.7c). In WT T cells, bleb area also increased with proximity to the leading edge, with a particularly sharp increase between the middle and front/lead regions (Fig. 3.7d). In contrast, blebs in DKO T cells were large irrespective of location (Fig. 3.7d). This inability to spatially regulate bleb frequency and size likely contributes to the profound directionality defects displayed by DKO T cells responding to S1P (Fig. 3.4e).

Finally, we asked how the location of ERM proteins within the cell relates to directional blebbing. WT T cells bound to VCAM were stimulated with S1P for 1, 2.5, or 5 minutes, after which they were fixed, labeled for phospho-ERM proteins and counterstained for tubulin to identify the centrosome, which is positioned in the rear of migratory lymphocytes. Consistent with the western blot data (Fig. 3.2), S1P drove an initial dephosphorylation of ERM proteins that recovered after 2.5-5 minutes. At 2.5 minutes, when cells are highly migratory and beginning to bleb, phosphorylated ERM

proteins primarily localized to the rear of the cell; labeling diminished gradually within the middle region and was largely absent from the front third of the cell (Fig. 3.7e-f). By five minutes post-stimulation, when cells have rounded up and ceased migration, active ERM proteins were found all around the cell cortex. Importantly, the regions where ERM proteins accumulate in WT cells correspond to regions of low bleb frequency. These are the same regions that show elevated blebbing frequency and size in DKO T cells. Taken together, these results show that ERM proteins in T cells are largely dispensable for lamellipodial migration, but play a critical role in facilitating polarized protrusions during bleb-based migration.

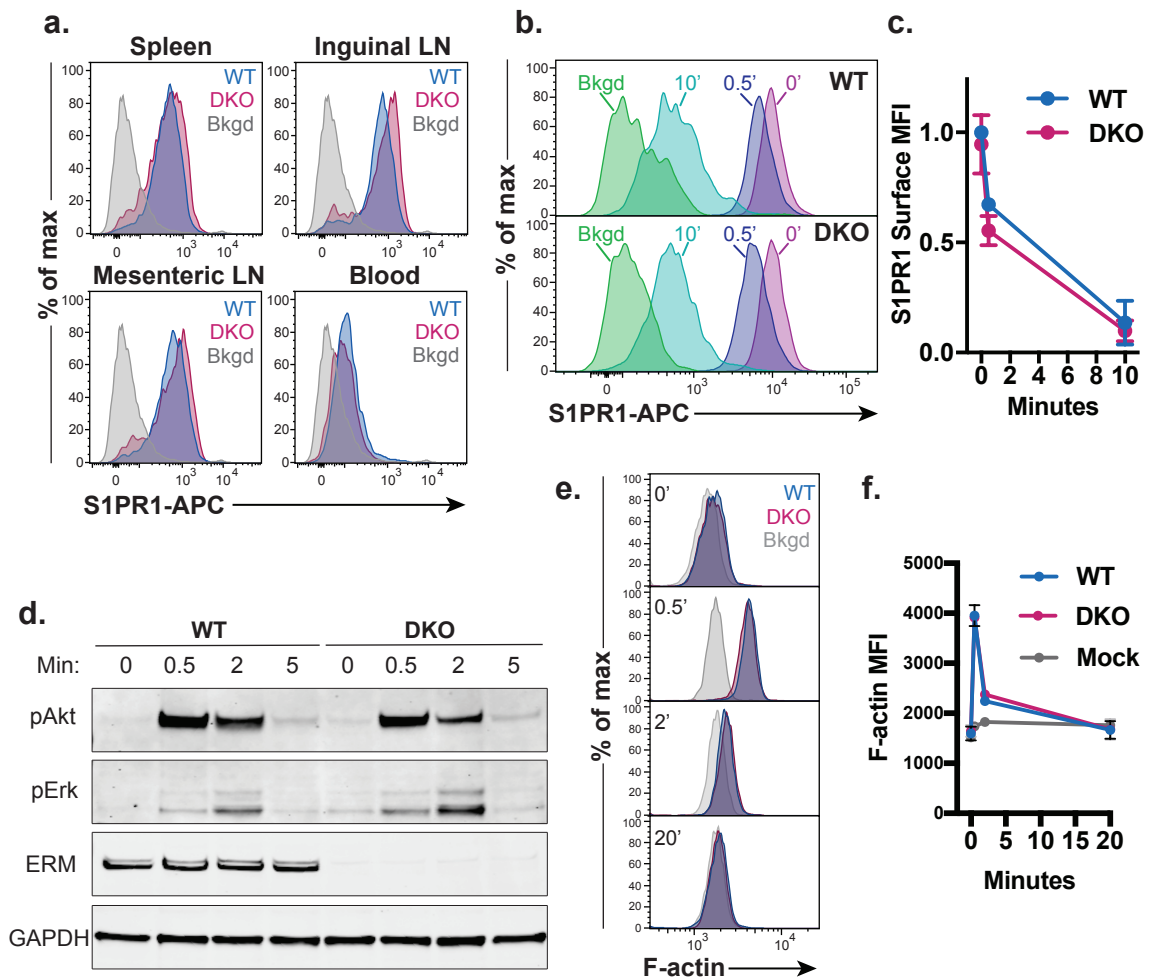


Figure 3.1 ERM proteins are dispensable for S1PR1 expression, endocytosis, and signaling.

(a) Ex vivo surface expression of S1PR1 on WT and DKO naïve CD4⁺ T cells (gated on Live, CD4⁺, CD62L^{Hi} CD44^{Low}) from the spleens, lymph nodes, and blood. Bkgd refers to WT CD4⁺CD8⁺ thymocytes stained in parallel. Representative flow panels from 3 independent experiments shown. **(b-c)** Ligand-induced S1PR1 endocytosis. WT and DKO naïve CD4⁺ T cells were stimulated with S1P (10 nM) for 0, 0.5, or 10 minutes, stained for surface S1PR1, and analyzed by flow cytometry. Bkgd refers to cells stained without primary anti-S1PR1 antibody. Pooled data from 4 independent experiments normalized to WT levels prior to stimulation are shown as means \pm StdDev and compared at each time point using an t-tests and the Holm-Sidak correction for multiple comparisons. **(d)** S1P-induced signaling. WT and DKO naïve CD4⁺ T cells were stimulated with S1P (1 nM), lysed after 0, 0.5, 2, and 5 minutes, and immunoblotted for phospho-Erk (Thr202/Tyr204), phospho-Akt (Ser473), total ERM proteins, and GAPDH. Blot representative of 3 independent experiments. **(e-f)** S1P-induced actin polymerization. WT and DKO naïve CD4⁺ T cells cultured were stimulated with S1P (1 nM) for 0, 0.5, 2, or 20 minutes, fixed, stained with phalloidin-AF488, and analyzed by flow cytometry. Representative plots and pooled data from four independent experiments shown as means \pm StDev and compared at each time point using multiple t-tests with the Holm-Sidak correction for multiple comparisons. No statistically significant differences were observed between WT and DKO T cell responses.

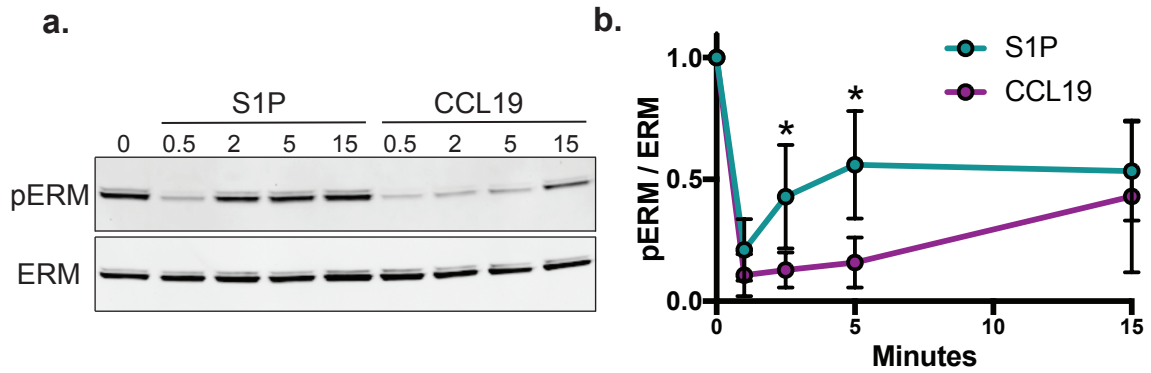


Figure 3.2 S1P-induced ERM inactivation is short-lived relative to chemokine
(a-b) ERM dephosphorylation and rephosphorylation. WT naïve CD4⁺ T cells were stimulated for 0, 0.5, 2, 5, or 15 minutes with S1P (100 nM) or CCL19 (100 ng/mL), lysed, and immunoblotted for phospho-ERM (Thr558 for moesin) and total ERM. Quantified band intensities displayed as the phospho/total ratio pooled from five independent experiments. Means for the S1P and CCL19 group compared at each time point using a multiple t-tests and the Holm-Sidak correction for multiple comparisons. *p<0.5

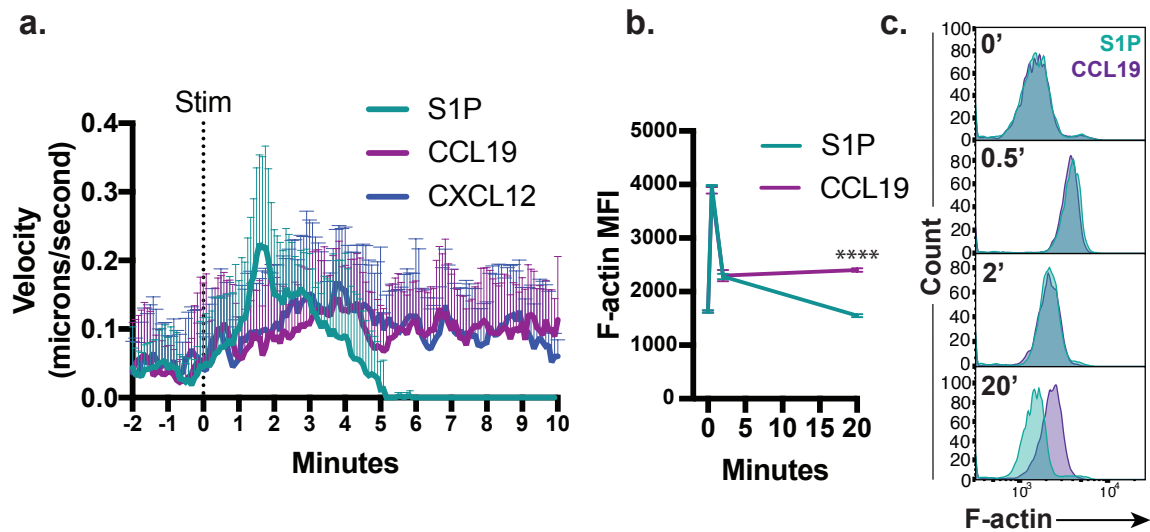


Figure 3.3 S1P promotes a rapid, highly transient mode of migration

(a) Instantaneous velocity following S1P or chemokine stimulation. WT naïve CD4⁺ T cells were imaged by DIC microscopy before and after stimulation with S1P (100 nM), CCL19 (100 ng/mL), or CXCL12 (100 ng/mL), and manually tracked at one-second intervals. Instantaneous velocities were smoothed over 5-second windows. Averages + StDev for twelve representative cells per condition are shown. **(b-c)** Actin polymerization kinetics following S1P vs Chemokine stimulation. WT naïve CD4⁺ T cells cultured overnight were stimulated with S1P (1 nM) or CCL19 (100 ng/mL), fixed after 0, 0.5, 2, or 20 minutes, stained for F-actin, and analyzed by flow cytometry. Representative data from three independent experiments shown with representative flow plots (gated on CD4⁺ singlets).

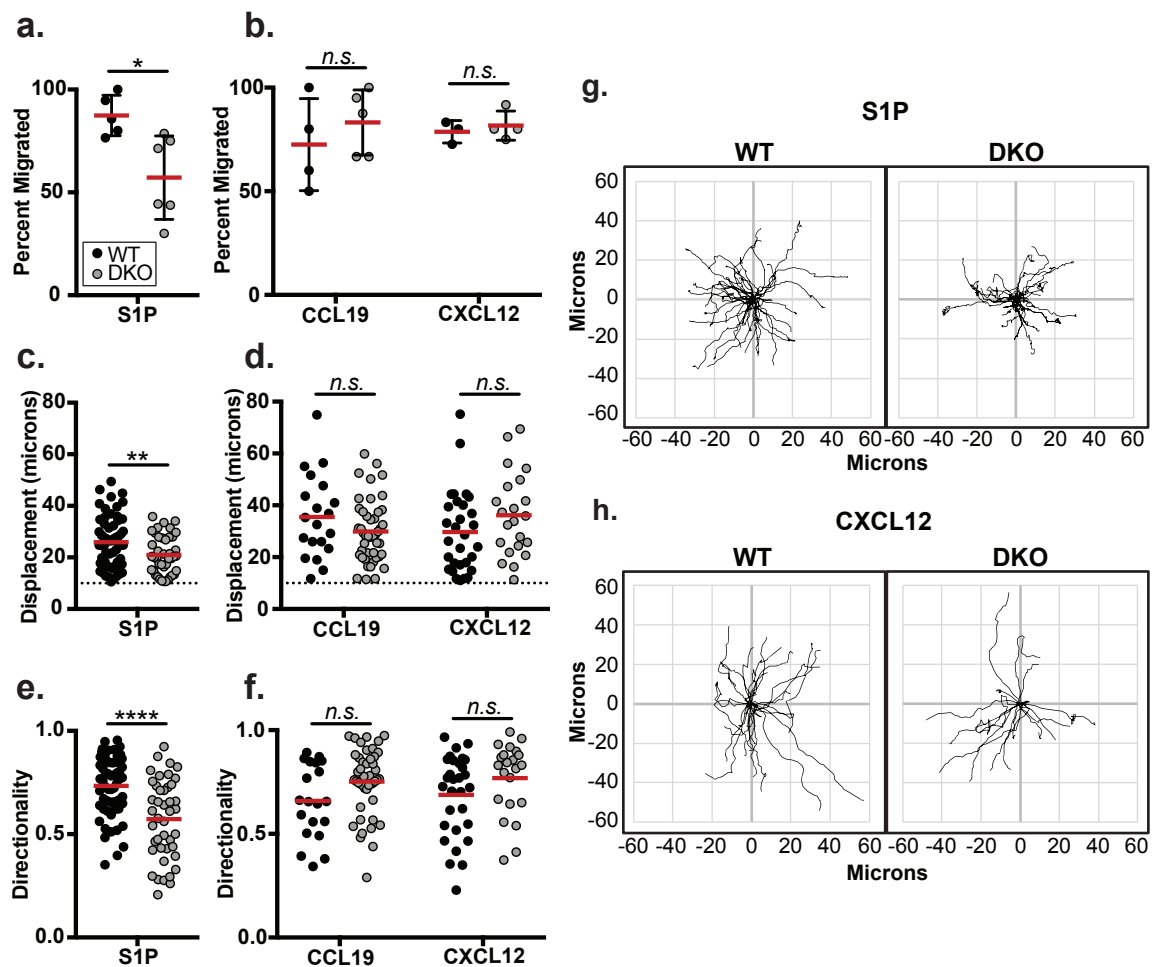


Figure 3.4 ERM proteins are required for S1P-induced chemokinetic responses

Migration of WT and DKO naïve CD4⁺ T cells in response to S1P or chemokine. Cells were added to VCAM-coated chambers and monitored by DIC microscopy following stimulation with S1P (100 nM), CCL19 (100 ng/mL), or CXCL12 (100 ng/mL). **(a-b)** Percentage of cells that displace at least 10 microns during the response. Each dot corresponds to a field of cells pooled from three independent experiments shown. Mean \pm Std Dev shown and compared individually using t-tests. **(c-d)** Displacement of WT and DKO migratory cells following S1P or chemokine stimulation. Dashed lines show 10-micron threshold for analysis from (a-b). **(e-f)** Directionality of migratory WT and DKO cells. Directionality was calculated by dividing displacement by total track length. For (c-f), pooled data from three independent experiments displayed as individual cells (dots) and means (horizontal bars) and compared using Mann-Whitney (non-parametric) t-tests. * $p < 0.05$, ** $p < 0.01$, **** $p < 0.0001$ **(g-h)** Tracks of individual cells with the same origin are shown, representative of three individual experiments.

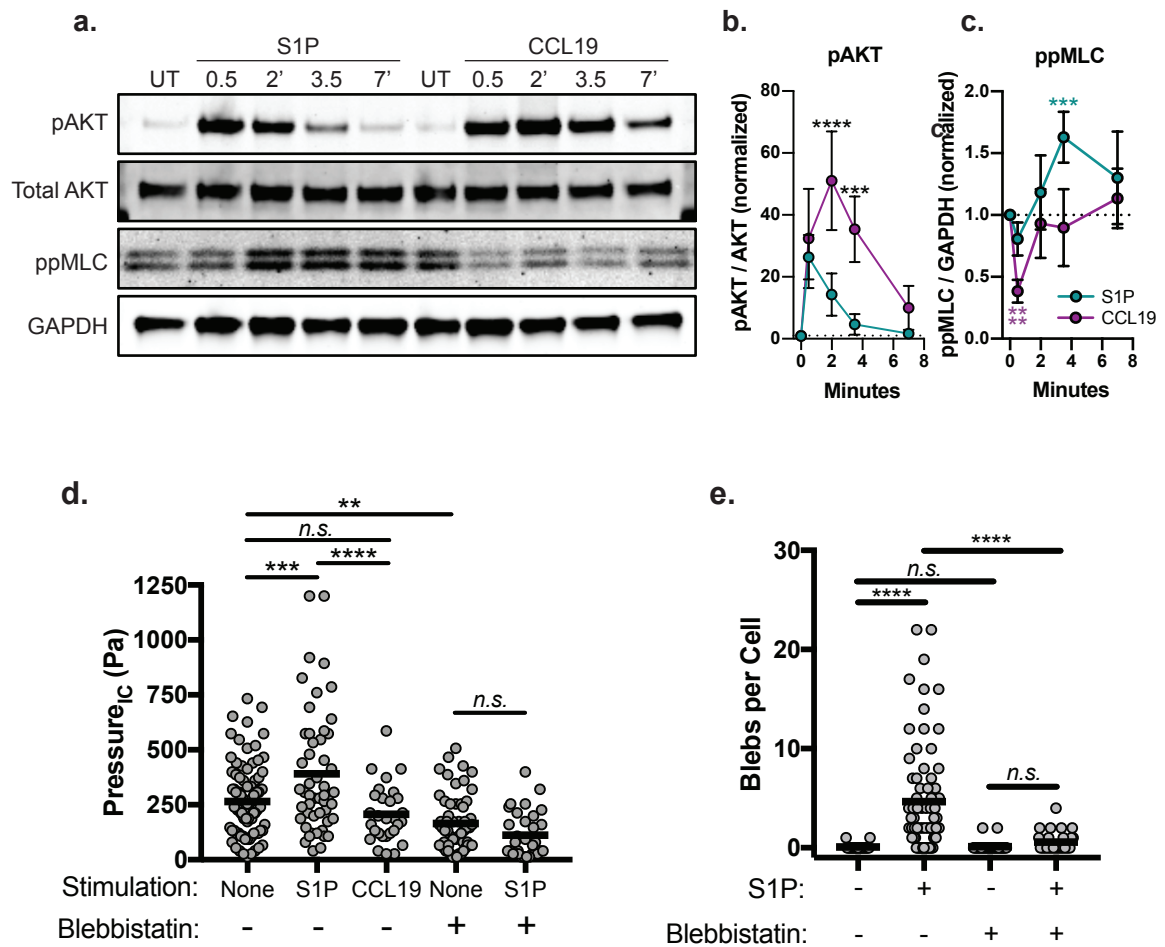


Figure 3.6 S1P activates myosin to drive intracellular pressurization and bleb-based migration

(a-c) WT naïve CD4⁺ T cells were stimulated with S1P (1 nM) or CCL19 (100 ng/mL) for 0, 0.5, 2, 3.5, or 7 minutes and immunoblotted for phospho-AKT (pAKT; Ser473), total AKT, phospho-myosin light chain (ppMLC; Thr18/Ser19), and GAPDH. A representative blot (a) is shown with quantitation pooled from four independent experiments (b-c). S1P vs CCL19 AKT phosphorylation (b) was compared using a two-way ANOVA with a Sidak correction for multiple comparisons. (c) Activation of myosin was determined using a one-sample t test to determine if normalized ppMLC/GAPDH levels were significantly different from a hypothetical mean of 1. (d) Intracellular pressure following S1P or chemokine stimulation. WT naïve CD4⁺ T cells were added to PLL-coated plates and left untreated or stimulated with S1P (100 nM) or CCL19 (100 ng/mL), and pressure was measured by the servo null method between 0-12 minutes of stimulation. Where indicated, blebbistatin (50 micromolar) was added at least 30 minutes prior to stimulation and pressure measurement. Each dot corresponds to a cell, pooled from 4 independent experiments. Means (horizontal bars) of the S1P and CCL19-treated groups compared to control using a Kruskal-Wallis One-way ANOVA. (e) Bleb quantitation following S1P or chemokine stimulation as in fig 3.5. Blebs were manually counted from DIC movies of control or S1P-stimulated (100 nM) cells on VCAM. Where indicated, cells were pre-treated with s-nitro-blebbistatin (5 micromolar) at least 10 minutes prior to stimulation and imaging. Each dot corresponds to a cell pooled from one experiment. Means (horizontal bars) of S1P, CCL19, and CXCL12 groups compared to control using a Kruskal-Wallis One-way ANOVA. **p < 0.01, ***p < 0.001, ****p < 0.0001

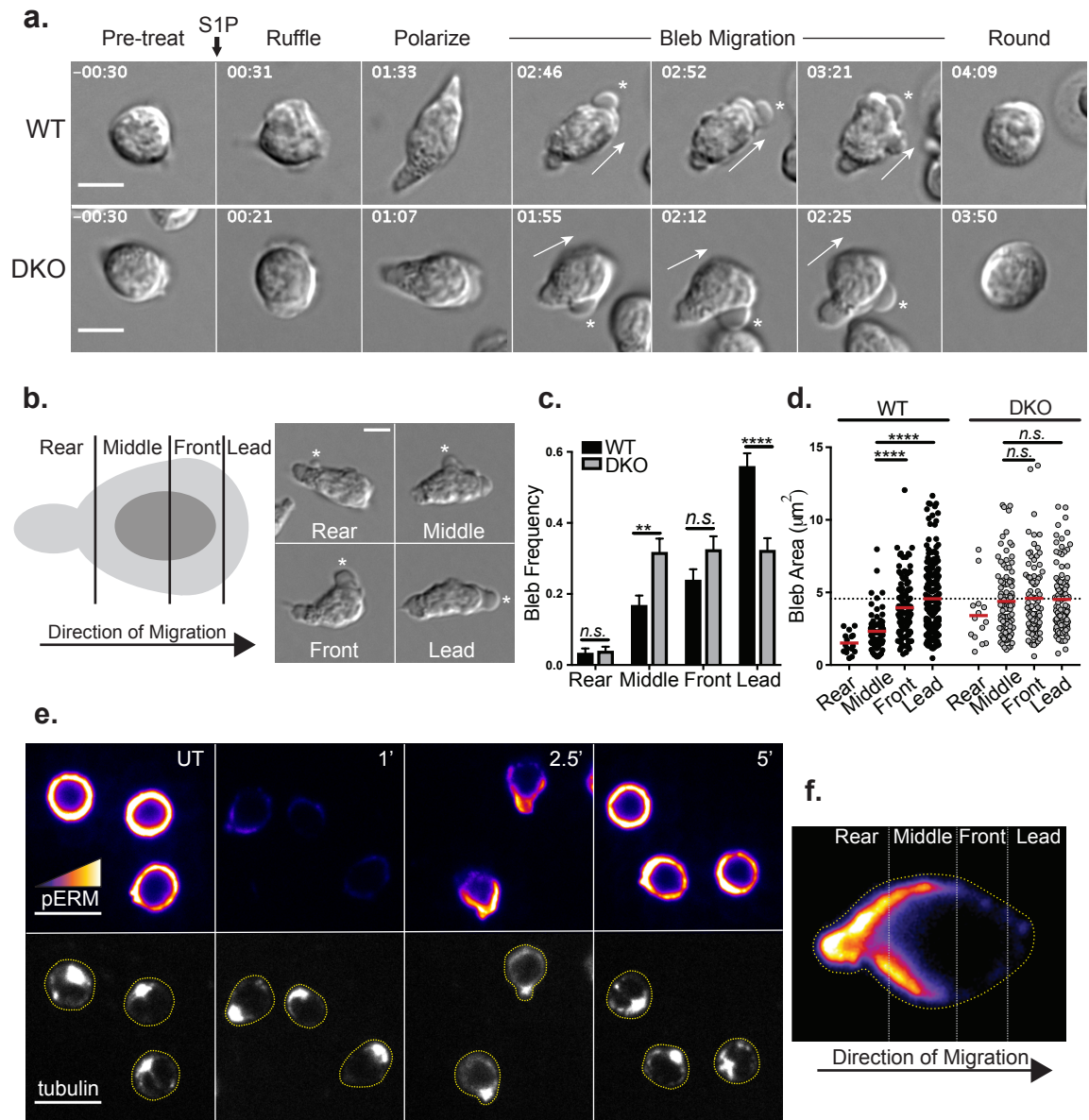


Figure 3.7. ERM proteins facilitate S1P-induced migration by limiting blebs to the leading edge. (a) Representative S1P-induced bleb-based migration for WT and DKO naive CD4⁺ T cells. Cells were imaged by DIC microscopy before and after stimulation with S1P (100 nM). Full arrows = direction of migration, asterisks = blebs. Time in mm:ss relative to S1P stimulation. Scale bar = 5 microns. (b) An illustration depicting a cell divided along the axis of migration and an example of S1P-induced blebs occurring in each region (asterisks). Scale bar = 5 microns. (c-d) Bleb frequency and area along the axis of migration. Individual cells were tracked during S1P-induced migration, and blebs were binned into the appropriate region and area was measured. (c) More than 50 cells pooled from three independent experiments shown as the mean \pm SEM compared using multiple t-tests and the Holm-Sidak correction for multiple comparisons. (d) Each dot corresponds to an individual bleb (>300 per group), and means compared (red horizontal bars) using a Kruskal-Wallis one-way ANOVA. **p < 0.01, ****p < 0.0001. Dashed line at WT lead mean. (e) Active ERM protein localization during S1P migratory responses. WT naive CD4⁺ T cells were stimulated with S1P, fixed at the indicated time (minutes), stained for phospho-ERM proteins (top) and tubulin (bottom), and imaged by confocal fluorescence microscopy. UT = untreated, scale bar = 10 microns. Cells outlined in yellow in tubulin channel. Representative images from 3 independent experiments. (f) A representative cell from the 2.5-minute time point in (e) enlarged and oriented in the same direction as (b).

CHAPTER 4: DISCUSSION

4.1 Summary and Reconciliation with Previous Work

The experiments detailed in this dissertation show that S1P promotes a mode of cell motility in T cells that is fundamentally different from the response elicited by chemokines. Rather than relying solely on actin polymerization-based lamellipodial migration, S1P promotes pressurization and blebbing, a mode of migration typically reserved for cells tasked with migrating in confinement. During this bleb-based migratory response, ERM proteins localize to the rear and sides of polarized T cells where they tether the membrane to the underlying actin cortex to limit bleb formation. This process restricts blebbing to the leading edge, thereby promoting forward movement of the cell. ERM-deficient T cells show dysregulated blebbing, resulting in compromised chemokinetic and transmigration responses towards S1P *in vitro* and defective egress from lymphoid tissues *in vivo* (modelled in Fig. 4.1).

The phenotypes of our MKO and DKO mice are essentially identical to those of MKO mice independently derived by Hirata et al [224]. They also report lymphocyte increases in the spleen, decreases in the lymph nodes, severe decreases in the blood, and an accumulation of mature single positive thymocytes in the thymus [224]. While T cells in these animals are ezrin-replete, our own data confirms that moesin deficiency alone causes perturbations in T cell trafficking, despite the functionally overlapping roles typically played by ERM proteins (Fig 2.3). In our hands, many of the trafficking phenotypes observed in the MKO mice, including lymphocyte reductions in the blood and lymph nodes are worsened by loss of ezrin (Fig 2.3). These data point towards functional overlap between ezrin and moesin in T cell trafficking, but with moesin playing

a more important role. This is likely due to the higher expression levels of moesin in T cells (Fig 2.1). Hirata et al. further pinned down the cell-intrinsic egress defect by using integrin-blocking antibodies to stop lymph node entry and show that moesin-deficient T cells display significantly lowered egress rates from lymph nodes and the spleen alike. With the cell-intrinsic egress defect well-established by our work and that of Hirata et al., I focused most of my efforts on understanding the cellular and molecular biology behind this egress defect.

Hirata et al. report that MKO T cells show defective actin polymerization in response to S1P, and a follow-up report by the Hirata group (Nomachi et al. [289]) finds that moesin is required for S1PR1 endocytosis. Curiously, Nomachi et al., in direct contradiction to the previous paper, shows that MKO T cells display *enhanced* transmigration towards S1P. This enhancement is observed without any drug treatment, but is made more prominent when WT and MKO T cells are isolated from mice treated with FTY720, an S1PR1 functional antagonist that works by driving sustained S1PR1 internalization and subsequent unresponsiveness to S1P [289]. No attempts were made to resolve this contradiction; indeed, the first paper is cited only in regard to the generation of the moesin knockout mouse. Like the initial Hirata paper, we show that ERM-deficient T cells display *diminished* S1P transmigration (Fig 2.8). In our hands, ERM deficiency had no effect on resting surface S1PR1 levels, consistent with the initial Hirata paper (Fig 3.1). Moreover, our quantitative analysis showed no change in the magnitude or kinetics of ligand-driven receptor endocytosis or actin polymerization (Fig 3.1). The basis for these discrepancies is unclear, but one major difference is our use of an optimized overnight cell culture protocol, which results in robust responses more suitable for quantitative analysis (Fig. 2.7).

Poor *in vitro* responses to S1P have long plagued the T cell field, and our overnight culture approach allowed us to address fundamental questions about S1P-induced T cell migration. In the sections that follow, I address two major questions that emerge from my work. First, how does S1PR1 instruct such a profoundly different migratory response than the chemokine receptors tested in this report (4.2)? Second, among the various protrusions a T cell can make, are blebs particularly well-suited for passage through specialized endothelial layers during egress (4.3)?

4.2 S1PR1 vs Chemokine Receptor Signaling

One of the major findings from my work is that chemokines prompt lamellipodial migration in T cells, whereas S1P prompts initial lamellipodial migration followed by subsequent myosin-dependent bleb-based migration. S1PR1, CCR7, and CXCR4, the receptors tested in my experiments, are all GPCRs, but S1PR1 belongs to the *Edg* family of GPCRs along with other S1P and LPA receptors, whereas CCR7 and CXCR4 are both members of the chemokine receptor family. Chemokines, by definition, are proteins [290], whereas both S1P and LPA are lipids. While S1PR1 is commonly lumped in with the chemokine receptors during discussions of T cell trafficking, it is worth noting that phylogenetic analysis of *Edg* and chemokine receptor families reveals these two groups are evolutionarily distinct from one another [291, 292]. Despite these genetic differences, side-by-side comparisons of cellular responses following *Edg* vs chemokine receptor ligation are rare. All of these GPCRs transmit signals by coupling to heterotrimeric G proteins, which are typically classified by their alpha subunits. These alpha subunits are organized into four distinct families: $G\alpha_s$, $G\alpha_i$, $G\alpha_q$, and $G\alpha_{12}$ [293]. S1PR1, CCR7, and CXCR4 all associate with and signal through $G\alpha_i$ under normal circumstances [294-299]. As expected, knockout of $G\alpha_i$ or inhibition with pertussis toxin

potently interferes with numerous aspects leukocyte trafficking and chemotaxis, including S1PR1- and CCR7-dependent processes for T cells *in vivo* [300-304].

While $G\alpha_i$ appears to be crucial for the signaling of all three receptors, it remains unclear how the same G alpha protein could mediate the diverse effects observed following S1PR1 vs CCR7/CXCR4 ligation. In addition to signaling through G alpha proteins, GPCRs can also signal through GRK family proteins, which phosphorylate the intracellular tail of activated receptors [305]. Classically, the GRK-mediated phosphorylation of active GPCRs and their subsequent arrestin-mediated endocytosis is associated with signal termination [306-308]. However, more recent data indicate that GRK proteins can influence and sustain GPCR-dependent signaling by serving as a protein scaffold [309]. This phenomenon is almost exclusively studied outside the context of either leukocytes or cell migration, so there is limited evidence to suggest that differential GRK usage between S1PR1 and CCR7/CXCR4 receptors mediates the different responses elicited by each receptor detailed in this report. That being said, the existing data points towards some interesting differences. First, unlike for $G\alpha_i$, CCR7 and CXCR4 utilize a different GRK protein than S1PR1. CCR7 and CXCR4 are both phosphorylated by GRK6 under most circumstances [310-312], whereas S1PR1 utilizes GRK2 [248]. GRK6 and GRK2 are in different subfamilies and localize to active GPCRs at the PM by completely different mechanisms: GRK6 is palmitoylated and therefore membrane-bound, whereas GRK2 is cytoplasmic and binds to $\beta\gamma$ subunits that have dissociated from $G\alpha_i$ following activation [309, 313-315]. Deletion of GRK6 enhances or prolongs chemokine receptor signaling for CCR7 and CXCR4 [311, 312]. A similar enhancement has been reported for S1PR1 in T cells deficient in GRK2 for *in vitro* migratory responses, but it is worth noting that GRK2-deficiency results in lymphopenia,

which is more suggestive of defective S1PR1 function *in vivo* [248]. The existing data points towards some potentially important differences in GRK protein function downstream of S1PR1 vs CCR7/CXCR4, but dedicated studies are required to determine what impact, if any, these have on the mode of motility elicited by ligation of these different receptors.

An important component of dissecting differential GPCR function will be to look directly at Rho GTPase activation. GPCRs that modulate cell migration typically exert their effects through the activation of the Rho superfamily of small GTPases, which include the Rac, Rho, and Cdc42 subfamilies. Classically, Rac activity is necessary for lamellipodia formation, Cdc42 for filopodia formation, and Rho for contractility [316-319]. For T cells, chemokine receptor signaling typically activates Rac, while S1PR1 signaling activates Rho but not Rac [320]. These authors measured Rac activation at 2-minutes post-stimulation, so it is presently unclear if S1P does not activate Rac or if the authors simply measured too late [320]. Time course studies looking at Rac vs Rho activation following S1P and chemokine stimulation are warranted. While we did not specifically measure Rac or Rho activation, the literature is consistent with our data showing that CCL19 and CXCL12 promote lamellipodia formation and S1P promotes myosin-dependent blebbing (Fig 3.5). Interestingly, LPA signaling through the receptor Lpar2 also promotes robust Rho activation in T cells [321], indicating that Rho activation may be a common feature of *Edg* family receptors in T cells.

Notably, S1PR1-dependent activation of Rho is not observed in most cell systems. In Chinese hamster ovary epithelial cell lines (CHO) [322], primary human umbilical vein endothelial cells (HUVECs) [323-325] and megakaryocytes [266], S1PR1 activates Rac, often without any detectable Rho activation. Yet in some cell lines,

S1PR1 drives modifications of cell-cell adhesions through Rho and not Rac [326]. This differential activation of Rac and Rho through S1PR1 in various cell types may help to explain why S1PR1 ligation results such disparate biological outcomes for different cell types, as detailed in the Introduction. One group has attributed these Rac/Rho discrepancies to different S1PR1 expression levels among different cell types or experimental conditions [327], but I propose here an alternative explanation: endocytosis of the receptor.

Classically, GPCR endocytosis is associated with signal extinction, but recent reports have shown that some GPCRs not only continue to signal following ligand-induced internalization but engage different signaling cascades from intracellular organelles than they do from the plasma membrane [269]. S1PR1 has been shown to signal for hours from endosomes in CHO cells when stimulated with the agonist FTY720 [268]. However, prolonged endosomal signaling in this study is likely secondary to the fact that FTY720 cannot be degraded easily by cells through normal S1P lyase-dependent mechanisms [328]. Still, the natural ligand S1P has been shown to both ligate and activate S1PR1 in endosomes in HeLa cells in the context of endosomal maturation [273]. Whether endosomal S1PR1 signals in T cells is unknown. Notably, T cells appear much more sensitive to ligand-induced S1PR1 endocytosis than endothelial cells [267]. Therefore, S1PR1 signaling differences at the PM vs endosomes could begin to explain and reconcile the aforementioned Rho GTPase data in T cells vs other cell types as well as the different biological outcomes mediated by S1PR1.

In further support of this hypothesis are our data showing that S1PR1 doesn't immediately promote blebbing, but instead drives a delayed lamellipodia-to-bleb transition. If S1PR1 switched from signaling through Rac at the PM to signaling through

Rho in endosomes, it would explain why S1P-stimulated T cells first utilize lamellipodia and only transition to myosin-dependent blebbing after 2-3 minutes, when the receptor is mostly internalized (Fig 3.1, 3.5, 3.6). This mechanism could also explain why GRK2-deficient T cells are hyper-responsive to S1P in transwell assays, but potentially defective at actual *in vivo* egress [248]. Sustained Rac activation at the plasma membrane may be sufficient for migration through transwell pores, as this would mimic a CCR7 response, but if subsequent activation of Rho by internalized S1PR1 was critical for actual passage through lymphatic endothelial cells *in vivo*, it would create an *in vitro* vs *in vivo* discrepancy like the one observed [248]. Although I was unable to address this particular hypothesis during my thesis work, other members of the Burkhardt lab are currently doing so by using inhibitors of clathrin-mediated endocytosis to elucidate the role of S1PR1 subcellular localization on signaling and T cell migratory responses.

In summary, the signaling and cellular responses elicited by S1PR1 in T cells is simultaneously distinct from chemokine receptors in T cells and from S1PR1 in endothelial cells. Despite using the same G alpha protein, S1PR1 and CCR7/CXCR4 elicit fundamentally different migratory response in T cells, with S1P uniquely activating bleb-based motility. S1PR1 utilizes a different GRK protein and activates different small GTPases than the aforementioned chemokine receptors, which likely mediate the different migratory responses observed in these experiments. The S1PR1-dependent activation of Rho reported by Mou et al. [320] appears to be atypical and may be limited to lymphocytes due to significant differences in ligand-induced receptor internalization and shuttling between lymphocytes and endothelial cells. While data on the signaling cascades needs to be clarified, our data provides a mechanistic explanation for how

S1PR1 uniquely promotes blebbing: through myosin activation and intracellular pressurization.

4.3 The role of lamellipodia, blebs, and other protrusions for migration *in vivo*

Perhaps the most obvious question arising from my finding that S1P promotes bleb-based migration is why would an egress signal specifically promote blebbing? Are blebs better-suited for breaching the lymphatic sinuses or splenic vasculature where egress occurs than actin-based protrusions? Understanding the role of the specific types of protrusions during T cell trafficking is difficult for several reasons. First, live intravital imaging experiments, while incredibly informative, often lack the spatial or temporal resolution to definitively identify different protrusive structures. The model organism best-suited for live cell imaging, the zebrafish, lacks lymph nodes, which precludes studies of intranodal migration or typical egress events. Relative to other protrusions, blebs are particularly transient and protein-dim, making them hard to visualize during intravital imaging experiments in mice. However, careful interpretation of *in vitro* migration studies and *in vivo* phenotypes can begin to clarify how various protrusions facilitate different aspects of T cell trafficking. This section begins with a summary of how different protrusive structures – especially lamellipodia and blebs – facilitate migration in different contexts *in vitro* and *in vivo* and ends with a focus on the morphology of egress portals as it relates to bleb-based passage.

One particularly crucial distinction between lamellipodial and bleb-based migration is that lamellipodial migration requires an adhesive substrate, typically provided in the form of immobilized integrin ligands, whereas bleb-based migration occurs optimally in minimally adhesive settings, not requiring any specific adhesive

contacts [128]. Intravital imaging experiments have shown that T cells migrate directly on the network of FRCs in the paracortex [27], which indicates some kind of contact-dependent guidance, presumably through one or more adhesive interaction. While FRCs express the ligands for LFA-1 (ICAM-1) and VLA-4 (VCAM-1), integrins seem to play only a minor role in intranodal T cell migration [329]. Woolf et al. found that LFA-1-deficient T cells show only modest speed and directionality defects relative to WT T cells, and that VLA-4 does not provide any compensatory adhesive interactions [329]. Similarly, deletion of all integrins from dendritic cells doesn't detectably impact migration to and within lymph nodes [330]. Therefore, while LFA-1 plays a critical role in lymph node entry through HEVs, it is not particularly important for intranodal migration.

Another candidate for an adhesive ligand that could facilitate lamellipodial migration is CCL21. Unlike CCL19, CCL21 remains immobilized on the surface of FRCs [331-334]. Surfaces coated with CCL21 alone, in the absence of any integrin ligands, promote profound and sustained migration of mouse or human T cells, suggesting that CCR7 can function as a weak adhesive receptor in its own right [329]. In this study, Immobilized CCL21 drives lamellipodial formation in T cells in the absences of any other receptor engagement. Moreover, CCL21 is a potent activator of Rac in T cells and Rac is crucial for intranodal migration [320, 329, 335]. Likewise, CCR7 deficiency has a much more profound impact on intranodal T cell migration than LFA-1-deficiency does, even when HEV entry is bypassed [31]. Although further study is warranted, these data point towards a model where immobilized CCL21 promotes Rac activation to drive lamellipodial T cell migration on the FRC network in the paracortex. Utilizing lamellipodial migration in the paracortex likely has an added benefit, as T cell receptors within lamellipodia are particularly sensitive to stimulation [336, 337]. Thus, a single

protrusive structure could facilitate both migration and the scanning of APCs that have collected in the paracortex for rare, cognate antigen [338].

While intravital imaging studies have shown that T cells are almost always associated with the stromal network in the paracortex, T cells do occasionally appear either weakly associated or fully detached from any FRC [27]. *In vitro* studies have shown that T cells can migrate in collagen matrices in the absence of any specific integrin ligands or immobilized chemokines, a process that is especially important in non-lymphoid organs where specialized FRC networks are not present [339, 340]. Work by Lämmerman et al. found that dendritic cell migration through collagen gels was independent of integrins or any specific adhesive interactions, instead relying heavily on Cdc42 activity and actomyosin contractions [330, 341]. Notably, Cdc42 is much more critical for three-dimensional collagen matrix migration than two-dimensional adhesion-dependent migration [341]. The authors were unable to study Cdc42-deficiency during intranodal migration because the defect in these cells in getting to the lymph node was too profound [341]. In three-dimensional environments, the leading edges of leukocytes are often broad and actin-rich, but lacking the telltale characteristics of both lamellipodia or filipodia and therefore are more aptly referred to simply as pseudopods or leading edges. The role of Cdc42 in T cell migration has been difficult to study due to the fact that this GTPase is absolutely critical for T cell development [342, 343], but these data collectively point towards Cdc42 being especially important in leukocytes for adhesion-independent, actin-based migration in three-dimensional environments.

Rho-depleted T cells either fail to polarize or they show defects in trailing edge retraction that results in inefficient transendothelial migration *in vitro* [344]. To my knowledge, intravital imaging studies have not been performed for Rho-deficient T cells,

but T cells deficient in myosin, the major Rho effector protein, display defective motility within the lymph nodes [345]. However, these defects in intranodal migration are mild compared to Rac-deficiency: Rac-deficient T display a roughly 70% decrease in median instantaneous velocity compared to a 30% decrease for myosin-deficient T cells [335, 345]. In addition to their mild intranodal migration defects, myosin-deficient T cells display decreased entry into lymph nodes, often remaining bound to HEVs apparently unable to transverse. These cells are also retained in lymph nodes for abnormally long periods of time, suggestive of an egress defect, although egress has not been directly tested [345]. Mou et al [320] showed previously that S1P selectively activates Rho in T cells, and we now demonstrate S1P activates myosin to promote bleb-base migration (Fig 3.6). Consistent with a barrier-crossing role for myosin, *in vitro* studies have shown that myosin becomes increasingly important for T cell transwell migration as the pores become increasingly narrow and restrictive [346]. Taken together, these data support a model in which S1P signaling through S1PR1 activates Rho to promote myosin-dependent bleb-based migration, which in turn promotes passage through confined spaces, and egress from lymphoid organs.

To summarize, the functions of Rac, Cdc42, Rho, and their associated protrusions in leukocyte migration are diverse, and their depletion or inhibition often results in complex phenotypes. However, the extant data on leukocytes point towards Rac being particularly critical for adhesion-mediated migration on FRC networks, Cdc42 being particularly critical for adhesion-independent migration in extracellular matrices, and Rho being particularly critical for myosin-dependent rear retraction and barrier crossing events. In this context, we propose that S1P induces lymphatic sinus and

splenic endothelial crossing events by promoting myosin-dependent blebbing rather than relying solely on actin-based protrusions.

Egress portals are unique barriers

This leads to most important topic in this discussion, which is the question of why blebs useful for egress. To begin to answer this question, I will first discuss *in vitro* data and modeling that compares the effectiveness of actin-based and bleb-based motility in varying contexts. This will then be followed by a discussion of the morphology of the endothelial barriers that stand between T cells and the circulatory fluids, where blebs are implicated for passage.

One particularly salient study (Tozluoğlu et al. [347]) modeled the migration of metastatic cancer cells, which show extreme plasticity in their protrusion type, in three separate environments: two-dimensional surfaces, continuous confinement, and discontinuous confinement. Continuous confinement is similar to migration in a microchannel, and discontinuous confinement is more akin to a dense collagen gel with various pore sizes that must be traversed. In line with previous experimental data, these models predict blebs to be minimally effective in two-dimensions, where actin-based protrusions are preferred [347, 348]. Both actin-based and bleb-based migration are effective in continuous confinement, but somewhat surprisingly, blebs are significantly more effective than actin-based protrusions in discontinuous confinement, especially when adhesive ligands are scant or entirely absent [347]. These models predict that the pressure-driven nature of blebs allows them to easily find pre-existing discontinuities in the complex matrix, allowing the cell to identify paths of least resistance.

How do paths of least resistance relate to cells traversing an endothelial layer during egress? Most endothelial layers form tight, continuous “zipper-like” cell-to-cell junctions that do not resemble the discontinuous confinement modeled by Tozluoğlu et al. [347], and T cells conspicuously do not use S1PR1 or blebs to cross at these sites, instead relying on chemokine receptors and actin-rich podosomes [349, 350]. However, Baluk et al. [351] report that blunt-end lymphatic sinus endothelial cells, where S1PR1-dependent egress occurs, form overlapping flaps with discontinuous adhesion molecules, resulting in “button-like” barriers [351]. These button-like barriers permit perpetual passage of fluid into lymphatics, which is important for antigen delivery to lymph nodes and the prevention of edema. Leukocytes enter these sinuses by squeezing through pre-existing discontinuities in the sinus barrier [352]. These “button-like” vessels were initially described from imaging studies of lymphatics that drain peripheral non-lymphoid tissues, and were observed at entry sites but not deeper into the vessels, where lymph needs to be efficiently transported [351]. The morphology of lymphatic sinuses in lymph nodes is less well-characterized, due in part to the extreme heterogeneity of lymphatic endothelial cells in these sites [353]. Our understanding of the morphology of sinuses in the lymph node cortex comes almost entirely from electron microscopy characterization of lymph nodes from various species conducted from the 1960s to 1980s. While some reports concluded that LEC layers in lymph nodes are continuous [354], others report the presence of pre-existing discontinuities on the scale reported by Baluk et al. [351] for peripheral lymphatics, some of which are filled with transmigrating leukocytes [353, 355-358]. T cell tracking in lymph nodes has shown that T cells tend to enter lymphatic sinuses through common portal sites, which is consistent with the presence of preformed discontinuities [36, 359].

More research dedicated to the morphology of LEC barriers in lymph nodes is warranted, but the existing data point towards discontinuous barriers being common at the regions where S1PR1-dependent egress occurs and where blebs are implicated. For T cells interacting with these lymphatic sinuses and sensing S1P, blebs may preferentially expand into these spaces between the “buttons” to pass from the lymph node parenchyma into the sinus. While the spatial and temporal resolution from the available intravital imaging studies is not high enough to confidently determine protrusive structures, T cells transmigrating *in vivo* appear to squeeze through adjacent LECs with large, rounded leading edges, potentially indicative of a bleb-based mechanism [36, 359]. This is consistent with electron micrographs showing invasive adenocarcinoma cells accessing peripheral lymphatics by extending rounded cytoplasmic projections, likely blebs, between adjacent LECs [360].

Almost everything that is known about tissue architecture at egress sites comes from analysis of lymph nodes, however S1P is also important for egress from the thymus and spleen, which occurs either primarily or exclusively into blood rather than lymph [39, 235, 361]. It is unclear if these vascular entry points resemble typical zipper-like blood endothelium or button-like lymphatic sinuses. Egress from the spleen has never been visualized despite extensive efforts, and the egress sites are unknown [46]. Vascular egress sites in the thymus, however, have been relatively well-characterized. Egress from the thymus occurs through blood vessels at the corticomedullary junction [361, 362]. These vessels are surrounded by a prominent perivascular space (PVS), which is further separated from the thymic epithelial space (TES) where thymopoiesis occurs by a prominent basement membrane and epithelial sheath [361, 363, 364]. PVSs are common in the brain, but uncommon in peripheral tissues where podosome-dependent

processes are thought to mediate T cell barrier crossing [365]. This PVS is often occupied with mature single positive thymocytes in the process of egressing, and forcing premature expression of S1PR1 causes a prominent accumulation of immature thymocytes in the perivascular space followed by their eventual release into circulation [361, 366]. It is unclear if S1PR1 only facilitates movement from the TES into the PVS or if it is also necessary subsequent passage into the venule. Notably, early electron microscopy studies of the rodent thymus demonstrated that thymocytes appear to breach this epithelial sheath surrounding the PVS through pre-existing discontinuities in the barrier [367, 368], suggesting this S1PR1-dependent step may occur in a similar fashion as lymphatic egress.

The emerging picture from these data is that the specialized entry and egress sites that facilitate homeostatic T cell trafficking are structurally different from “textbook” peripheral blood endothelial layers, and that these atypical structures may be particularly permissive to bleb-based passage. While chemokines are critical for passage across blood endothelial layers *in vitro* and *in vivo* [369], S1P is selectively critical for passage across lymphatic endothelium *in vitro* and *in vivo* [256]. This relationship between endothelial morphology and the permissiveness to different protrusions warrants further study, especially considering the central role that transendothelial migration plays in inflammatory diseases and the metastatic spread of cancers.

Concluding Remarks

Sphingosine is named after the Sphinx, a human/bird/lion hybrid in Greek mythology that devours travelers if they cannot answer her riddle: *What goes on four feet in the morning, two feet at noon, and three feet in the evening?* It was named after

the sphinx as a nod to the enigmatic, frustrating nature of the lipid [233, 370]. The fact that this riddle pertains to movement is purely coincidental. I can personally attest that S1P does justice to the family name, but I believe the data outlined in this thesis have begun to clarify the unique role for this lipid in T cell trafficking.

The role of blebs in T cell trafficking will be most directly solved by *in vivo* imaging, but current technology is unlikely to be able to detect blebs in lymph nodes. There are some compromises that can be made, however. If S1PR1-mediated egress from peripheral tissues also promotes bleb-based motility, substantially higher temporal and spatial resolution can be observed in ear explant imaging experiments, as routinely performed by Michael Sixt's lab (Compare, for instance, supplementary movie 3 in Grigorova et al. 2008 [36] to videos 4-6 in Pflücke et al. 2009 [352]). Zebrafish have lymphatic networks extremely similar to those present in mammals [371, 372], and may therefore be useful for determining the role of blebs in leukocyte trafficking. Zebrafish are the primary model organism where bleb-based motility has been unambiguously observed *in vivo*, although these observations are limited to primordial germ cell migration [135, 150, 373, 374].

Migration throughout the host is an incredibly complex process, and there are undoubtedly still many Sphinxes with many riddles. I hope the contributions detailed in this report add to our collective understanding of leukocyte trafficking and provide a foundation for future studies on S1P, blebbing, and egress.

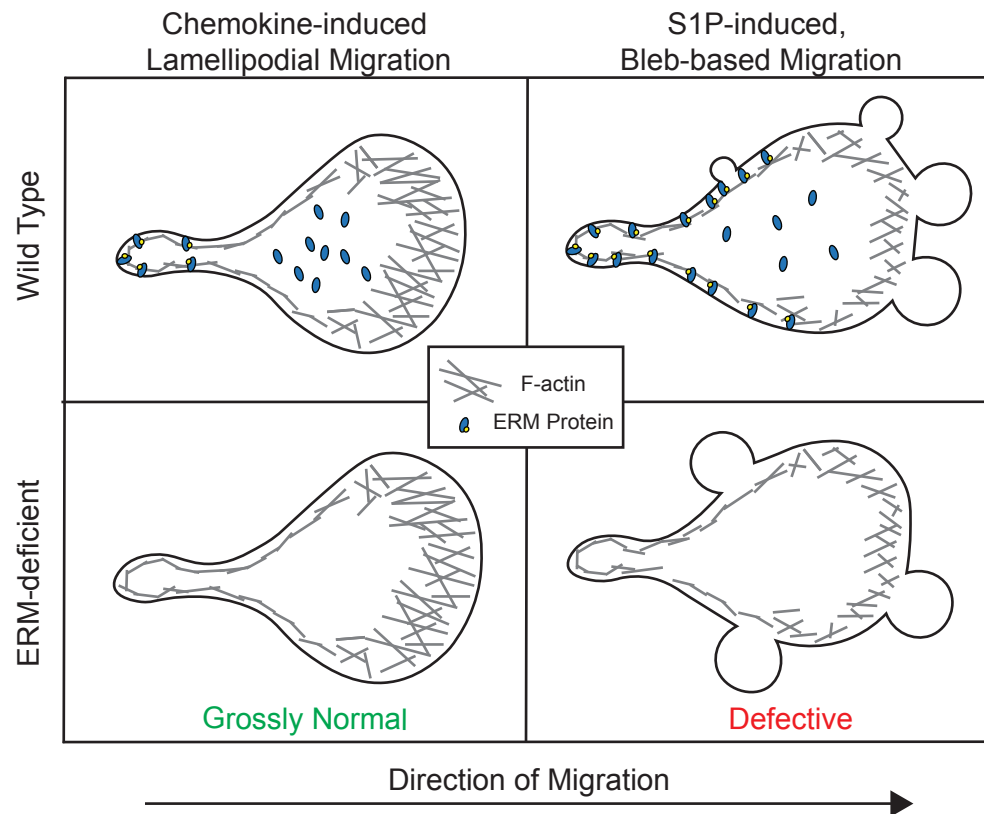


Figure 4.1 A model for the role of ERM proteins in lamellipodial and bleb-based migration

Illustrations showing cell morphology and protrusive structures in WT and ERM-deficient T cells migrating using lamellipodia (left) and blebs (right). Lamellipodial migration appears largely unaffected by the absence of ERM proteins. Wild type cells migrating by blebs primarily show protrusions at the front or leading edge of the cell. When a bleb forms outside the front region of the cell, it is typically small. This polarized blebbing is facilitated by the rearward localization of ERM proteins. In the absence of ERM proteins, blebs form indiscriminately over the cell body, precluding efficient directional migration.

Materials and Methods

Mice. Moesin knockout mice were generated by and purchased from the Texas A&M Institute for Genomic Medicine. A gene trap vector was inserted into the first intron of the *Msn* gene on the X chromosome in 129/Sv ES clones (OST432827), and live mice with germline insertion were generated on the 129Sv x C57BL/6 background. The resulting moesin knockout (MKO) mice were backcrossed for ten generations to mice of the C57BL/6 background (Jackson Laboratories). Mice homozygous for a floxed ezrin gene and transgenic for CD4-Cre (EKO, previously described in Shaffer et al. 2009 [217]) on the C57BL/6 background were then crossed to the MKO mice, to generate mice bearing germline deletion of moesin and deletion of ezrin late in T cell development (female: $Msn^{-/-}Ezrin^{flox/flox}CD4-Cre^{+}$ or male: $Msn^{-/Y}Ezrin^{flox/flox}CD4-Cre^{+}$). Loss of moesin and ezrin expression in mature T cells was confirmed by RT-PCR and western blotting. For most experiments, sex-matched WT littermates were used as controls. Age and sex matched controls were used when littermates were not available or possible. All mice were housed under barrier conditions in the Children's Hospital of Philadelphia animal facility, in accordance with protocols approved by the Institutional Animal Care and Use Committee.

Flow Cytometry. Spleens, lymph nodes, and thymi were harvested from 8-16-week-old mice, and single cell suspensions were prepared. PBMCs were isolated with Lymphoprep (STEMCELL). Cells were counted and stained with fluorochrome-conjugated antibodies towards CD3, CD4, CD8, CD44, CD62L, B220, and NK1.1 (Biolegend, BD Biosciences, Tonbo) and live-dead aqua or blue (Thermo Fisher Scientific). For S1PR1, staining was done in lipid-free FACS buffer (PBS + 1% CS-FBS + 1 mM EDTA). Cells were stained sequentially with rat anti-S1PR1 (R&D MAB7089),

donkey anti rat IgG-biotin F(ab')₂ (Jackson ImmunoResearch 712-066-153), and Streptavidin-APC (Biolegend 405207). For S1PR1 endocytosis experiments, cells were stimulated with S1P (10 nM) for the indicated times, and endocytosis was stopped by adding ice-cold PBS and washing twice with lipid-free FACS buffer prior to surface staining. For F-actin measurements, cells were stimulated with S1P (1 nM) or CCL19 (100 ng/mL) and fixed with 3% paraformaldehyde at the indicated times. Cells were then permeabilized with PSG (PBS + 0.01% saponin + 0.25% fish skin gelatin) and labeled with phalloidin Alexa Fluor 488 (Invitrogen) and anti-CD4-APC (RM4-5, BioLegend). All samples were analyzed on either an LSR Fortessa or LSR II (BD biosciences) equipped with FACSDiva software (BD Biosciences). Data was analyzed using FlowJo software (v.10.4.2).

Immunofluorescence on tissue sections. Spleens and lymph nodes were fixed for 2-4 hours in 4% PFA in PBS, washed, and incubated overnight in 30% sucrose in PBS. Tissues were embedded in OCT and sectioned using a cryostat. Sections were blocked for 30 minutes in staining solution (5% donkey serum in PBS-Tween) containing FcRblock and subsequently incubated overnight at 4°C in staining solution with 1-2 ng/μL of fluorescently-labelled anti-mouse antibodies against CD3-AF647 (Clone 17A2, Biolegend), B220-BV421 (Clone RA3-6B2, Biolegend) and Laminin 1+2 (rabbit anti-mouse, AB7463, Abcam, labelled with CF568 Mix-n-stain™ antibody labelling kit from Biotium). After washing in PBS, slides were mounted using ProLong™ Diamond antifade (Invitrogen), and imaged at 10-20X using a Zeiss LSM710 confocal microscope. Images were processed and analyzed using Zeiss Blue 3.1 (Zeiss) and Velocity 6.3. (Perkin Elmer) software.

Competitive In Vivo Migration. Naïve CD4⁺ T cells isolated from the spleens and lymph nodes of age and sex matched DKO (CD45.2⁺) and congenic WT CD45.1⁺ B6.SJL-Ptprc^a mice (Jackson) were labelled with 1 μ M CellTracker Green CMFDA (Thermo), washed, and mixed at a 1:1 ratio in PBS. 1×10^6 total cells were injected into the tail veins of recipient animals. Recipients were euthanized at 1 or 24 hours after injection. Cells from blood, spleens, and lymph nodes were harvested, stained for CD4, CD45.1, CD45.2 and with a L/D stain (Biolegend, Tonbo), and analyzed by flow cytometry. Input cells were analyzed in parallel. CellTracker Green was used to distinguish between donor and recipient cells, and WT and DKO were further distinguished by CD45.1/CD45.2 expression. Final ratios were normalized to the corresponding input ratios.

T cell purification and culture. For functional studies, lymphoid organs were harvested into ice cold PBS, 0.5% fatty acid free BSA, 1mM EDTA (MACS Buffer) and cell suspensions were prepared. Naïve CD4⁺ T cells were harvested by negative magnetic selection (Miltenyi), washed extensively in MACS buffer, and resuspended in DMEM with 10% charcoal-stripped FBS (Gibco). Cells were cultured overnight at 37°C and 5% CO₂ prior to use.

S1P preparation. Sphingosine-1-Phosphate d18:1 (Avanti) powder was solubilized in methanol:water 95:5 at 50°C with sonication. The solvent was evaporated using dry nitrogen to create a film of S1P on the interior of the vessel, which was resuspended in Milli-Q water supplemented with 4 mg/mL of fatty acid free BSA (Roche) to a final concentration of 100 μ M. The S1P-BSA solution was stored at -20°C in tightly-sealed glass vials and diluted into cell culture media immediately prior to use.

Transmigration Assays. 1×10^5 T cells in DMEM supplemented with 10% CS-FBS were added into a 5-micron transwell insert (Corning) in an empty well to allow them settle for 20 minutes. The insert was gently lowered into a well containing the indicated chemoattractant. In some experiments, the 20-minute settling phase doubled as a pre-incubation with 100 nM of Ex26 (Tocris). An identical concentration of the drug was included in the lower chamber. After 90 minutes, transwell inserts were gently removed, and the number of cells in the lower chamber were enumerated on a hemocytometer.

Microscopy. Eight well chambers (Lab-Tek #1.0 Borosilicate) were coated with 2 $\mu\text{g/mL}$ recombinant mouse VCAM-1 (R&D) overnight at 4°C and washed before use. For live cell imaging, cells in Phenol Red-free L-15 medium (Gibco) + glucose (2 mg/mL) were allowed to settle in the chambers for 30 minutes and then imaged by DIC microscopy at 37°C using either a 40x or 63x objective on a Zeiss Axiovert 200M inverted microscope equipped with an MS-2000 automatic stage (Applied Scientific Instruments) and a Roper Scientific electron-multiplying CCD camera. For experiments that include blebbistatin (5 μM s-nitro-blebbistatin, Cayman), this settling phase doubled as a pre-incubation period. Time-lapse imaging was performed using Slidebook 6 software (Intelligent Imaging Innovations Inc.). Cells were imaged for several minutes at which point S1P, CCL19, or CXCL12 was dripped into the chamber, and acquisition was continued for 10 minutes. Images were collected at 1-second intervals. For studies involving immunofluorescence microscopy of fixed cells, cells were allowed to adhere to VCAM-coated surfaces and stimulated with S1P. At the indicated time after addition of S1P, the media was gently removed and the cells were fixed for 20 minutes in a solution of 10% w/v trichloroacetic acid to preserve ERM phosphorylation [375]. Cells were then permeabilized with 0.1% Triton X-100 in PBS, blocked with PBS, 0.01% saponin, and 0.25% gelatin, stained with

rabbit with anti-phospho ERM (CST#3141) and rat anti-tubulin (clone YL1/2) for 1 hour in PSG, washed three times, stained with anti-rabbit AlexaFluor647 and anti-rat AlexaFluor488 (Invitrogen), washed, and imaged using a 63x PLAN Apo 1.4 NA objective on an Axiovert 200M (Zeiss) with a spinning disc confocal system (UltraVIEW ERS6, Perkin Elmer) equipped with an ORCA-ER camera (Hamamatsu). Image processing was performed both using Volocity v6.3 software (Perkin Elmer) and ImageJ (NIH). All images were prepared for publication in ImageJ.

Cell tracking. DIC chemokinesis assay movies were exported into ImageJ and cells were tracked using the Manual Tracking plugin. For analyzing velocity (Fig. 5c), twelve representative cells were tracked at the one-second acquisition rate, and the instantaneous velocity was smoothed over five-second intervals before displaying. For ease, most videos were reduced to every fifth frame prior to tracking. The different response kinetics with S1P and chemokines forced us to analyze and track cells in each stimulation condition differently. Following stimulation, S1P-treated cells were tracked until the cell characteristically stopped migrating and rounded up, which generally occurred 4-5 minutes post-stimulation (Fig. 5c). Given the slower but more sustained chemokine response, chemokine-treated cells were tracked for 7 minutes. Due to these differences in analysis, the different treatment conditions are graphed separately. Cells that left the field of view, landed after stimulation, or dislodged while tracking were not included. Dislodgement was a minor issue for S1P-treated cells, and generally only occurred after the cell had rounded up. Dislodgement was a serious issue with CCL19 and CXCL12 treatment, affecting roughly half of the otherwise analyzable cells. We considered this a tolerable problem since it allowed S1P and chemokine treatment to be compared under the same experimental conditions.

Bleb quantitation. In order for a protrusion to be classified as a bleb by DIC microscopy, three criteria had to be met. First, the protrusion had to form rapidly, generally in less than one second. Second, the edge of the bleb has to appear smooth and symmetrical, which contrasts with the roughness and irregularity of actin-rich protrusions and edges. Third, the contents of the protrusion had to be clear and devoid of any obvious granules or organelles. These metrics were modified from Zatulovskiy et al [152]. Once a bleb was identified, it was outlined in ImageJ and the area was calculated. Based on the direction of migration, the bleb was then determined to have occurred in either the rear, middle, front, or lead regions of the cell.

Immunoblotting. For experiments involving stimulation, 200 μ L of cells in DMEM were added to an Eppendorf and stimulated with 50 μ L of 5x S1P (1 nM final). To stop, 1 mL of ice-cold PBS was added, cells were rapidly centrifuged, and resuspended in lysis buffer (50 mM Tris-HCl, 50 mM NaCl, 5 mM EDTA, 50 mM NaF, 30 mM $\text{Na}_4\text{P}_2\text{O}_7$, 50 mM β -glycerophosphate, and 1% Triton X-100 in water). Cells were lysed on ice for 30 minutes with occasional vortexing then microfuged for 10 minutes. Lysates were moved to tubes containing NuPAGE LDS sample buffer (Thermo) and boiled for 5 minutes. Samples were then resolved on Bis-Tris 4-12% gradient gels (NuPAGE), transferred to nitrocellulose membranes, washed with TBST, and immunoblotted overnight at 4°C in 2% BSA (w/v) TBST. The following antibodies were used for immunoblotting in this report: Anti-ERM (Cell Signaling Technology #3142), anti-moesin (BD Biosciences clone 38, recognizes all family members), anti-phospho ERM (Cell Signaling #3141), anti-GAPDH (Millipore Sigma MAB374), anti-phospho Erk1/2 Thr202/Tyr204 (Cell Signaling #9101), anti-phospho Akt Ser473 (Cell Signaling #4060). Following overnight incubation, membranes were washed multiple times with TBST and then stained with anti-rabbit or

anti-mouse secondary antibodies conjugated to AlexaFluor680 (Thermo) or IRDye 800CW (Licor). Immunoblots were read on a Licor Odyssey imaging system and quantified using ImageStudioLite (v. 5.2.5).

Measuring intracellular pressure (Pic). The intracellular pressure of T cells was directly measured using the micropressure measurement technique [288]. We used a 900A micropressure system (World Precision Instruments) connected to a 0.5 μ M micropipette that is filled with a 1 M KCl solution and calibrated in a chamber with 0.1 M KCl solution to set the overall electrical resistance of the system to zero or null. When measuring the intracellular pressure, the tip of the micropipette is inserted through the plasma membrane. A positive intracellular pressure pushes the electrolyte solution further up the micropipette. The micropressure machine compensates by increasing the pressure of an air column until a null setting is restored. This pressure value is equivalent to the intracellular pressure. An MPC-325 micromanipulator (Sutter Instrument) installed on an LSM700 laser scanning confocal microscope (Zeiss) was used to position micropipette within the chamber (37°C and 10% CO₂). For these experiments, T cells were plated in chambers coated with Poly-L Lysine (Sigma) in DMEM. Cells were left untreated (control), or stimulated with either S1P or CCL19. For experiments using blebbistatin (50 μ M), cells were pre-treated for 30-60 minutes prior to stimulation. T cell pressure measurements were taken for 2-3 seconds and the average pressure reading during this interval was taken as the cytoplasmic hydraulic pressure of the cell.

Statistical analysis. All statistical tests were performed and graphs were made using GraphPad Prism (GraphPad Software v7.0d), with specific tests indicated in figure legends.

BIBLIOGRAPHY

1. Wadhams, G.H. and J.P. Armitage, *Making sense of it all: bacterial chemotaxis*. Nature Reviews Molecular Cell Biology, 2004. **5**(12): p. 1024-1037.
2. Friedl, P. and K. Wolf, *Plasticity of cell migration: a multiscale tuning model*. Journal of Cell Biology, 2009. **188**(1): p. 11-19.
3. Metchnikoff, É., *Immunity in Infective Diseases*. Cambridge University Press, 1905.
4. Medzhitov, R. and C.A. Janeway, Jr., *Innate Immunity: The Virtues of a Nonclonal System of Recognition*. Cell, 1997. **91**(3): p. 295-298.
5. Kolaczowska, E. and P. Kubes, *Neutrophil recruitment and function in health and inflammation*. Nat Rev Immunol, 2013. **13**(3): p. 159-75.
6. Jung, D. and F.W. Alt, *Unraveling V(D)J Recombination: Insights into Gene Regulation*. Cell, 2004. **116**(2): p. 299-311.
7. Moon, J.J., et al., *Naive CD4(+) T Cell Frequency Varies for Different Epitopes and Predicts Repertoire Diversity and Response Magnitude*. Immunity, 2007. **27**(2): p. 203-213.
8. Obar, J.J., K.M. Khanna, and L. Lefrançois, *Endogenous Naive CD8+ T Cell Precursor Frequency Regulates Primary and Memory Responses to Infection*. Immunity, 2008. **28**(6): p. 859-869.
9. Bajénoff, M., S. Granjeaud, and S. Guerder, *The Strategy of T Cell Antigen-presenting Cell Encounter in Antigen-draining Lymph Nodes Revealed by Imaging of Initial T Cell Activation*. Journal of Experimental Medicine, 2003. **198**(5): p. 715-724.
10. Gowans, J.L. and a.E.J. Knight, *The route of re-circulation of lymphocytes in the rat*. Proc. R. Soc. Lond. B. , 1964. **159**(975): p. 257-282.
11. Hiraoka, N., et al., *A novel, high endothelial venule-specific sulfotransferase expresses 6-sulfo sialyl Lewis(x), an L-selectin ligand displayed by CD34*. Immunity, 1999. **11**(1): p. 79-89.
12. Gallatin, W.M., I.L. Weissman, and E.C. Butcher, *A cell-surface molecule involved in organ-specific homing of lymphocytes*. Nature, 1983. **304**(5921): p. 30-34.
13. Rosen, S.D., *Ligands for L-Selectin: Homing, Inflammation, and Beyond*. Annual Review of Immunology, 2004. **22**(1): p. 129-156.
14. Butcher, E.C. and L.J. Picker, *Lymphocyte Homing and Homeostasis*. Science, 1996. **272**(5258): p. 60.
15. Bao, X., et al., *Endothelial heparan sulfate controls chemokine presentation in recruitment of lymphocytes and dendritic cells to lymph nodes*. Immunity, 2010. **33**(5): p. 817-829.
16. Shamri, R., et al., *Lymphocyte arrest requires instantaneous induction of an extended LFA-1 conformation mediated by endothelium-bound chemokines*. Nature Immunology, 2005. **6**(5): p. 497-506.
17. Arbonés, M.L., et al., *Lymphocyte homing and leukocyte rolling and migration are impaired in L-selectin-deficient mice*. Immunity, 1994. **1**(4): p. 247-60.
18. Förster, R., et al., *CCR7 Coordinates the Primary Immune Response by Establishing Functional Microenvironments in Secondary Lymphoid Organs*. Cell 1999. **99**(1): p. 23-33.
19. Berlin-Rufenach, C., et al., *Lymphocyte migration in lymphocyte function-associated antigen (LFA)-1-deficient mice*. J Exp Med, 1999. **189**(9): p. 1467-78.

20. Hamann, A., et al., *Evidence for an accessory role of LFA-1 in lymphocyte-high endothelium interaction during homing*. J Immunol, 1988. **140**(3): p. 693-9.
21. Masopust, D. and J.M. Schenkel, *The integration of T cell migration, differentiation and function*. Nature Reviews Immunology, 2013. **13**(5): p. 309-320.
22. Bai, Z., et al., *Constitutive Lymphocyte Transmigration across the Basal Lamina of High Endothelial Venules Is Regulated by the Autotaxin/Lysophosphatidic Acid Axis*. The Journal of Immunology, 2013. **190**(5): p. 2036.
23. Zhang, Y., et al., *Autotaxin through lysophosphatidic acid stimulates polarization, motility, and transendothelial migration of naive T cells*. Journal of immunology (Baltimore, Md. : 1950), 2012. **189**(8): p. 3914-3924.
24. Knowlden, S.A., et al., *Regulation of T Cell Motility In Vitro and In Vivo by LPA and LPA2*. PLOS ONE, 2014. **9**(7): p. e101655.
25. Mionnet, C., et al., *High endothelial venules as traffic control points maintaining lymphocyte population homeostasis in lymph nodes*. Blood, 2011. **118**(23): p. 6115-22.
26. Gretz, J.E., et al., *Sophisticated strategies for information encounter in the lymph node: the reticular network as a conduit of soluble information and a highway for cell traffic*. The Journal of Immunology, 1996. **157**(2): p. 495.
27. Bajénoff, M., et al., *Stromal Cell Networks Regulate Lymphocyte Entry, Migration, and Territoriality in Lymph Nodes*. Immunity, 2006. **25**(6): p. 989-1001.
28. Katakai, T., et al., *Lymph node fibroblastic reticular cells construct the stromal reticulum via contact with lymphocytes*. J Exp Med, 2004. **200**(6): p. 783-95.
29. Katakai, T., et al., *A novel reticular stromal structure in lymph node cortex: an immuno-platform for interactions among dendritic cells, T cells and B cells*. Int Immunol, 2004. **16**(8): p. 1133-42.
30. Mori, S., et al., *Mice Lacking Expression of the Chemokines Ccl21-Ser and Ccl19 (plT Mice) Demonstrate Delayed but Enhanced T Cell Immune Responses*. Journal of Experimental Medicine, 2001. **193**(2): p. 207-218.
31. Braun, A., et al., *Afferent lymph–derived T cells and DCs use different chemokine receptor CCR7–dependent routes for entry into the lymph node and intranodal migration*. Nature Immunology, 2011. **12**(9): p. 879-887.
32. Wang, X., et al., *Follicular dendritic cells help establish follicle identity and promote B cell retention in germinal centers*. Journal of Experimental Medicine, 2011. **208**(12): p. 2497-2510.
33. Katakai, T., et al., *Organizer-Like Reticular Stromal Cell Layer Common to Adult Secondary Lymphoid Organs*. The Journal of Immunology, 2008. **181**(9): p. 6189.
34. Cyster, J.G., et al., *Follicular stromal cells and lymphocyte homing to follicles*. Immunol Rev, 2000. **176**: p. 181-93.
35. Mandl, J.N., et al., *Quantification of lymph node transit times reveals differences in antigen surveillance strategies of naive CD4+ and CD8+ T cells*. Proceedings of the National Academy of Sciences, 2012. **109**(44): p. 18036.
36. Grigorova, I.L., et al., *Cortical sinus probing, S1P1-dependent entry and flow-based capture of egressing T cells*. Nature Immunology, 2009. **10**(1): p. 58-65.
37. Schwab, S.R., et al., *Lymphocyte Sequestration Through S1P Lyase Inhibition and Disruption of S1P Gradients*. Science, 2005. **309**(5741): p. 1735.

38. Allende, M.L., et al., *Expression of the Sphingosine 1-Phosphate Receptor, S1P1, on T-cells Controls Thymic Emigration*. Journal of Biological Chemistry, 2004. **279**(15): p. 15396-15401.
39. Matloubian, M., et al., *Lymphocyte egress from thymus and peripheral lymphoid organs is dependent on S1P receptor 1*. Nature, 2004. **427**(6972): p. 355-360.
40. Mebius, R.E. and G. Kraal, *Structure and function of the spleen*. Nat Rev Immunol, 2005. **5**(8): p. 606-16.
41. Bajénoff, M., N. Glaichenhaus, and R.N. Germain, *Fibroblastic Reticular Cells Guide T Lymphocyte Entry into and Migration within the Splenic T Cell Zone*. The Journal of Immunology, 2008. **181**(6): p. 3947.
42. Neely, H.R. and M.F. Flajnik, *CXCL13 Responsiveness but Not CXCR5 Expression by Late Transitional B Cells Initiates Splenic White Pulp Formation*. The Journal of Immunology, 2015: p. 1401905.
43. Gray, D., et al., *Marginal zone B cells express CR1 and CR2 receptors*. European Journal of Immunology, 1984. **14**(1): p. 47-52.
44. Ferguson, A.R., M.E. Youd, and R.B. Corley, *Marginal zone B cells transport and deposit IgM-containing immune complexes onto follicular dendritic cells*. Int Immunol, 2004. **16**(10): p. 1411-22.
45. Cinamon, G., et al., *Follicular shuttling of marginal zone B cells facilitates antigen transport*. Nature immunology, 2008. **9**(1): p. 54-62.
46. Chauveau, A., et al., *Visualization of T Cell Migration in the Spleen Reveals a Network of Perivascular Pathways that Guide Entry into T Zones*. Immunity, 2020. **52**(5): p. 794-807.e7.
47. Conley, J.M., M.P. Gallagher, and L.J. Berg, *T Cells and Gene Regulation: The Switching On and Turning Up of Genes after T Cell Receptor Stimulation in CD8 T Cells*. Front Immunol, 2016. **7**: p. 76.
48. Taniuchi, I., *CD4 Helper and CD8 Cytotoxic T Cell Differentiation*. Annu Rev Immunol, 2018. **36**: p. 579-601.
49. Shiow, L.R., et al., *CD69 acts downstream of interferon-alpha/beta to inhibit S1P1 and lymphocyte egress from lymphoid organs*. Nature, 2006. **440**(7083): p. 540-4.
50. Benechet, A.P., et al., *T cell-intrinsic S1PR1 regulates endogenous effector T-cell egress dynamics from lymph nodes during infection*. Proceedings of the National Academy of Sciences, 2016: p. 201516485.
51. Siegelman, M.H., D. Stanescu, and P. Estess, *The CD44-initiated pathway of T-cell extravasation uses VLA-4 but not LFA-1 for firm adhesion*. J Clin Invest, 2000. **105**(5): p. 683-91.
52. Lesley, J. and R. Hyman, *CD44 can be activated to function as an hyaluronic acid receptor in normal murine T cells*. Eur J Immunol, 1992. **22**(10): p. 2719-23.
53. DeGrendele, H.C., P. Estess, and M.H. Siegelman, *Requirement for CD44 in Activated T Cell Extravasation into an Inflammatory Site*. Science, 1997. **278**(5338): p. 672.
54. Venturi, G.M., et al., *Leukocyte migration is regulated by L-selectin endoproteolytic release*. Immunity, 2003. **19**(5): p. 713-24.
55. Chen, A., P. Engel, and T.F. Tedder, *Structural requirements regulate endoproteolytic release of the L-selectin (CD62L) adhesion receptor from the cell surface of leukocytes*. J Exp Med, 1995. **182**(2): p. 519-30.

56. Galkina, E., et al., *L-selectin shedding does not regulate constitutive T cell trafficking but controls the migration pathways of antigen-activated T lymphocytes*. J Exp Med, 2003. **198**(9): p. 1323-35.
57. Pereira, J.P., et al., *EBI2 mediates B cell segregation between the outer and centre follicle*. Nature, 2009. **460**(7259): p. 1122-6.
58. Pereira, J.P., L.M. Kelly, and J.G. Cyster, *Finding the right niche: B-cell migration in the early phases of T-dependent antibody responses*. Int Immunol, 2010. **22**(6): p. 413-9.
59. Okada, T., et al., *Antigen-Engaged B Cells Undergo Chemotaxis toward the T Zone and Form Motile Conjugates with Helper T Cells*. PLOS Biology, 2005. **3**(6): p. e150.
60. Coffey, F., B. Alabyev, and T. Manser, *Initial clonal expansion of germinal center B cells takes place at the perimeter of follicles*. Immunity, 2009. **30**(4): p. 599-609.
61. Hannedouche, S., et al., *Oxysterols direct immune cell migration via EBI2*. Nature, 2011. **475**(7357): p. 524-7.
62. Liu, C., et al., *Oxysterols direct B-cell migration through EBI2*. Nature, 2011. **475**(7357): p. 519-23.
63. Li, J., et al., *EBI2 augments Tfh cell fate by promoting interaction with IL-2-quenching dendritic cells*. Nature, 2016. **533**(7601): p. 110-114.
64. Green, J.A., et al., *The sphingosine 1-phosphate receptor S1P₂ maintains the homeostasis of germinal center B cells and promotes niche confinement*. Nature immunology, 2011. **12**(7): p. 672-680.
65. Lu, E., et al., *S-Geranylgeranyl-L-glutathione is a ligand for human B cell-confinement receptor P2RY8*. Nature, 2019. **567**(7747): p. 244-248.
66. Muppidi, J.R., E. Lu, and J.G. Cyster, *The G protein-coupled receptor P2RY8 and follicular dendritic cells promote germinal center confinement of B cells, whereas S1PR3 can contribute to their dissemination*. J Exp Med, 2015. **212**(13): p. 2213-22.
67. Moriyama, S., et al., *Sphingosine-1-phosphate receptor 2 is critical for follicular helper T cell retention in germinal centers*. J Exp Med, 2014. **211**(7): p. 1297-305.
68. Muppidi, J.R., et al., *Loss of signalling via Gα13 in germinal centre B-cell-derived lymphoma*. Nature, 2014. **516**(7530): p. 254-258.
69. Allen, C.D., et al., *Germinal center dark and light zone organization is mediated by CXCR4 and CXCR5*. Nat Immunol, 2004. **5**(9): p. 943-52.
70. Sallusto, F., et al., *Two subsets of memory T lymphocytes with distinct homing potentials and effector functions*. Nature, 1999. **401**(6754): p. 708-12.
71. Weninger, W., et al., *Migratory Properties of Naive, Effector, and Memory Cd8⁺ T Cells*. Journal of Experimental Medicine, 2001. **194**(7): p. 953-966.
72. Mora, J.R. and U.H. von Andrian, *T-cell homing specificity and plasticity: new concepts and future challenges*. Trends Immunol, 2006. **27**(5): p. 235-43.
73. Martín-Fontecha, A., et al., *CD40L⁺ CD4⁺ memory T cells migrate in a CD62P-dependent fashion into reactive lymph nodes and license dendritic cells for T cell priming*. Journal of Experimental Medicine, 2008. **205**(11): p. 2561-2574.
74. Guarda, G., et al., *L-selectin-negative CCR7⁻ effector and memory CD8⁺ T cells enter reactive lymph nodes and kill dendritic cells*. Nature Immunology, 2007. **8**(7): p. 743-752.
75. Campbell, J.J., et al., *The chemokine receptor CCR4 in vascular recognition by cutaneous but not intestinal memory T cells*. Nature, 1999. **400**(6746): p. 776-80.

76. Morales, J., et al., *CTACK, a skin-associated chemokine that preferentially attracts skin-homing memory T cells*. Proceedings of the National Academy of Sciences, 1999. **96**(25): p. 14470.
77. Reiss, Y., et al., *CC chemokine receptor (CCR)4 and the CCR10 ligand cutaneous T cell-attracting chemokine (CTACK) in lymphocyte trafficking to inflamed skin*. J Exp Med, 2001. **194**(10): p. 1541-7.
78. Berlin, C., et al., *α 4 β 7 integrin mediates lymphocyte binding to the mucosal vascular addressin MAdCAM-1*. Cell, 1993. **74**(1): p. 185-195.
79. Wagner, N., et al., *Critical role for beta7 integrins in formation of the gut-associated lymphoid tissue*. Nature, 1996. **382**(6589): p. 366-70.
80. Lefrançois, L., et al., *The Role of β 7 Integrins in CD8 T Cell Trafficking During an Antiviral Immune Response*. Journal of Experimental Medicine, 1999. **189**(10): p. 1631-1638.
81. Svensson, M., et al., *CCL25 mediates the localization of recently activated CD8 α beta(+) lymphocytes to the small-intestinal mucosa*. J Clin Invest, 2002. **110**(8): p. 1113-21.
82. Gebhardt, T., et al., *Memory T cells in nonlymphoid tissue that provide enhanced local immunity during infection with herpes simplex virus*. Nat Immunol, 2009. **10**(5): p. 524-30.
83. Jiang, X., et al., *Skin infection generates non-migratory memory CD8⁺ T(RM) cells providing global skin immunity*. Nature, 2012. **483**(7388): p. 227-31.
84. Glennie, N.D., et al., *Skin-resident memory CD4⁺ T cells enhance protection against Leishmania major infection*. J Exp Med, 2015. **212**(9): p. 1405-14.
85. Masopust, D., et al., *Dynamic T cell migration program provides resident memory within intestinal epithelium*. J Exp Med, 2010. **207**(3): p. 553-64.
86. Teijaro, J.R., et al., *Cutting Edge: Tissue-Retentive Lung Memory CD4 T Cells Mediate Optimal Protection to Respiratory Virus Infection*. The Journal of Immunology, 2011. **187**(11): p. 5510.
87. Hofmann, M. and H. Pircher, *E-cadherin promotes accumulation of a unique memory CD8 T-cell population in murine salivary glands*. Proceedings of the National Academy of Sciences, 2011: p. 201107200.
88. Wakim, L.M., A. Woodward-Davis, and M.J. Bevan, *Memory T cells persisting within the brain after local infection show functional adaptations to their tissue of residence*. Proceedings of the National Academy of Sciences, 2010. **107**(42): p. 17872.
89. Skon, C.N., et al., *Transcriptional downregulation of S1pr1 is required for the establishment of resident memory CD8⁺ T cells*. Nat Immunol, 2013. **14**(12): p. 1285-93.
90. Mackay, L.K., et al., *The developmental pathway for CD103⁺CD8⁺ tissue-resident memory T cells of skin*. Nature Immunology, 2013. **14**(12): p. 1294-1301.
91. Casey, K.A., et al., *Antigen-Independent Differentiation and Maintenance of Effector-like Resident Memory T Cells in Tissues*. The Journal of Immunology, 2012. **188**(10): p. 4866.
92. Schön, M.P., et al., *Mucosal T lymphocyte numbers are selectively reduced in integrin α E (CD103)-deficient mice*. J Immunol, 1999. **162**(11): p. 6641-9.
93. Svitkina, T.M., *Actin Cell Cortex: Structure and Molecular Organization*. Trends in Cell Biology, 2020. **30**(7): p. 556-565.
94. Dai, J. and M.P. Sheetz, *Membrane tether formation from blebbing cells*. Biophysical journal, 1999. **77**(6): p. 3363-3370.

95. Nambiar, R., R.E. McConnell, and M.J. Tyska, *Control of cell membrane tension by myosin-I*. Proceedings of the National Academy of Sciences, 2009. **106**(29): p. 11972.
96. Stewart, M.P., et al., *Hydrostatic pressure and the actomyosin cortex drive mitotic cell rounding*. Nature, 2011. **469**(7329): p. 226-230.
97. Chengappa, P., et al., *Intracellular Pressure: A Driver of Cell Morphology and Movement*. Int Rev Cell Mol Biol, 2018. **337**: p. 185-211.
98. Foth, B.J., M.C. Goedecke, and D. Soldati, *New insights into myosin evolution and classification*. Proceedings of the National Academy of Sciences of the United States of America, 2006. **103**(10): p. 3681.
99. Trivedi, D.V., et al., *The Myosin Family of Mechanoenzymes: From Mechanisms to Therapeutic Approaches*. Annual Review of Biochemistry, 2020. **89**(1): p. 667-693.
100. Rayment, I., et al., *Three-dimensional structure of myosin subfragment-1: a molecular motor*. Science, 1993. **261**(5117): p. 50.
101. Sweeney, H.L. and A. Houdusse, *Structural and functional insights into the Myosin motor mechanism*. Annu Rev Biophys, 2010. **39**: p. 539-57.
102. Lymn, R.W. and E.W. Taylor, *Mechanism of adenosine triphosphate hydrolysis by actomyosin*. Biochemistry, 1971. **10**(25): p. 4617-4624.
103. Titus, M.A., *Myosin-Driven Intracellular Transport*. Cold Spring Harb Perspect Biol, 2018. **10**(3).
104. Côté, G.P., Robinson, E. A., Appella, E., and Korn, E. D, J. Biol. Chem., 1984. **259**: p. 12781-12787.
105. Craig, R., R. Smith, and J. Kendrick-Jones, *Light-chain phosphorylation controls the conformation of vertebrate non-muscle and smooth muscle myosin molecules*. Nature, 1983. **302**(5907): p. 436-439.
106. Pecci, A., et al., *MYH9: Structure, functions and role of non-muscle myosin IIA in human disease*. Gene, 2018. **664**: p. 152-167.
107. Niederman, R. and T.D. Pollard, *Human platelet myosin. II. In vitro assembly and structure of myosin filaments*. Journal of Cell Biology, 1975. **67**(1): p. 72-92.
108. Mabuchi, I. and M. Okuno, *The effect of myosin antibody on the division of starfish blastomeres*. Journal of Cell Biology, 1977. **74**(1): p. 251-263.
109. Powell, K., *Myosin powers cytokinesis*. Journal of Cell Biology, 2005. **170**(4): p. 515-515.
110. Crowley, E. and A.F. Horwitz, *Tyrosine phosphorylation and cytoskeletal tension regulate the release of fibroblast adhesions*. Journal of Cell Biology, 1995. **131**(2): p. 525-537.
111. Chrzanowska-Wodnicka, M. and K. Burridge, *Rho-stimulated contractility drives the formation of stress fibers and focal adhesions*. Journal of Cell Biology, 1996. **133**(6): p. 1403-1415.
112. WorthyLake, R.A., et al., *RhoA is required for monocyte tail retraction during transendothelial migration*. Journal of Cell Biology, 2001. **154**(1): p. 147-160.
113. Bhadriraju, K., et al., *Activation of ROCK by RhoA is regulated by cell adhesion, shape, and cytoskeletal tension*. Exp Cell Res, 2007. **313**(16): p. 3616-23.
114. Discher, D.E., P. Janmey, and Y.-I. Wang, *Tissue Cells Feel and Respond to the Stiffness of Their Substrate*. Science, 2005. **310**(5751): p. 1139.
115. Ikebe, M., J. Koretz, and D.J. Hartshorne, *Effects of phosphorylation of light chain residues threonine 18 and serine 19 on the properties and conformation of smooth muscle myosin*. J Biol Chem, 1988. **263**(13): p. 6432-7.

116. Umemoto, S., A.R. Bengur, and J.R. Sellers, *Effect of multiple phosphorylations of smooth muscle and cytoplasmic myosins on movement in an in vitro motility assay*. J Biol Chem, 1989. **264**(3): p. 1431-6.
117. Wendt, T., et al., *Three-dimensional image reconstruction of dephosphorylated smooth muscle heavy meromyosin reveals asymmetry in the interaction between myosin heads and placement of subfragment 2*. Proceedings of the National Academy of Sciences, 2001. **98**(8): p. 4361.
118. Amano, M., et al., *Phosphorylation and activation of myosin by Rho-associated kinase (Rho-kinase)*. J Biol Chem, 1996. **271**(34): p. 20246-9.
119. Somlyo, A.P. and A.V. Somlyo, *Ca²⁺ sensitivity of smooth muscle and nonmuscle myosin II: modulated by G proteins, kinases, and myosin phosphatase*. Physiol Rev, 2003. **83**(4): p. 1325-58.
120. Kamm, K.E. and J.T. Stull, *Dedicated myosin light chain kinases with diverse cellular functions*. J Biol Chem, 2001. **276**(7): p. 4527-30.
121. Mullins, R.D., J.A. Heuser, and T.D. Pollard, *The interaction of Arp2/3 complex with actin: Nucleation, high affinity pointed end capping, and formation of branching networks of filaments*. Proceedings of the National Academy of Sciences, 1998. **95**(11): p. 6181.
122. Svitkina, T.M. and G.G. Borisy, *Arp2/3 complex and actin depolymerizing factor/cofilin in dendritic organization and treadmilling of actin filament array in lamellipodia*. J Cell Biol, 1999. **145**(5): p. 1009-26.
123. Pruyne, D., et al., *Role of formins in actin assembly: nucleation and barbed-end association*. Science, 2002. **297**(5581): p. 612-5.
124. Sagot, I., et al., *An actin nucleation mechanism mediated by Bni1 and profilin*. Nat Cell Biol, 2002. **4**(8): p. 626-31.
125. Zigmond, S.H., et al., *Formin leaky cap allows elongation in the presence of tight capping proteins*. Curr Biol, 2003. **13**(20): p. 1820-3.
126. Korobova, F. and T. Svitkina, *Arp2/3 complex is important for filopodia formation, growth cone motility, and neuritogenesis in neuronal cells*. Mol Biol Cell, 2008. **19**(4): p. 1561-74.
127. Yang, C., et al., *Novel Roles of Formin mDia2 in Lamellipodia and Filopodia Formation in Motile Cells*. PLOS Biology, 2007. **5**(11): p. e317.
128. Charras, G. and E. Paluch, *Blebs lead the way: how to migrate without lamellipodia*. Nat Rev Mol Cell Biol. , 2008. **9**: p. 730-736.
129. Cunningham, C.C., *Actin polymerization and intracellular solvent flow in cell surface blebbing*. Journal of Cell Biology, 1995. **129**(6): p. 1589-1599.
130. Paluch, E., et al., *Cortical actomyosin breakage triggers shape oscillations in cells and cell fragments*. Biophys J, 2005. **89**(1): p. 724-33.
131. Paluch, E., J. van der Gucht, and C.c. Sykes, *Cracking up: symmetry breaking in cellular systems*. Journal of Cell Biology, 2006. **175**(5): p. 687-692.
132. Taloni, A., et al., *Volume Changes During Active Shape Fluctuations in Cells*. Physical Review Letters, 2015. **114**(20): p. 208101.
133. Kleinschmidt, J.H., *Folding kinetics of the outer membrane proteins OmpA and FomA into phospholipid bilayers*. Chemistry and Physics of Lipids, 2006. **141**(1): p. 30-47.
134. Goudarzi, M., et al., *Bleb Expansion in Migrating Cells Depends on Supply of Membrane from Cell Surface Invaginations*. Dev Cell, 2017. **43**(5): p. 577-587.e5.

135. Blaser, H., et al., *Migration of zebrafish primordial germ cells: a role for myosin contraction and cytoplasmic flow*. Dev Cell, 2006. **11**(5): p. 613-27.
136. Keller, H., P. Rentsch, and J. Hagmann, *Differences in cortical actin structure and dynamics document that different types of blebs are formed by distinct mechanisms*. Exp Cell Res, 2002. **277**(2): p. 161-72.
137. Charras, G.T., et al., *Reassembly of contractile actin cortex in cell blebs*. The Journal of Cell Biology, 2006. **175**(3): p. 477-490.
138. Charras, G.T., et al., *Non-equilibration of hydrostatic pressure in blebbing cells*. Nature, 2005. **435**(7040): p. 365-369.
139. Tinevez, J.-Y., et al., *Role of cortical tension in bleb growth*. Proceedings of the National Academy of Sciences, 2009. **106**(44): p. 18581.
140. Strychalski, W. and R.D. Guy, *Intracellular Pressure Dynamics in Blebbing Cells*. Biophys J, 2016. **110**(5): p. 1168-79.
141. Rossy, J., et al., *Ezrin/moesin in motile Walker 256 carcinosarcoma cells: signal-dependent relocalization and role in migration*. Exp Cell Res, 2007. **313**(6): p. 1106-20.
142. Lorentzen, A., et al., *An ezrin-rich, rigid uropod-like structure directs movement of amoeboid blebbing cells*. Journal of Cell Science, 2011. **124**(8): p. 1256.
143. Diz-Muñoz, A., et al., *Control of Directed Cell Migration In Vivo by Membrane-to-Cortex Attachment*. PLOS Biology, 2010. **8**(11): p. e1000544.
144. Trinkaus, J.P., *Surface activity and locomotion of Fundulus deep cells during blastula and gastrula stages*. Developmental Biology, 1973. **30**(1): p. 68-103.
145. Johnson, K.E., *Circus movements and blebbing locomotion in dissociated embryonic cells of an amphibian, Xenopus laevis*. Journal of Cell Science, 1976. **22**(3): p. 575.
146. Kubota, H.Y., *Creeping locomotion of the endodermal cells dissociated from gastrulae of the Japanese newt, Cynops pyrrhogaster*. Exp Cell Res, 1981. **133**(1): p. 137-48.
147. Fink, R.D. and J.P. Trinkaus, *Fundulus deep cells: directional migration in response to epithelial wounding*. Dev Biol, 1988. **129**(1): p. 179-90.
148. Pollard, T.D. and G.G. Borisy, *Cellular motility driven by assembly and disassembly of actin filaments*. Cell, 2003. **112**(4): p. 453-65.
149. Robertson, A.M.G., et al., *Morphological aspects of glucocorticoid-induced cell death in human lymphoblastoid cells*. The Journal of Pathology, 1978. **126**(3): p. 181-187.
150. Goudarzi, M., et al., *Fluid dynamics during bleb formation in migrating cells in vivo*. PLOS ONE, 2019. **14**(2): p. e0212699.
151. Yoshida, K. and T. Soldati, *Dissection of amoeboid movement into two mechanically distinct modes*. Journal of Cell Science, 2006. **119**(18): p. 3833.
152. Zatulovskiy, E., et al., *Bleb-driven chemotaxis of Dictyostelium cells*. Journal of Cell Biology, 2014. **204**(6): p. 1027-1044.
153. Haston, W.S. and J.M. Shields, *Contraction waves in lymphocyte locomotion*. Journal of Cell Science, 1984. **68**(1): p. 227.
154. Yan, S.L.S., et al., *In Vivo F-Actin Filament Organization during Lymphocyte Transendothelial and Interstitial Migration Revealed by Intravital Microscopy*. iScience, 2019. **16**: p. 283-297.
155. Bretscher, A., *Purification of an 80,000-dalton protein that is a component of the isolated microvillus cytoskeleton, and its localization in nonmuscle cells*. Journal of Cell Biology, 1983. **97**(2): p. 425-432.

156. Lankes, W., et al., *A heparin-binding protein involved in inhibition of smooth-muscle cell proliferation*. The Biochemical journal, 1988. **251**(3): p. 831-842.
157. Tsukita, S. and S. Tsukita, *Isolation of cell-to-cell adherens junctions from rat liver*. Journal of Cell Biology, 1989. **108**(1): p. 31-41.
158. Funayama, N., et al., *Radixin is a novel member of the band 4.1 family*. J Cell Biol, 1991. **115**(4): p. 1039-48.
159. Takeuchi, K., et al., *Perturbation of cell adhesion and microvilli formation by antisense oligonucleotides to ERM family members*. Journal of Cell Biology, 1994. **125**(6): p. 1371-1384.
160. McClatchey, A.I., *ERM proteins at a glance*. Journal of cell science, 2014. **127**(Pt 15): p. 3199-3204.
161. Fehon, R.G., A.I. McClatchey, and A. Bretscher, *Organizing the cell cortex: the role of ERM proteins*. Nature Reviews Molecular Cell Biology, 2010. **11**(4): p. 276-287.
162. Ingraffea, J., D. Reczek, and A. Bretscher, *Distinct cell type-specific expression of scaffolding proteins EBP50 and E3KARP: EBP50 is generally expressed with ezrin in specific epithelia, whereas E3KARP is not*. Eur J Cell Biol, 2002. **81**(2): p. 61-8.
163. Kitajiri, S.-i., et al., *Radixin deficiency causes deafness associated with progressive degeneration of cochlear stereocilia*. Journal of Cell Biology, 2004. **166**(4): p. 559-570.
164. McCartney, B.M. and R.G. Fehon, *Distinct cellular and subcellular patterns of expression imply distinct functions for the Drosophila homologues of moesin and the neurofibromatosis 2 tumor suppressor, merlin*. Journal of Cell Biology, 1996. **133**(4): p. 843-852.
165. Göbel, V., et al., *Lumen morphogenesis in C. elegans requires the membrane-cytoskeleton linker erm-1*. Dev Cell, 2004. **6**(6): p. 865-73.
166. Van Fürden, D., et al., *The C. elegans ezrin-radixin-moesin protein ERM-1 is necessary for apical junction remodelling and tubulogenesis in the intestine*. Dev Biol, 2004. **272**(1): p. 262-76.
167. Dong, B., W. Deng, and D. Jiang, *Distinct cytoskeleton populations and extensive crosstalk control Ciona notochord tubulogenesis*. Development, 2011. **138**(8): p. 1631.
168. Bretscher, A., K. Edwards, and R.G. Fehon, *ERM proteins and merlin: integrators at the cell cortex*. Nat Rev Mol Cell Biol, 2002. **3**(8): p. 586-99.
169. Shabardina, V., et al., *Emergence and Evolution of ERM Proteins and Merlin in Metazoans*. Genome Biology and Evolution, 2020. **12**(1): p. 3710-3724.
170. Algrain, M., et al., *Ezrin contains cytoskeleton and membrane binding domains accounting for its proposed role as a membrane-cytoskeletal linker*. Journal of Cell Biology, 1993. **120**(1): p. 129-139.
171. Niggli, V., et al., *Identification of a phosphatidylinositol-4,5-bisphosphate-binding domain in the N-terminal region of ezrin*. FEBS Letters, 1995. **376**(3): p. 172-176.
172. Turunen, O., T. Wahlström, and A. Vaheri, *Ezrin has a COOH-terminal actin-binding site that is conserved in the ezrin protein family*. J Cell Biol, 1994. **126**(6): p. 1445-53.
173. Gary, R. and A. Bretscher, *Ezrin self-association involves binding of an N-terminal domain to a normally masked C-terminal domain that includes the F-actin binding site*. Molecular Biology of the Cell, 1995. **6**(8): p. 1061-1075.
174. Magendantz, M., et al., *Interdomain Interactions of Radixin in Vitro*. Journal of Biological Chemistry, 1995. **270**(43): p. 25324-25327.

175. Nakamura, F., et al., *Regulation of F-actin binding to platelet moesin in vitro by both phosphorylation of threonine 558 and polyphosphatidylinositides*. Mol Biol Cell, 1999. **10**(8): p. 2669-85.
176. Hamada, K., et al., *Structural basis of the membrane-targeting and unmasking mechanisms of the radixin FERM domain*. Embo j, 2000. **19**(17): p. 4449-62.
177. Yonemura, S., et al., *Rho-dependent and -independent activation mechanisms of ezrin/radixin/moesin proteins: an essential role for polyphosphoinositides in vivo*. Journal of Cell Science, 2002. **115**(12): p. 2569.
178. Matsui, T., et al., *Rho-kinase phosphorylates COOH-terminal threonines of ezrin/radixin/moesin (ERM) proteins and regulates their head-to-tail association*. J Cell Biol, 1998. **140**(3): p. 647-57.
179. Simons, P.C., et al., *C-terminal threonine phosphorylation activates ERM proteins to link the cell's cortical lipid bilayer to the cytoskeleton*. Biochem Biophys Res Commun, 1998. **253**(3): p. 561-5.
180. Pearson, M.A., et al., *Structure of the ERM protein moesin reveals the FERM domain fold masked by an extended actin binding tail domain*. Cell, 2000. **101**(3): p. 259-70.
181. Fievet, B.T., et al., *Phosphoinositide binding and phosphorylation act sequentially in the activation mechanism of ezrin*. Journal of Cell Biology, 2004. **164**(5): p. 653-659.
182. Oshiro, N., Y. Fukata, and K. Kaibuchi, *Phosphorylation of Moesin by Rho-associated Kinase (Rho-kinase) Plays a Crucial Role in the Formation of Microvilli-like Structures*. Journal of Biological Chemistry, 1998. **273**(52): p. 34663-34666.
183. Polesello, C., et al., *Dmoesin controls actin-based cell shape and polarity during Drosophila melanogaster oogenesis*. Nat Cell Biol, 2002. **4**(10): p. 782-9.
184. Brown, M.J., et al., *Chemokine stimulation of human peripheral blood T lymphocytes induces rapid dephosphorylation of ERM proteins, which facilitates loss of microvilli and polarization*. Blood, 2003. **102**(12): p. 3890-3899.
185. Liu, Y., et al., *Constitutively active ezrin increases membrane tension, slows migration, and impedes endothelial transmigration of lymphocytes in vivo in mice*. Blood, 2012. **119**(2): p. 445-453.
186. Viswanatha, R., et al., *Interactome Analysis Reveals Ezrin Can Adopt Multiple Conformational States*. Journal of Biological Chemistry, 2013. **288**(49): p. 35437-35451.
187. Ng, T., et al., *Ezrin is a downstream effector of trafficking PKC-integrin complexes involved in the control of cell motility*. The EMBO journal, 2001. **20**(11): p. 2723-2741.
188. Pietromonaco, S.F., et al., *Protein kinase C-theta phosphorylation of moesin in the actin-binding sequence*. J Biol Chem, 1998. **273**(13): p. 7594-603.
189. Hébert, M., et al., *Rho-ROCK-Dependent Ezrin-Radixin-Moesin Phosphorylation Regulates Fas-Mediated Apoptosis in Jurkat Cells*. The Journal of Immunology, 2008. **181**(9): p. 5963.
190. Baumgartner, M., et al., *The Nck-interacting kinase phosphorylates ERM proteins for formation of lamellipodium by growth factors*. Proceedings of the National Academy of Sciences, 2006. **103**(36): p. 13391.
191. Belkina, N.V., et al., *LOK is a major ERM kinase in resting lymphocytes and regulates cytoskeletal rearrangement through ERM phosphorylation*. Proceedings of the National Academy of Sciences, 2009. **106**(12): p. 4707.
192. Viswanatha, R., et al., *Local phosphocycling mediated by LOK/SLK restricts ezrin function to the apical aspect of epithelial cells*. Journal of Cell Biology, 2012. **199**(6): p. 969-984.

193. Clucas, J. and F. Valderrama, *ERM proteins in cancer progression*. Journal of Cell Science, 2014. **127**(2): p. 267.
194. Fukata, Y., et al., *Association of the Myosin-binding Subunit of Myosin Phosphatase and Moesin: Dual Regulation of Moesin Phosphorylation by Rho-associated Kinase and Myosin Phosphatase*. Journal of Cell Biology, 1998. **141**(2): p. 409-418.
195. Kim, K.-M., et al., *Molecular characterization of myosin phosphatase in endothelium*. Journal of cellular physiology, 2012. **227**(4): p. 1701-1708.
196. Kovacs-Kasa, A., et al., *The protective role of MLCP-mediated ERM dephosphorylation in endotoxin-induced lung injury in vitro and in vivo*. Scientific reports, 2016. **6**: p. 39018-39018.
197. Canals, D., P. Roddy, and Y.A. Hannun, *Protein phosphatase 1 α mediates ceramide-induced ERM protein dephosphorylation: a novel mechanism independent of phosphatidylinositol 4, 5-bisphosphate (PIP₂) and myosin/ERM phosphatase*. J Biol Chem, 2012. **287**(13): p. 10145-55.
198. Kunda, P., et al., *Moesin controls cortical rigidity, cell rounding, and spindle morphogenesis during mitosis*. Curr Biol, 2008. **18**(2): p. 91-101.
199. Carreno, S., et al., *Moesin and its activating kinase Slik are required for cortical stability and microtubule organization in mitotic cells*. J Cell Biol, 2008. **180**(4): p. 739-46.
200. Roubinet, C., et al., *Molecular networks linked by Moesin drive remodeling of the cell cortex during mitosis*. Journal of Cell Biology, 2011. **195**(1): p. 99-112.
201. Kunda, P., et al., *PP1-mediated moesin dephosphorylation couples polar relaxation to mitotic exit*. Curr Biol, 2012. **22**(3): p. 231-6.
202. Rodrigues, N.T., et al., *Kinetochore-localized PP1-Sds22 couples chromosome segregation to polar relaxation*. Nature, 2015. **524**(7566): p. 489-92.
203. Funamoto, S., et al., *Spatial and temporal regulation of 3-phosphoinositides by PI 3-kinase and PTEN mediates chemotaxis*. Cell, 2002. **109**(5): p. 611-23.
204. von Stein, W., et al., *Direct association of Bazooka/PAR-3 with the lipid phosphatase PTEN reveals a link between the PAR/aPKC complex and phosphoinositide signaling*. Development, 2005. **132**(7): p. 1675-86.
205. Gassama-Diagne, A., et al., *Phosphatidylinositol-3,4,5-trisphosphate regulates the formation of the basolateral plasma membrane in epithelial cells*. Nat Cell Biol, 2006. **8**(9): p. 963-70.
206. Martin-Belmonte, F., et al., *PTEN-mediated apical segregation of phosphoinositides controls epithelial morphogenesis through Cdc42*. Cell, 2007. **128**(2): p. 383-97.
207. Leslie, N.R., et al., *Understanding PTEN regulation: PIP₂, polarity and protein stability*. Oncogene, 2008. **27**(41): p. 5464-5476.
208. Saotome, I., M. Curto, and A.I. McClatchey, *Ezrin is essential for epithelial organization and villus morphogenesis in the developing intestine*. Dev Cell, 2004. **6**(6): p. 855-64.
209. Speck, O., et al., *Moesin functions antagonistically to the Rho pathway to maintain epithelial integrity*. Nature, 2003. **421**(6918): p. 83-87.
210. Iijima, M. and P. Devreotes, *Tumor suppressor PTEN mediates sensing of chemoattractant gradients*. Cell, 2002. **109**(5): p. 599-610.
211. Lokuta, M.A., et al., *Type I γ PIP kinase is a novel uropod component that regulates rear retraction during neutrophil chemotaxis*. Mol Biol Cell, 2007. **18**(12): p. 5069-80.
212. Matsuoka, S. and M. Ueda, *Mutual inhibition between PTEN and PIP₃ generates bistability for polarity in motile cells*. Nature Communications, 2018. **9**(1): p. 4481.

213. Prentice-Mott, H.V., et al., *Directional memory arises from long-lived cytoskeletal asymmetries in polarized chemotactic cells*. Proc Natl Acad Sci U S A, 2016. **113**(5): p. 1267-72.
214. Yoshinaga-Ohara, N., et al., *Spatiotemporal regulation of moesin phosphorylation and rear release by Rho and serine/threonine phosphatase during neutrophil migration*. Exp Cell Res, 2002. **278**(1): p. 112-22.
215. Lee, J.-H., et al., *Roles of p-ERM and Rho-ROCK signaling in lymphocyte polarity and uropod formation*. Journal of Cell Biology, 2004. **167**(2): p. 327-337.
216. Shaffer, M.H., et al., *Ezrin Is Highly Expressed in Early Thymocytes, but Dispensable for T Cell Development in Mice*. PLOS ONE, 2010. **5**(8): p. e12404.
217. Shaffer, M.H., et al., *Ezrin and Moesin Function Together to Promote T Cell Activation*. J Immunol, 2009. **182**: p. 1021-1032.
218. Parameswaran, N., K. Matsui, and N. Gupta, *Conformational Switching in Ezrin Regulates Morphological and Cytoskeletal Changes Required for B Cell Chemotaxis*. The Journal of Immunology, 2011. **186**(7): p. 4088.
219. del Pozo, M.A., et al., *Chemokines regulate cellular polarization and adhesion receptor redistribution during lymphocyte interaction with endothelium and extracellular matrix. Involvement of cAMP signaling pathway*. The Journal of cell biology, 1995. **131**(2): p. 495-508.
220. Chen, E.J.H., et al., *Ezrin and Moesin Are Required for Efficient T Cell Adhesion and Homing to Lymphoid Organs*. PLOS One, 2013. **8**(2).
221. Martinelli, S., et al., *Ezrin/Radixin/Moesin Proteins and Flotillins Cooperate to Promote Uropod Formation in T Cells*. Frontiers in Immunology, 2013. **4**(84).
222. Panicker, S.R., et al., *Neutrophils lacking ERM proteins polarize and crawl directionally but have decreased adhesion strength*. Blood Advances, 2020. **4**(15): p. 3559-3571.
223. Doi, Y., et al., *Normal development of mice and unimpaired cell adhesion/cell motility/actin-based cytoskeleton without compensatory up-regulation of ezrin or radixin in moesin gene knockout*. J Biol Chem, 1999. **274**(4): p. 2315-21.
224. Hirata, T., et al., *Moesin-deficient mice reveal a non-redundant role for moesin in lymphocyte homeostasis*. International Immunology, 2012. **24**(11): p. 705-717.
225. Lagresle-Peyrou, C., et al., *X-linked primary immunodeficiency associated with hemizygous mutations in the moesin (MSN) gene*. Journal of Allergy and Clinical Immunology, 2016. **138**(6): p. 1681-1689.e8.
226. Delmonte, O.M., et al., *First Case of X-Linked Moesin Deficiency Identified After Newborn Screening for SCID*. Journal of Clinical Immunology, 2017. **37**(4): p. 336-338.
227. Bradshaw, G., et al., *Exome Sequencing Diagnoses X-Linked Moesin-Associated Immunodeficiency in a Primary Immunodeficiency Case*. Frontiers in immunology, 2018. **9**: p. 420-420.
228. Henrickson, S.E., et al., *Hematopoietic Stem Cell Transplant for the Treatment of X-MAID*. Frontiers in pediatrics, 2019. **7**: p. 170-170.
229. Pore, D., et al., *Ezrin Tunes the Magnitude of Humoral Immunity*. The Journal of Immunology, 2013. **191**(8): p. 4048.
230. Allenspach, E.J., et al., *ERM-dependent movement of CD43 defines a novel protein complex distal to the immunological synapse*. Immunity, 2001. **15**(5): p. 739-50.
231. Satooka, H., et al., *The ERM Protein Moesin Regulates CD8(+) Regulatory T Cell Homeostasis and Self-Tolerance*. J Immunol, 2017. **199**(10): p. 3418-3426.

232. Yatomi, Y., et al., *Sphingosine 1-phosphate: synthesis and release*. Prostaglandins Other Lipid Mediat, 2001. **64**(1-4): p. 107-22.
233. Spiegel, S. and S. Milstien, *Sphingosine-1-phosphate: an enigmatic signalling lipid*. Nat Rev Mol Cell Biol, 2003. **4**(5): p. 397-407.
234. Stunff, H.L., S. Milstien, and S. Spiegel, *Generation and metabolism of bioactive sphingosine-1-phosphate*. Journal of Cellular Biochemistry, 2004. **92**(5): p. 882-899.
235. Pappu, R., et al., *Promotion of Lymphocyte Egress into Blood and Lymph by Distinct Sources of Sphingosine-1-Phosphate*. Science, 2007. **316**(5822): p. 295.
236. Yatomi, Y., et al., *Sphingosine-1-phosphate: a platelet-activating sphingolipid released from agonist-stimulated human platelets*. Blood, 1995. **86**(1): p. 193-202.
237. Yatomi, Y., et al., *Sphingosine 1-Phosphate, a Bioactive Sphingolipid Abundantly Stored in Platelets, Is a Normal Constituent of Human Plasma and Serum*. The Journal of Biochemistry, 1997. **121**(5): p. 969-973.
238. Shivdasani, R.A., et al., *Transcription factor NF-E2 is required for platelet formation independent of the actions of thrombopoietin/MGDF in megakaryocyte development*. Cell, 1995. **81**(5): p. 695-704.
239. Vu, T.M., et al., *Mfsd2b is essential for the sphingosine-1-phosphate export in erythrocytes and platelets*. Nature, 2017. **550**(7677): p. 524-528.
240. Pham, T.H., et al., *Lymphatic endothelial cell sphingosine kinase activity is required for lymphocyte egress and lymphatic patterning*. J Exp Med, 2010. **207**(1): p. 17-27.
241. Mendoza, A., et al., *The Transporter Spns2 Is Required for Secretion of Lymph but Not Plasma Sphingosine-1-Phosphate*. Cell Reports, 2012. **2**(5): p. 1104-1110.
242. Fukuhara, S., et al., *The sphingosine-1-phosphate transporter Spns2 expressed on endothelial cells regulates lymphocyte trafficking in mice*. The Journal of Clinical Investigation, 2012. **122**(4): p. 1416-1426.
243. Hisano, Y., et al., *Mouse SPNS2 Functions as a Sphingosine-1-Phosphate Transporter in Vascular Endothelial Cells*. PLOS ONE, 2012. **7**(6): p. e38941.
244. Serra, M. and J.D. Saba, *Sphingosine 1-phosphate lyase, a key regulator of sphingosine 1-phosphate signaling and function*. Advances in enzyme regulation, 2010. **50**(1): p. 349-362.
245. Vogel, P., et al., *Incomplete Inhibition of Sphingosine 1-Phosphate Lyase Modulates Immune System Function yet Prevents Early Lethality and Non-Lymphoid Lesions*. PLOS ONE, 2009. **4**(1): p. e4112.
246. Zamora-Pineda, J., et al., *Dendritic cell sphingosine-1-phosphate lyase regulates thymic egress*. Journal of Experimental Medicine, 2016. **213**(12): p. 2773-2791.
247. Pham, T.H., et al., *S1P1 receptor signaling overrides retention mediated by G alpha i-coupled receptors to promote T cell egress*. Immunity, 2008. **28**(1): p. 122-33.
248. Arnon, T.I., et al., *GRK2-Dependent S1PR1 Desensitization Is Required for Lymphocytes to Overcome Their Attraction to Blood*. Science, 2011. **333**(6051): p. 1898.
249. Willinger, T., et al., *Dynamin 2-dependent endocytosis is required for sustained S1PR1 signaling*. Journal of Experimental Medicine, 2014. **211**(4): p. 685-700.
250. Mackay, C.R., W.L. Marston, and L. Dudley, *Naive and memory T cells show distinct pathways of lymphocyte recirculation*. J Exp Med, 1990. **171**(3): p. 801-17.
251. Klonowski, K.D., et al., *Dynamics of blood-borne CD8 memory T cell migration in vivo*. Immunity, 2004. **20**(5): p. 551-62.

252. Mendoza, A., et al., *Lymphatic endothelial S1P promotes mitochondrial function and survival in naive T cells*. Nature, 2017. **546**(7656): p. 158-161.
253. Blaho, V.A., et al., *HDL-bound sphingosine-1-phosphate restrains lymphopoiesis and neuroinflammation*. Nature, 2015. **523**(7560): p. 342-6.
254. Liu, G., et al., *The S1P(1)-mTOR axis directs the reciprocal differentiation of T(H)1 and T(reg) cells*. Nature immunology, 2010. **11**(11): p. 1047-1056.
255. Olesch, C., et al., *Beyond Immune Cell Migration: The Emerging Role of the Sphingosine-1-phosphate Receptor S1PR4 as a Modulator of Innate Immune Cell Activation*. Mediators of Inflammation, 2017. **2017**: p. 6059203.
256. Xiong, Y., et al., *CD4 T cell sphingosine 1-phosphate receptor (S1PR)1 and S1PR4 and endothelial S1PR2 regulate afferent lymphatic migration*. Science immunology, 2019. **4**(33): p. eaav1263.
257. Drouillard, A., et al., *S1PR5 is essential for human natural killer cell migration toward sphingosine-1 phosphate*. Journal of Allergy and Clinical Immunology, 2018. **141**(6): p. 2265-2268.e1.
258. Walzer, T., et al., *Natural killer cell trafficking in vivo requires a dedicated sphingosine 1-phosphate receptor*. Nat Immunol, 2007. **8**(12): p. 1337-44.
259. Tedford, K., et al., *The opposing forces of shear flow and sphingosine-1-phosphate control marginal zone B cell shuttling*. Nature Communications, 2017. **8**(1): p. 2261.
260. Drouillard, A., et al., *Human Naive and Memory T Cells Display Opposite Migratory Responses to Sphingosine-1 Phosphate*. The Journal of Immunology, 2018. **200**(2): p. 551.
261. Baeyens, A., et al., *Exit Strategies: S1P Signaling and T Cell Migration*. Trends Immunol, 2015. **36**(12): p. 778-787.
262. Liu, Y., et al., *Edg-1, the G protein-coupled receptor for sphingosine-1-phosphate, is essential for vascular maturation*. The Journal of Clinical Investigation, 2000. **106**(8): p. 951-961.
263. Allende, M.L., T. Yamashita, and R.L. Proia, *G-protein-coupled receptor S1P1 acts within endothelial cells to regulate vascular maturation*. Blood, 2003. **102**(10): p. 3665-3667.
264. Mendelson, K., et al., *Sphingosine 1-Phosphate Receptor Signaling Regulates Proper Embryonic Vascular Patterning*. Journal of Biological Chemistry, 2013. **288**(4): p. 2143-2156.
265. Shoham, A.B., et al., *S1P1 inhibits sprouting angiogenesis during vascular development*. Development, 2012. **139**(20): p. 3859.
266. Zhang, L., et al., *A novel role of sphingosine 1-phosphate receptor S1pr1 in mouse thrombopoiesis*. Journal of Experimental Medicine, 2012. **209**(12): p. 2165-2181.
267. Cahalan, S.M., et al., *Actions of a picomolar short-acting S1P₁ agonist in S1P₁-eGFP knock-in mice*. Nature chemical biology, 2011. **7**(5): p. 254-256.
268. Mullershausen, F., et al., *Persistent signaling induced by FTY720-phosphate is mediated by internalized S1P1 receptors*. Nature Chemical Biology, 2009. **5**(6): p. 428-434.
269. Godbole, A., et al., *Internalized TSH receptors en route to the TGN induce local Gs-protein signaling and gene transcription*. Nature Communications, 2017. **8**(1): p. 443.
270. Hanson, M.A., et al., *Crystal structure of a lipid G protein-coupled receptor*. Science, 2012. **335**(6070): p. 851-5.
271. Parrill, A.L., S. Lima, and S. Spiegel, *Structure of the First Sphingosine 1-Phosphate Receptor*. Science Signaling, 2012. **5**(225): p. pe23.

272. Stanley, N., L. Pardo, and G.D. Fabritiis, *The pathway of ligand entry from the membrane bilayer to a lipid G protein-coupled receptor*. Scientific Reports, 2016. **6**(1): p. 22639.
273. Kajimoto, T., et al., *Ongoing activation of sphingosine 1-phosphate receptors mediates maturation of exosomal multivesicular endosomes*. Nature Communications, 2013. **4**(1): p. 2712.
274. Rosen, H., et al., *Sphingosine 1-phosphate receptor signaling*. Annu Rev Biochem, 2009. **78**: p. 743-68.
275. Murata, N., et al., *Interaction of sphingosine 1-phosphate with plasma components, including lipoproteins, regulates the lipid receptor-mediated actions*. The Biochemical journal, 2000. **352 Pt 3**(Pt 3): p. 809-815.
276. Hammad, S.M., et al., *Sphingosine 1-Phosphate Distribution in Human Plasma: Associations with Lipid Profiles*. Journal of Lipids, 2012. **2012**: p. 180705.
277. Christoffersen, C., et al., *Endothelium-protective sphingosine-1-phosphate provided by HDL-associated apolipoprotein M*. Proceedings of the National Academy of Sciences, 2011. **108**(23): p. 9613.
278. Galvani, S., et al., *HDL-bound sphingosine 1-phosphate acts as a biased agonist for the endothelial cell receptor S1P1 to limit vascular inflammation*. Science signaling, 2015. **8**(389): p. ra79-ra79.
279. Obinata, H., et al., *Identification of ApoA4 as a sphingosine 1-phosphate chaperone in ApoM- and albumin-deficient mice*. J Lipid Res, 2019. **60**(11): p. 1912-1921.
280. Smith, M.E. and W.L. Ford, *The recirculating lymphocyte pool of the rat: a systematic description of the migratory behaviour of recirculating lymphocytes*. Immunology, 1983. **49**(1): p. 83-94.
281. Lyons, A.B. and C.R. Parish, *Are murine marginal-zone macrophages the splenic white pulp analog of high endothelial venules?* European Journal of Immunology, 1995. **25**(11): p. 3165-3172.
282. Grayson, M.H., et al., *Intravital microscopy comparing T lymphocyte trafficking to the spleen and the mesenteric lymph node*. American Journal of Physiology-Heart and Circulatory Physiology, 2003. **284**(6): p. H2213-H2226.
283. Gandy, K.Alexa O., et al., *Sphingosine 1-phosphate induces filopodia formation through S1PR2 activation of ERM proteins*. Biochemical Journal, 2013. **449**(3): p. 661-672.
284. Cahalan, S.M., et al., *Sphingosine 1-phosphate receptor 1 (S1P(1)) upregulation and amelioration of experimental autoimmune encephalomyelitis by an S1P(1) antagonist*. Molecular pharmacology, 2013. **83**(2): p. 316-321.
285. Bai, Z., et al., *CXC Chemokine Ligand 12 Promotes CCR7-Dependent Naive T Cell Trafficking to Lymph Nodes and Peyer's Patches*. The Journal of Immunology, 2009. **182**(3): p. 1287.
286. Vrzalikova, K., et al., *S1PR1 drives a feedforward signalling loop to regulate BATF3 and the transcriptional programme of Hodgkin lymphoma cells*. Leukemia, 2018. **32**(1): p. 214-223.
287. Paluch, E.K. and E. Raz, *The role and regulation of blebs in cell migration*. Current opinion in cell biology, 2013. **25**(5): p. 582-590.
288. Petrie, R.J. and H. Koo, *Direct Measurement of Intracellular Pressure*. Current Protocols in Cell Biology, 2014. **63**(1): p. 12.9.1-12.9.9.
289. Nomachi, A., et al., *Moesin Controls Clathrin-Mediated S1PR1 Internalization in T Cells*. PLOS ONE, 2013. **8**(12): p. e82590.

290. Hughes, C.E. and R.J.B. Nibbs, *A guide to chemokines and their receptors*. The FEBS Journal, 2018. **285**(16): p. 2944-2971.
291. Fredriksson, R., et al., *The G-Protein-Coupled Receptors in the Human Genome Form Five Main Families. Phylogenetic Analysis, Paralogon Groups, and Fingerprints*. Molecular Pharmacology, 2003. **63**(6): p. 1256.
292. Katritch, V., V. Cherezov, and R.C. Stevens, *Structure-Function of the G Protein–Coupled Receptor Superfamily*. Annual Review of Pharmacology and Toxicology, 2013. **53**(1): p. 531-556.
293. Syrovatkina, V., et al., *Regulation, Signaling, and Physiological Functions of G-Proteins*. Journal of Molecular Biology, 2016. **428**(19): p. 3850-3868.
294. Davis, C.B., et al., *Signal transduction due to HIV-1 envelope interactions with chemokine receptors CXCR4 or CCR5*. The Journal of experimental medicine, 1997. **186**(10): p. 1793-1798.
295. Haribabu, B., et al., *Regulation of human chemokine receptors CXCR4. Role of phosphorylation in desensitization and internalization*. J Biol Chem, 1997. **272**(45): p. 28726-31.
296. Roland, J., et al., *Role of the intracellular domains of CXCR4 in SDF-1-mediated signaling*. Blood, 2003. **101**(2): p. 399-406.
297. Okada, T. and J.G. Cyster, *CC Chemokine Receptor 7 Contributes to Gi-Dependent T Cell Motility in the Lymph Node*. The Journal of Immunology, 2007. **178**(5): p. 2973.
298. Hwang, I.-Y., et al., *Biased S1PR1 Signaling in B Cells Subverts Responses to Homeostatic Chemokines, Severely Disorganizing Lymphoid Organ Architecture*. The Journal of Immunology, 2019. **203**(9): p. 2401.
299. Sinha, R.K., et al., *B lymphocytes exit lymph nodes through cortical lymphatic sinusoids by a mechanism independent of sphingosine-1-phosphate-mediated chemotaxis*. Immunity, 2009. **30**(3): p. 434-46.
300. Chaffin, K.E. and R.M. Perlmutter, *A pertussis toxin-sensitive process controls thymocyte emigration*. European Journal of Immunology, 1991. **21**(10): p. 2565-2573.
301. Debes, G.F., et al., *Chemokine receptor CCR7 required for T lymphocyte exit from peripheral tissues*. Nat Immunol, 2005. **6**(9): p. 889-94.
302. Suzuki, G., et al., *Pertussis Toxin-Sensitive Signal Controls the Trafficking of Thymocytes Across the Corticomedullary Junction in the Thymus*. The Journal of Immunology, 1999. **162**(10): p. 5981.
303. Spangrude, G.J., et al., *Inhibition of lymphocyte and neutrophil chemotaxis by pertussis toxin*. J Immunol, 1985. **135**(6): p. 4135-43.
304. Hla, T., *Signaling and biological actions of sphingosine 1-phosphate*. Pharmacological Research, 2003. **47**(5): p. 401-407.
305. Gurevich, V.V. and E.V. Gurevich, *GPCR Signaling Regulation: The Role of GRKs and Arrestins*. Frontiers in Pharmacology, 2019. **10**(125).
306. Carman, C.V., et al., *Selective regulation of Galpha(q/11) by an RGS domain in the G protein-coupled receptor kinase, GRK2*. J Biol Chem, 1999. **274**(48): p. 34483-92.
307. Wilden, U., S.W. Hall, and H. Kühn, *Phosphodiesterase activation by photoexcited rhodopsin is quenched when rhodopsin is phosphorylated and binds the intrinsic 48-kDa protein of rod outer segments*. Proc Natl Acad Sci U S A, 1986. **83**(5): p. 1174-8.

308. Krasel, C., et al., *Beta-arrestin binding to the beta2-adrenergic receptor requires both receptor phosphorylation and receptor activation*. J Biol Chem, 2005. **280**(10): p. 9528-35.
309. Gurevich, E.V., et al., *G protein-coupled receptor kinases: more than just kinases and not only for GPCRs*. Pharmacol Ther, 2012. **133**(1): p. 40-69.
310. Zidar, D.A., et al., *Selective engagement of G protein coupled receptor kinases (GRKs) encodes distinct functions of biased ligands*. Proceedings of the National Academy of Sciences, 2009. **106**(24): p. 9649.
311. Busillo, J.M., et al., *Site-specific phosphorylation of CXCR4 is dynamically regulated by multiple kinases and results in differential modulation of CXCR4 signaling*. J Biol Chem, 2010. **285**(10): p. 7805-17.
312. Vroon, A., et al., *Reduced GRK2 level in T cells potentiates chemotaxis and signaling in response to CCL4*. Journal of Leukocyte Biology, 2004. **75**(5): p. 901-909.
313. Koch, W.J., et al., *The binding site for the beta gamma subunits of heterotrimeric G proteins on the beta-adrenergic receptor kinase*. Journal of Biological Chemistry, 1993. **268**(11): p. 8256-8260.
314. Touhara, K., et al., *Binding of G protein beta gamma-subunits to pleckstrin homology domains*. Journal of Biological Chemistry, 1994. **269**(14): p. 10217-10220.
315. Lodowski, D.T., et al., *The structure of G protein-coupled receptor kinase (GRK)-6 defines a second lineage of GRKs*. J Biol Chem, 2006. **281**(24): p. 16785-93.
316. Nobes, C.D. and A. Hall, *Rho GTPases Control Polarity, Protrusion, and Adhesion during Cell Movement*. Journal of Cell Biology, 1999. **144**(6): p. 1235-1244.
317. Allen, W.E., et al., *A Role for Cdc42 in Macrophage Chemotaxis*. Journal of Cell Biology, 1998. **141**(5): p. 1147-1157.
318. Ridley, A.J., *Rho GTPases and cell migration*. J Cell Sci, 2001. **114**(Pt 15): p. 2713-22.
319. Ridley, A.J., *Rho GTPase signalling in cell migration*. Curr Opin Cell Biol, 2015. **36**: p. 103-12.
320. Mou, F., et al., *The Mst1 and Mst2 kinases control activation of rho family GTPases and thymic egress of mature thymocytes*. Journal of Experimental Medicine, 2012. **209**(4): p. 741-759.
321. Takeda, A., et al., *Fibroblastic reticular cell-derived lysophosphatidic acid regulates confined intranodal T-cell motility*. eLife, 2016. **5**: p. e10561.
322. Okamoto, H., et al., *Inhibitory regulation of Rac activation, membrane ruffling, and cell migration by the G protein-coupled sphingosine-1-phosphate receptor EDG5 but not EDG1 or EDG3*. Mol Cell Biol, 2000. **20**(24): p. 9247-61.
323. Lee, M.J., et al., *Vascular endothelial cell adherens junction assembly and morphogenesis induced by sphingosine-1-phosphate*. Cell, 1999. **99**(3): p. 301-12.
324. Reinhard, N.R., et al., *The balance between Gai-Cdc42/Rac and Ga12/13-RhoA pathways determines endothelial barrier regulation by sphingosine-1-phosphate*. Molecular Biology of the Cell, 2017. **28**(23): p. 3371-3382.
325. Li, Q., et al., *Differential activation of receptors and signal pathways upon stimulation by different doses of sphingosine-1-phosphate in endothelial cells*. Experimental Physiology, 2015. **100**(1): p. 95-107.
326. Lee, M.-J., et al., *Sphingosine-1-Phosphate as a Ligand for the G Protein-Coupled Receptor EDG-1*. Science, 1998. **279**(5356): p. 1552.

327. Donati, C. and P. Bruni, *Sphingosine 1-phosphate regulates cytoskeleton dynamics: implications in its biological response*. Biochim Biophys Acta, 2006. **1758**(12): p. 2037-48.
328. Bandhuvula, P., et al., *The immune modulator FTY720 inhibits sphingosine-1-phosphate lyase activity*. J Biol Chem, 2005. **280**(40): p. 33697-700.
329. Woolf, E., et al., *Lymph node chemokines promote sustained T lymphocyte motility without triggering stable integrin adhesiveness in the absence of shear forces*. Nat Immunol, 2007. **8**(10): p. 1076-85.
330. Lämmermann, T., et al., *Rapid leukocyte migration by integrin-independent flowing and squeezing*. Nature, 2008. **453**(7191): p. 51-5.
331. de Paz, J.L., et al., *Profiling Heparin–Chemokine Interactions Using Synthetic Tools*. ACS Chemical Biology, 2007. **2**(11): p. 735-744.
332. Hirose, J., et al., *Chondroitin sulfate B exerts its inhibitory effect on secondary lymphoid tissue chemokine (SLC) by binding to the C-terminus of SLC*. Biochim Biophys Acta, 2002. **1571**(3): p. 219-24.
333. Patel, D.D., et al., *Chemokines have diverse abilities to form solid phase gradients*. Clin Immunol, 2001. **99**(1): p. 43-52.
334. Schumann, K., et al., *Immobilized chemokine fields and soluble chemokine gradients cooperatively shape migration patterns of dendritic cells*. Immunity, 2010. **32**(5): p. 703-13.
335. Faroudi, M., et al., *Critical roles for Rac GTPases in T-cell migration to and within lymph nodes*. Blood, 2010. **116**(25): p. 5536-5547.
336. Negulescu, P.A., et al., *Polarity of T Cell Shape, Motility, and Sensitivity to Antigen*. Immunity, 1996. **4**(5): p. 421-430.
337. Wei, X., B.J. Tromberg, and M.D. Cahalan, *Mapping the sensitivity of T cells with an optical trap: Polarity and minimal number of receptors for Ca^{2+} signaling*. Proceedings of the National Academy of Sciences, 1999. **96**(15): p. 8471.
338. Dustin, M.L., *The cellular context of T cell signaling*. Immunity, 2009. **30**(4): p. 482-92.
339. Friedl, P. and E.B. Bröcker, *T cell migration in three-dimensional extracellular matrix: guidance by polarity and sensations*. Dev Immunol, 2000. **7**(2-4): p. 249-66.
340. Friedl, P., et al., *CD4⁺ T lymphocytes migrating in three-dimensional collagen lattices lack focal adhesions and utilize beta1 integrin-independent strategies for polarization, interaction with collagen fibers and locomotion*. Eur J Immunol, 1998. **28**(8): p. 2331-43.
341. Lämmermann, T., et al., *Cdc42-dependent leading edge coordination is essential for interstitial dendritic cell migration*. Blood, 2009. **113**(23): p. 5703-5710.
342. Guo, F., et al., *Coordination of IL-7 receptor and T-cell receptor signaling by cell-division cycle 42 in T-cell homeostasis*. Proceedings of the National Academy of Sciences, 2010. **107**(43): p. 18505.
343. Guo, F., et al., *Distinct Roles of Cdc42 in Thymopoiesis and Effector and Memory T Cell Differentiation*. PLOS ONE, 2011. **6**(3): p. e18002.
344. Heasman, S.J., et al., *Coordinated RhoA signaling at the leading edge and uropod is required for T cell transendothelial migration*. Journal of Cell Biology, 2010. **190**(4): p. 553-563.
345. Jacobelli, J., et al., *Confinement-optimized three-dimensional T cell amoeboid motility is modulated via myosin IIA–regulated adhesions*. Nature Immunology, 2010. **11**(10): p. 953-961.

346. Jacobelli, J., et al., *Activated T Cell Trans-Endothelial Migration Relies on Myosin-IIA Contractility for Squeezing the Cell Nucleus through Endothelial Cell Barriers*. PLOS ONE, 2013. **8**(9): p. e75151.
347. Tozluoğlu, M., et al., *Matrix geometry determines optimal cancer cell migration strategy and modulates response to interventions*. Nature Cell Biology, 2013. **15**(7): p. 751-762.
348. Bergert, M., et al., *Cell mechanics control rapid transitions between blebs and lamellipodia during migration*. Proceedings of the National Academy of Sciences, 2012. **109**(36): p. 14434.
349. Carman, C.V., et al., *Transcellular diapedesis is initiated by invasive podosomes*. Immunity, 2007. **26**(6): p. 784-797.
350. Carman, C.V. and T.A. Springer, *A transmigratory cup in leukocyte diapedesis both through individual vascular endothelial cells and between them*. J Cell Biol, 2004. **167**(2): p. 377-88.
351. Baluk, P., et al., *Functionally specialized junctions between endothelial cells of lymphatic vessels*. Journal of Experimental Medicine, 2007. **204**(10): p. 2349-2362.
352. Pflücke, H. and M. Sixt, *Preformed portals facilitate dendritic cell entry into afferent lymphatic vessels*. Journal of Experimental Medicine, 2009. **206**(13): p. 2925-2935.
353. Jalkanen, S. and M. Salmi, *Lymphatic endothelial cells of the lymph node*. Nature Reviews Immunology, 2020. **20**(9): p. 566-578.
354. Farr, A.G., Y. Cho, and P.P.H. de Bruyn, *The structure of the sinus wall of the lymph node relative to its endocytic properties and transmural cell passage*. American Journal of Anatomy, 1980. **157**(3): p. 265-284.
355. Spalding, H.J. and T.J. Heath, *Fine structure of lymph pathways in nodes from the superficial inguinal lymph centre in the pig*. Journal of anatomy, 1989. **166**: p. 43-54.
356. Clark, S.L., Jr., *The reticulum of lymph nodes in mice studied with the electron microscope*. Am J Anat, 1962. **110**: p. 217-57.
357. Forkert, P.-G., J.A. Thliveris, and F.D. Bertalanffy, *Structure of sinuses in the human lymph node*. Cell and Tissue Research, 1977. **183**(1): p. 115-130.
358. van Ewijk, W., et al., *Lymphoid microenvironments in the thymus and lymph node*. Scanning Microsc, 1988. **2**(4): p. 2129-40.
359. Wei, S.H., et al., *Sphingosine 1-phosphate type 1 receptor agonism inhibits transendothelial migration of medullary T cells to lymphatic sinuses*. Nat Immunol, 2005. **6**(12): p. 1228-35.
360. Azzali, G., *Tumor cell transendothelial passage in the absorbing lymphatic vessel of transgenic adenocarcinoma mouse prostate*. Am J Pathol, 2007. **170**(1): p. 334-46.
361. Zachariah, M.A. and J.G. Cyster, *Neural crest-derived pericytes promote egress of mature thymocytes at the corticomedullary junction*. Science (New York, N.Y.), 2010. **328**(5982): p. 1129-1135.
362. Mori, K., et al., *The perivascular space as a path of hematopoietic progenitor cells and mature T cells between the blood circulation and the thymic parenchyma*. Int Immunol, 2007. **19**(6): p. 745-53.
363. Kato, S. and G.I. Schoefl, *Microvasculature of normal and involuted mouse thymus. Light- and electron-microscopic study*. Acta Anat (Basel), 1989. **135**(1): p. 1-11.
364. James, K.D., W.E. Jenkinson, and G. Anderson, *T-cell egress from the thymus: Should I stay or should I go?* J Leukoc Biol, 2018. **104**(2): p. 275-284.

365. Wardlaw, J.M., et al., *Perivascular spaces in the brain: anatomy, physiology and pathology*. Nat Rev Neurol, 2020. **16**(3): p. 137-153.
366. White, A.J., et al., *A type 2 cytokine axis for thymus emigration*. J Exp Med, 2017. **214**(8): p. 2205-2216.
367. Ushiki, T., *A scanning electron-microscopic study of the rat thymus with special reference to cell types and migration of lymphocytes into the general circulation*. Cell Tissue Res, 1986. **244**(2): p. 285-98.
368. Kato, S., *Thymic microvascular system*. Microscopy Research and Technique, 1997. **38**(3): p. 287-299.
369. Shulman, Z., et al., *Transendothelial migration of lymphocytes mediated by intraendothelial vesicle stores rather than by extracellular chemokine depots*. Nat Immunol, 2011. **13**(1): p. 67-76.
370. Thudichum, J.L.W., *A Treatise on the Chemical Constitution of the Brain: based throughout upon Original Researches* 1884. **149**.
371. Yaniv, K., et al., *Live imaging of lymphatic development in the zebrafish*. Nat Med, 2006. **12**(6): p. 711-6.
372. Jung, H.M., et al., *Development of the larval lymphatic system in zebrafish*. Development, 2017. **144**(11): p. 2070.
373. Grimaldi, C., et al., *E-cadherin focuses protrusion formation at the front of migrating cells by impeding actin flow*. Nature Communications, 2020. **11**(1): p. 5397.
374. Diz-Muñoz, A., et al., *Steering cell migration by alternating blebs and actin-rich protrusions*. BMC Biology, 2016. **14**(1): p. 74.
375. Hayashi, K., et al., *Immunofluorescence detection of ezrin/radixin/moesin (ERM) proteins with their carboxyl-terminal threonine phosphorylated in cultured cells and tissues*. Journal of Cell Science, 1999. **112**(8): p. 1149.